Implementation of 5G Private Networks at Portuguese Air Force

Ana Rita Fonseca Ramalho

Thesis to obtain the Master of Science Degree in

Electrical and Computer Engineering

Supervisors: Prof. Luís Manuel de Jesus Sousa Correia

Lieutenant Colonel Adalberto José Rocha Santos

Examination Committee

Chairperson: Prof. José Eduardo Charters Ribeiro da Cunha Sanguino

Supervisor: Prof. Luís Manuel de Jesus Sousa Correia

Members of Committee: Prof. António Manuel Raminhos Cordeiro Grilo

Major Eng. Gonçalo Cruz

November 2023

I declare that this document is an original work of my own authorship and that it fulfils all the requirements of the Code of Conduct and Good Practices of the *Universidade de Lisboa*.

“In the middle of difficulty lies opportunity.”

-Albert Einstein

Acknowledgements

To the Portuguese Air Force Academy and the Instituto Superior Técnico, for all the academic and personal support over the past few years.

To Professor Luís M. Correia as a teacher for the last two years and as an advisor and supervisor for the last year, I would like to thank him for all his availability, critical spirit, motivation, solutions, help and, above all, good humour when times were challenging.

To Lieutenant Colonel Adalberto Santos, for all his willingness to help, availability, attention, understanding and concern during the development of the work. I would like to thank him for all the inspiration and sharing of knowledge.

To all the GROW members, especially Francisco Graterol, José Reis, Pedro Mateus and Bernardo Galego, who shared this chapter with me, always promoting group spirit, sharing knowledge and, above all, friendship. I would like to thank them as a colleague and friend.

To Kaisers for all the shared moments and experiences, our friendship and for always overcoming adversity together.

To all my friends, who, despite being far away, were always there. For supporting my decisions and always believing in me. I owe all my achievements to them, too. Thank you.

To my family for being my strength at all times. For always believing in my abilities and never giving up on helping me, no matter how difficult it was. For always showing me all the paths but encouraging me to choose the best one. They have created every opportunity, with love, affection and persistence. I want to thank them for being the main part of who I have become today.

Finally, to my loved João for being there every day. For all his help, dedication, comfort, support, friendship and love. For always showing the positive side and turning every problem into a solution. I cannot thank him enough for everything.

Abstract

This thesis studies the implementation of 5G private networks at the Portuguese Air Force, focusing specifically on their potential applications and benefits. Private networks have been the centre of attention since 5G technology was introduced due to its capacity to provide increased connection, reduced latency, and data security. This research aims at identifying and studying the aspects and characteristics of 5G private networks. It also investigates real-world use services in restricted scenarios, such as an Airbase, the Portuguese Air Force Wide Area Multilateration System, and a Remote-Controlled UAV Squadron, to demonstrate the practical implications of this technology. To guarantee service performance, the developed model considers the MEC node deployment options, Splitting Option 7.2 functionalities, and network architectures as variables to analyse the deployment performance of a private network. The results show that even when adopting adequate latency reduction strategies and radio techniques applied to a 5G private network architecture, it is impossible to ensure some services' requirements, removing the possibility of deploying a private network integrated into a commercial Operator infrastructure.

Keywords

5G, Private Network, Military Communications, Critical Services, Latency, Capacity.

Resumo

Esta tese tem como principal objetivo estudar a implementação de redes privadas 5G, através do foco nas suas potenciais aplicações e benefícios para a Força Aérea Portuguesa. As redes privadas têm tido um grande impacto desde que a tecnologia 5G foi introduzida, devido à sua capacidade de conexão, latência reduzida e segurança na partilha de dados. Desta forma, este trabalho tem como intuito identificar e estudar os aspectos e características das redes móveis 5G e das respetivas redes privadas. Procede-se, de igual modo, à investigação de casos reais em cenários restritos tais como uma Base Aérea, o Sistema de Multilateração da Força Aérea Portuguesa, e a Esquadra de Controlo-Remoto de UAVs, para demonstrar as implicações práticas desta tecnologia. Por forma a garantir a implementação dos serviços, o modelo desenvolvido considera a opção de implementação do nó MEC, as funcionalidades da *Splitting Option* 7.2, e as arquitecturas de rede como variáveis que influenciam a performance da instalação de uma rede privada. Os resultados mostram que, mesmo adotando estratégias adequadas de redução de latência e técnicas de rádio aplicadas a uma arquitetura de rede 5G, é impossível garantir os requisitos de alguns serviços, retirando a possibilidade de implantação de uma rede privada integrada na infraestrutura de um Operador comercial.

Palavras-chave

5G, Redes Privadas, Comunicações Militares, Serviços Críticos, Latência, Capacidade.

Table of Contents

List of Figures

List of Tables

List of Abbreviations

3GPP	3rd Generation Partnership Project
4G	4th Generation of Mobile Communication Systems
5G	5th Generation of Mobile Communication Systems
5GC	5G Core
AF	Application Function
AL	Air Link
AM	Amplitude Modulation
AMF	Access and Mobility Management Function
AR	Augmented Reality
AUSF	Authentication Server Function
BBU	Base Band Unit
BH	Backhaul
BS	Base Station
BSS	Business Support Systems
CCTV	Closed-Circuit Television
CN	Core Network
CP	Control Plane
CPx	Cyclic Prefix
CPx-OFDMA	Cyclic Prefix Orthogonal Frequency Division Multiplexing Access
CQI	Channel Quality Indicator
C-RAN	Cloud-Radio Access Network
CU	Centralised Unit
DL	Downlink
DN	Data Network
DNS	Domain Name System
DU	Distributed Unit
E2E	End-to-End
EASDF	Edge Application Server Discovery Function
eCPRI	enhanced Common Public Radio Interface
EDC	External Data Centre
eMBB	enhanced Mobile Broadband
eNB	evolved Node B
FDD	Frequency Division Duplexing
FH	Fronthaul
FM	Frequency Modulation
FR1	Frequency Range 1

FR2	Frequency Range 2
GBR	Guaranteed Bit Rate
gNB	Next Generation Node B
GS	Ground Station
ICI	Inter Carrier Interference
IMT	International Mobile Telecommunications
IoT	Internet of Things
IP	Internet Protocol
ISI	Inter Symbol Interference
ISR	Intelligence, Surveillance, Reconnaissance
ITU	International Telecommunication Union
LAA	Licence Assisted Access
LAN	Local Area Network
LoS	Line of Sight
LTE	Long-Term Evolution
MANO	Management and Orchestration
MEC	Multi-Access Edge Computing
MH	Middlehaul
MIMO	Multiple-Input Multiple-Output
mMTC	massive Machine Type Communications
MNO	Mobile Network Operator
MSL	Mean Sea Level
NAV Portugal	Air Navigation Portugal
NEF	Network Exposure Function
NFV	Network Function Virtualisation
n-GBR	non-Guaranteed Bit Rate
NLoS	Non-Line of Sight
NR	New Radio
NRF	Network Repository Function
NR-U	New Radio Unlicensed
NSACF	Network Slice Access Control Function
NSSF	Network Slice Selection Function
NTN	Non-Terrestrial Network
OFDM	Orthogonal Frequency-Division Multiplexing
O-RAN	Open-Radio Access Network
OSS	Operations Support Systems
PCF	Policy Control Function
PDCP	Packet Data Convergence Protocol
PDU	Protocol Data Unit
PER	Packet Error Rate

QAM	Quadrature Amplitude Modulation
QoE	Quality of Experience
QoS	Quality of Service
QPSK	Quadrature Phase-Shift Keying
RAN	Radio Access Network
RB	Resource Block
RRC	Radio Resource Control
RRH	Remote Radio Head
RU	Radio Unit
SCP	Service Communication Proxy
SCS	Subcarrier Spacing
SDN	Software-Defined Networking
SLA	Service Level Agreement
SMF	Session Management Function
TDD	Time Division Duplexing
TL	Transport Link
TTI	Transmission Time Interval
UAV	Unmanned Aerial Vehicle
UDM	Unified Data Management
UE	User Equipment
UL	Uplink
UP	User Plane
UPF	User Plane Function
URLLC	Ultra-Reliable Low Latency Communications
VHF	Very High Frequency
VNF	Virtualised Network Function
VR	Virtual Reality
WAM	Wide Area Multilateration

List of Symbols

A_f	Average factor
B	System bandwidth
B_c	Bandwidth for control signals
b_c	Buffered traffic ratio
D	Data packet size
d	Distance between the origin and destination of the signal
d_{AL_Rx}	AL link length on the receiver side
d_{AL_Tx}	AL link length on the transmitter side
d_{BH_Rx}	BH link length on the receiver side
d_{BH_Tx}	BH link length on the transmitter side
d_{E2E}	E2E distance
d_{FH_Rx}	FH link length on the receiver side
d_{FH_Tx}	FH link length on the transmitter side
$D_{MAC_{info}}$	Maximum amount of data transmitted over the wireless network
d_{Max_E2E}	Maximum E2E distance
$d_{Max\_optical}$	Maximum optical link length
d_{MH_Rx}	MH link length on the receiver side
d_{MH_Tx}	MH link length on the transmitter side
d_{RH}	Radio horizon distance
$D_{serv,p}$	Packet size in bytes for a specific service with priority p
d_{TL_Rx}	TL length on the receiver side
d_{TL_Tx}	TL length on the transmitter side
F_{DL}	Percentage of the slot reserved for the DL
f_{ref}	Reference frequency
F_{UL}	Percentage of the slot reserved for the UL
f_s	Scaling factor
$h_{A,MSL}$	Aircraft height above the MSL

$h_{GS,MSL}$	GS height above the MSL
M	Modulation order
M_c	Modulation order for control signals
$M_{P,serv}$	Number of users connected to the node and utilising services with a higher or equal priority than the examined user
N_A	Number of antenna ports
$N_{L,c}$	Number of layers for control signalling
N_L	Number of layers in the system
$N_{PRB}^{B,\mu}$	Maximum number of physical RB in bandwidth B with numerology μ
N_Q	Bit width
N_{SC}	Number of subcarriers used in the system
N_{SY}	Number of symbols in the system
N_u	Number of users connected to the RU node
O	Overhead for control channels
Q_m	Average modulation order
R	Data rate provided by the link
r_A	Effective distance of the aircraft's antenna to the Earth's centre
R_c	Signalling rate
R_{code_max}	Maximum code rate
R_e	Effective Earth radius
R_{FDD}	Capacity of the 5G FDD radio link
r_{GS}	Effective distance of the GS's antenna to the Earth's centre
R_{max}	Maximum capacity offered by the link
$R_{Op.2}$	MH link capacity for Splitting Option 2
$R_{Op.7.2}$	FH link capacity for Splitting Option 7.2
R_p	Peak rate
R_s	Data rate of the services offered by the RU node
$R_{TDD/DL}$	Average throughput of the radio in 5G DL in TDD
$R_{TDD/UL}$	Average throughput of the radio in 5G UL in TDD
R_u	RU node required throughput
T_s^{μ}	Average subframe OFDM symbol duration

v	Velocity of the signal on the link
v_{Layers}	Number of MIMO layers
Z_c^{DL}	Aggregated buffered traffic size in DL
Z_c^{UL}	Aggregated buffered traffic size in UL
Δf_{subc}	SCS
δ_{AL_Rx}	AL latency on the receiver side
δ_{AL_Tx}	AL latency on the transmitter side
δ_{BH_Rx}	Propagation latency of the BH link on the receiver side
δ_{BH_Tx}	Propagation latency of the BH link on the transmitter side
δ_{CU_Proc}	CU node processing latency
δ_{CU_Queu}	CU node queuing latency
δ_{CU_Rx}	Latency of the CU node on the receiver side
δ_{CU_Trans}	CU node transmission latency
δ_{CU_Tx}	Latency of the CU node on the transmitter side
δ_{Core_Proc}	CN processing latency
δ_{Core_Rx}	Latency of the CN on the receiver side
δ_{Core_Trans}	CN transmission latency
δ_{Core_Tx}	Latency of the CN on the transmitter side
δ_{DU_Proc}	DU node processing latency
δ_{DU_Queu}	DU node queuing latency
δ_{DU_Rx}	Latency of the DU node on the receiver side
δ_{DU_Trans}	DU node transmission latency
δ_{DU_Tx}	Latency of the DU node on the transmitter side
δ_{E2E}	E2E latency
δ_{EDC}	Latency of the EDC node
δ_{EDC_Proc}	EDC node processing latency
δ_{EDC_Trans}	EDC node transmission latency
δ_{FH_Rx}	Propagation latency of the FH link on the receiver side
δ_{FH_Tx}	Propagation latency of the FH link on the transmitter side
δ_{MEC}	Latency of the MEC node
δ_{MEC_Proc}	MEC node processing latency

δ_{MEC_Trans}	MEC node transmission latency
δ_{MH_Rx}	Propagation latency of the MH link on the receiver side
δ_{MH_Tx}	Propagation latency of the MH link on the transmitter side
δ_{Max_E2E}	Maximum E2E latency
$\delta_{Max\_optical}$	Maximum optical link propagation latency
δ_{Prop}	Propagation latency
δ_{Queu}	Queuing latency
δ_{RU_Proc}	RU node processing latency
δ_{RU_Queu}	RU node queuing latency
δ_{RU_Rx}	Latency of the RU node on the receiver side
δ_{RU_Trans}	RU node transmission latency
δ_{RU_Tx}	Latency of the RU node on the transmitter side
$\delta_{service}$	Required latency associated with the chosen service
δ_{TL_Rx}	Propagation latency on the TL on the receiver side
δ_{TL_Tx}	Propagation latency on the TL on the transmitter side
δ_{Total_node}	Total node latency
δ_{Total_prop}	Total propagation latency
δ_{Trans}	Transmission latency
δ_{UE_Proc}	UE node processing latency
δ_{UE_Rx}	UE node latency on the receiver side
δ_{UE_Trans}	UE node transmission latency
δ_{UE_Tx}	UE node latency on the transmitter side
μ	Numerology number
μ_s	Subcarrier utilisation (load)
ρ_{CU}	Ratio of functionalities assigned to the CU node
ρ_{DU}	Ratio of functionalities assigned to the DU node
ρ_{func}	Number of functionalities executed by the MEC node
ρ_{lat}	Latency adaptation parameter
ρ_{RU}	Ratio of functionalities assigned to the RU node
ρ_{UE}	Latency processing ratio of the UE

List of Software

Google Earth	Map and geographical information software
MATLAB R2020a	Numerical computing software
Microsoft Excel	Spreadsheet application
Microsoft PowerPoint	Presentation and slide program
Microsoft Word	Text Editor Software

Chapter 1

Introduction

This chapter provides an introduction to the thesis. An overview of the fifth generation of mobile communications associated with the improvements applied by this network is provided. The Portuguese Air Force paradigm is presented with the motivation and a description of the problem under study. At the end, the work structure is presented.

1.1 Overview

The 5th Generation of Mobile Communication Systems (5G) represents a significant advancement in mobile network capabilities. The connectivity for consumers' tablets, smartphones, and laptops is forced to its limits concerning latency, capacity, and availability. In addition, new services, such as industrial Internet of Things (IoT) connectivity and critical communications, are being developed. This improvement is accomplished through flexible platforms that enable device connectivity, high reliability, and ultra-low latency, in which 5G targets are set with data rates up to 20 Gbps and capacity increases up to 1 000 times. Several new use cases and applications are being developed to run on top of 5G mobile networks. It is expected that 5G will profoundly impact society by improving productivity, efficiency, and safety, allowing Telecommunications Operators to assist customers in automating business processes due to the 5G implementation [1].

It is worth noticing that productivity gains in physical business processes, such as construction, manufacturing, and logistics, have lagged behind those in service industries, which have been able to digitalise and automate processes over the last decades. In some industries, uploading a large amount of image data and ensuring a guaranteed data rate is required as a service. In some cases, technology and Uplink (UL) enhancements to ensure performance are more important than general users' communication services. As illustrated in Figure 1.1, the 5G evolution promotes a highly reliable radio technology for applications while improving UL performance [1, 2].

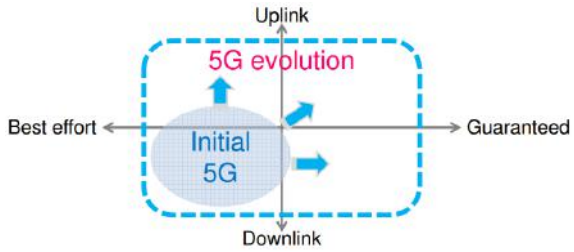

Figure 1.1 – Performance improvement of 5G evolution (extracted from [2]).

Because all these improvements, there is the need to harvest a spectrum that cellular technology has not previously used. In this way, 5G is considered a promising solution. However, spectrum is an expensive resource that is difficult to manage globally, especially considering the cost of devices and network equipment. Thus, moving to higher frequency bands not previously used in cellular systems is difficult, even if the antenna's size decreases as the carrier frequency increases [2].

Many other challenges arise due to higher frequency path loss. Power amplifier technologies must evolve to support sufficient transmit powers with reasonable energy efficiency in a consumer device price point. As a result, industry verticals are very interested in 5G and intend to build their own private dedicated networks or use Operator spectrum and network slicing technology [2].

In this way, an intriguing convergence of three inflexion points is observed: 5G as a new radio standard, the spread of the cloud concept in wireless networks, and the rapid adoption of artificial intelligence and machine learning.

Because of the new requirements and increased use cases, 5G system design and deployment differs from previous mobile network generations, driving the rise of private networks. This type of network provides a way to share data privately and independently. Companies can communicate information conveniently and securely by connecting to their members-only network, providing more access points. The number of private network deployments is increasing rapidly as a result. While private 5G has the same technological advantages as public 5G, it also gives users more control over the network's security, policies, services, and data. Compared to standard 5G networks, it provides higher flexibility, including improved coverage options for remote applications, fewer technical challenges for large indoor spaces, and access to more shared spectrum [3]. However, some limitations, such as regulatory, technical and integration challenges, are still associated with the private 5G deployment.

Armed Forces are one of the areas typo in these new features, aspiring to achieve a sustained mode of operation by using a 5G mobile network. The military scenarios make extensive use of services and communication technologies. These are frequently highly specialised communication services, such as critical communication, requiring high security, privacy, and availability. Other essential requirements include *ad hoc* connectivity and on-demand, resistance to jamming and End-to-End (E2E) encryption. Military personnel also use commercial services, like broadband and mobile voice. However, with the introduction of 5G and network slicing, where isolated/private networks can be established on a shared network infrastructure, it becomes more practical for the Armed Forces to use a commercial network. In this way, there is a possibility to ensure the requirements associated with various missions using 5G network properties [2, 4].

1.2 Portuguese Air Force Paradigm

The Portuguese Air Force, as an integral part of the national forces system, has the mission of cooperating in the military defence of the country and is responsible for carrying out air operations in defence of national space as well as missions in the public interest to meet the needs of the population [5].

Therefore, adopting a 5G private network is an enormous potential development. Several benefits provided by this cutting-edge technology revolutionise mission-critical operations, data transmission, and communication. In this way, the implementation of private networks is based on the need to improve the existing network structure that is unable to respond to services with very demanding requirements. Thus, improving the performance of the Portuguese Air Force systems in its various areas of operation can be supported by installing 5G private networks.

The thesis developed by [6], in 2021 assesses the Very High Frequency (VHF) Amplitude/Frequency Modulation (AM/FM) communications system installed on Azores Island. The thesis was developed to create and study a new system since the original, which consists of ground stations (GS) with transmitting antennas and an interconnection and remote monitoring system, had several problems locating aircraft in certain areas. Therefore, creating a new system with extensive coverage was an object of study. Based on this context, a 5G private network can coexist within the VHF AM/FM communication system in the same operational environment. However, the integration depends on the

specific communication needs of the organisation or facility, like an Air Force base. Thus, integrating a 5G private network can serve as a high-speed Backhaul (BH) connection for VHF AM/FM Base Stations (BS), improving network dependability and permitting effortless interaction between geographically separated VHF AM/FM locations. It can also ensure a backup or redundant communication link, enabling the Portuguese Air Force to maintain operations even if the VHF AM/FM system encounters problems or interruptions. This redundancy raises the dependability of overall coverage.

Regarding the extended coverage, by strategically deploying 5G BSs, the Portuguese Air Force can extend coverage to regions where VHF AM/FM signals may have limitations, such as rough terrain or densely wooded areas. Moreover, while VHF AM/FM systems primarily handle voice communication, combining data services or applications that request high-speed data access can also be requested. Therefore, the interoperability of the 5G private network can support these data-centric services, enabling simultaneous audio and data transmission and ensuring that personnel can switch between them as needed.

The 5G private network also supports advanced Quality of Service (QoS) management, allowing the prioritisation of these services and ensuring that the critical voice and data traffic receive the highest priority, even during network congestion. Integrating the system with the private network enables robust security features to protect sensitive data and communications, ensuring the confidentiality of mission-critical information.

There is also the possibility of installing a 5G private network in another communications system that continues to influence the Portuguese Air Force performance and whose constraints were introduced in the thesis developed by [7] in 2018. In this case, the main objective was to analyse the required coverage in *ad-hoc* networks of Unmanned Aerial Vehicle (UAV) to ensure military missions of maritime surveillance, reconnaissance, and target detection and tracking. Therefore, implementing a 5G private network can significantly improve the deployment of the UAV network. This migration extends coverage by providing ultra-high-speed communications, enabling UAVs to exchange large volumes of data. This benefits streaming high-resolution video, transmitting sensor data, and facilitating real-time decision-making. The 5G private network also allows UAVs operating in challenging environments to benefit from stable and uninterrupted connectivity, improving mission success rates.

Furthermore, the edge computing capabilities integrated into the private network enable UAVs to offload processing tasks, and the fact that these networks are highly scalable makes it easy to add more UAVs to the network as needed. Therefore, this integration is valuable for mission-critical applications across public safety, defence and infrastructure inspection, where UAVs improve efficiency and effectiveness.

Moreover, the efficient spectrum usage provided by the 5G private network optimises available frequencies, reducing interference, which is crucial in crowded UAV environments. Thus, data-intensive missions have the support of high-speed 5G connectivity for transmitting large volumes of data.

The two studies' examples correspond to analyses applied to the Portuguese Air Force communication systems. However, other areas can also benefit from this type of installation. Thus, integrating systems

enhances the Portuguese Air Force's mission flexibility by providing a versatile communication platform that can adapt to various scenarios and operational requirements.

When analysing the Portuguese Air Force paradigm, it is possible to verify that the integration has many benefits, including increased connection, improved communication, real-time data transmission, and support for mission-critical activities. This innovative project is not a technological indulgence but an urgent necessity based on several elements that collectively transform the national defence strategy. These advantages allow the Portuguese Air Force to be more operationally effective, situationally aware, and mission-ready.

1.3 Motivation and Contents

The current thesis is motivated by studying 5G private military communications methods to develop and optimise the respective performance parameters in airbases, manoeuvring aerodromes and radar stations. Like many military units worldwide, the Portuguese Air Force constantly seeks to improve communication and networking capabilities. Introducing a 5G private network provides an opportunity to improve connectivity and data transmission, thus improving mission-critical operations and overall efficiency. The study has two main components: a model to calculate the capacities, required throughputs, latency and distance leading to the first outputs, and a model to determine the best private network to deploy considering the associated conditions. The influence of different scenarios on the various parameters is compared with other results from the literature.

The presented work is divided into five chapters. Chapter 1 includes an introduction to the study, a description of the topic, and the corresponding motivation and contents. Then, Chapter 2 addresses the fundamental concepts required for the model’s development, such as 5G architectures, 5G radio interface, network slicing and virtualisation concepts, cloud and edge networks, Ultra-Reliable Low Latency Communications (URLLC), enhanced Mobile Broadband (eMBB), massive Machine Type Communications (mMTC) services, and private networks. Finally, the State of the Art is provided with references and explanations of essential literacy for model and thesis development. The explanation and development of the model are covered in Chapter 3. The inputs, intermediate parameters and the respective calculations lead to the outputs used to elaborate the analysis presented in Chapter 4. The network architectures, the data rates, the latency contributions and the throughput calculation expressions are also detailed in Chapter 3. The assessment tests used to validate the model are depicted at the end. Chapter 4 presents and analyses the results. It begins by describing the simulated scenarios and then analyses the typo outputs for each simulation. Chapter 5 finalises the thesis, providing the main results from the work, conclusions from the various chapters, and recommendations for future implementations of 5G private network systems inside and outside the Portuguese Air Force context.

Chapter 2

Fundamental Concepts

This chapter provides an overview of the 5G system. Section 2.1 addresses the two primary network architectures for 5G, describes the Standalone (SA) architecture network functions, and introduces the radio interface characteristics. Section 2.2 is dedicated to the complementary concepts that enable the virtualisation of network functions and the network slicing implementation. Section 2.3 introduces the MEC concept and the characteristics of the cloud and edge network. Section 2.4 refers to the services and applications of 5G. Section 2.5 approaches the characteristics of a 5G private network. Finally, Section 2.6 concludes the chapter with a State of the Art on the thesis' subject.

2.1 5G Aspects

2.1.1 Network Architecture

The 3rd Generation Partnership Project (3GPP) introduces two architecture options for 5G: Non-Standalone (NSA) and SA, presented in Figure 2.1 [8].

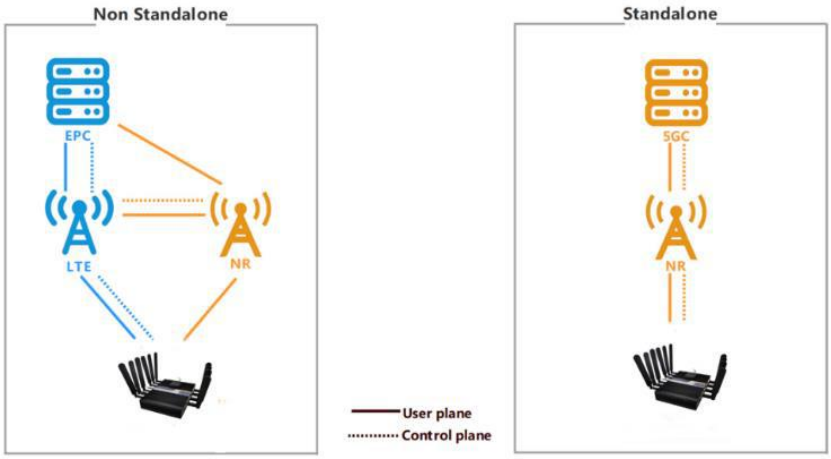

Figure 2.1 – NSA and SA versions (extracted from [9]).

In the NSA architecture, 5G infrastructure is built upon the existing 4th Generation of Mobile Communication Systems (4G). In Long-Term Evolution (LTE), the Evolved Node B (eNB) acts as the primary node, and the 5G Next Generation Node B (gNB), which is a 5G BS that supports 5G New Radio (NR), as the secondary node. Both are connected to the Evolved Packet Core [10]. On the other hand, the SA architecture consists of a 5G gNB and a 5G Core (5GC). Only 5G systems use the Radio Access Network (RAN) and the Core Network (CN). The User Equipment (UE) is linked to the New Generation RAN via gNBs.

The SA network architecture of 5G is presented in Figure 2.2. The corresponding network functions are described below [11]:

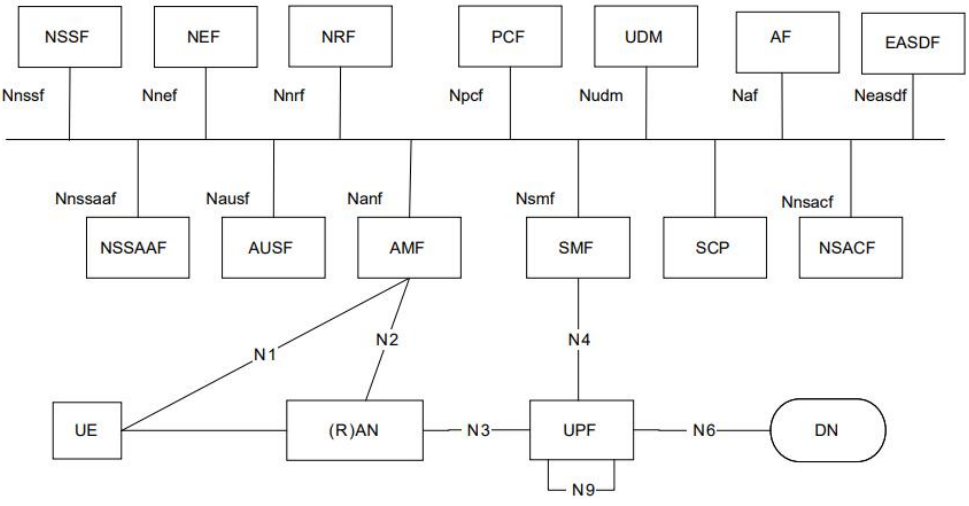

Figure 2.2 – The SA network architecture of 5G (extracted from [13]).

- The Network Slice Selection Function (NSSF) chooses a set of network slice instances to

accommodate a UE service request.

- The Network Exposure Function (NEF) provides an interface for external applications to communicate with the 5G network to obtain network-related information.
- The Network Repository Function (NRF) allows network functions to register their functionality and discover the services provided by other network functions. It gets discoverable by Access and Mobility Management Function (AMF) when UE tries to access a service type served by Session Management Function (SMF).
- The Policy Control Function (PCF) controls and manages policy rules, including QoS enforcement, charging and traffic routing rules.
- The Unified Data Management (UDM) oversees access authorisation and subscription management. UDM collaborates with the AMF and Authentication Server Function (AUSF). The AMF monitors UE authentication, authorisation, and mobility, while the AUSF stores data for UE authentication.
- The Application Function (AF) accesses the NEF to retrieve resources, interacts with the PCF for policy control and exposes services to end users.
- The Edge Application Server Discovery Function (EASDF) registers to NRF for discovery and selection, handles the Domain Name System (DNS) messages according to the instruction from the Session Management Function (SMF) and terminates the DNS security if used.
- The AUSF allows the AMF to authenticate the UE and access 5G CN services.
- The AMF performs operations like mobility, registration, and connection management. The AMF chooses the appropriate SMF for managing the user session based on the service requested by the UE. It indicates the end of the RAN interface connected by N2.
- The SMF establishes, modifies, and releases Protocol Data Unit (PDU) sessions between the UE and the data network.
- The Service Communication Proxy (SCP) helps Operators to efficiently secure and manage their 5G network by providing routing control, resiliency, and observability to the CN.
- The Network Slice Access Control Function (NSACF) provides the network slice access control for all AMFs by counting the number of registered UEs.
- UE is any device used directly by an end-user to communicate.
- The RAN provides access to a 5G CN and connects individual devices to other network parts through a radio link.
- The User Plane Function (UPF) performs operations like packet routing and forwarding, inspection, User Plane (UP) policy enforcement and QoS handling. It transports Internet Protocol (IP) data traffic between the UE and external networks. UPF supports the 5G architecture's Intra/Inter Radio Access Technology anchor point.
- Data Network (DN) allows UE to connect by a PDU session logically.

The functional components are organised into two groups: one implemented in the Control Plane (CP), which includes the functions AMF, SMF, PCF, UDM, AUSF, NEF, NRF and NSSF, and another implemented in the UP, which includes only the UPF [12].

2.1.2 Radio Interface

NR is an Orthogonal Frequency-Division Multiplexing (OFDM) radio interface resistant to frequency selective fading that makes better use of the currently available spectrum, i.e., Orthogonal Frequency-Division Multiple Access (OFDMA). NR operates in the 0.7 GHz to 60 GHz frequency range, enabling the use of a wide range of radio spectrum for various applications. OFDMA allows multiple users to use at the same time the cell's frequency resource [10].

Three categories define the NR spectrum: low bands (below 1 GHz), medium bands (from 1 GHz up to 6 GHz) and high bands (above 24 GHz). NR can be used in lower bands for applications that require a more extended range (e.g., massive IoT), ensuring coverage. Medium bands are used in applications that must support many devices (e.g., eMBB and mission-critical). High data rates and capacity characterise the use of high bands. However, in high-frequency bands, there is an increase in the Doppler Effect, resulting in higher Inter Carrier Interference (ICI) and lower data rates when the terminal moves [14].

The Frequency Range 1 (FR1) and Frequency Range 2 (FR2) terminology are used to distinguish cases that require a specific frequency range-dependent operation. The FR1 refers to an operation in bands below 6.0 GHz, whereas the FR2 refers to an operation between 24.25 GHz and 52.6 GHz. The latter has less coverage and is more sensitive to interference from objects like buildings and trees, but it provides better data rates and reduced latency compared with the FR1. The FR2 is intended for localised applications like high-speed links and indoor wireless networks. Waveforms from the OFDMA family are a good choice in FR1 and FR2 operations due to their high flexibility in multiple access and compatibility with Multiple-Input Multiple-Output (MIMO) [11].

Table 2.1 shows the frequency bands for 5G selected for use in Portugal and their corresponding duplex mode [15]. 5G equipment that uses 6.0 GHz is being developed and already has the support of several large markets. Currently, 3GPP band N104 covers the 6.0 GHz band, with a UL of 5 295 MHz and a downlink (DL) of 6 425 MHz and operates in the Time Division Duplexing (TDD) duplex mode.

Table 2.1 – 5G frequency bands used in Portugal (extracted from [16, 17]).

Band	Frequency [GHz]	UL [MHz]	DL [MHz]	Duplex Mode
N28	0.7	[758, 788]	[703, 733]	FDD
N78	3.6	[3 400, 3 800]	[3 400, 3 800]	TDD
N104	6.0	5 925	6 425	TDD

The frequency band of 0.7 GHz can cover tens of kilometres from a single BS in rural or less densely populated areas. Coverage may extend for several kilometres in urban areas with more obstacles and interference. Due to its limited availability and spectrum allocation, this frequency band cannot support significant data rates; however, it has excellent signal propagation. The medium band of 3.6 GHz offers the required capacity to handle many 5G devices. Despite having a shorter range than lower spectrum bands, it offers faster data rates, making it ideal for urban macrocells but with the potential to be more widespread. Lastly, the 6.0 GHz band can provide extremely high data rates. However, the mobile spectrum signal is minimal and more susceptible to attenuation than others, requiring a massive density

of BSs. In this way, the coverage radius is approximately a few hundred metres. Thus, the shadow fading values and the different large-scale path loss models lead to a noticeable difference in the cell range evaluation given to a certain cell-edge signal-to-noise ratio [18, 19].

A DL and UL symmetric use of Cyclic Prefix Orthogonal Frequency-Division Multiple Access (CPx-OFDMA) is an excellent choice to localise the waveform in time to achieve high capacity. The term Cyclic Prefix (CPx) associated with the OFDMA consists of a copy of the end part of the symbol added to the beginning, creating a guard interval, eliminating Inter Symbol Interference (ISI) and ICI. Therefore, different users can be separated for transmitting and receiving, typo themselves to use a particular frequency resource at a particular time, allowing the use of higher-order modulations [11, 20].

5G NR supports Frequency Division Duplexing (FDD) and TDD schemes. TDD is the primary duplexing mode for higher frequencies, where the UL and DL transmissions share a single frequency band at different time intervals. On the other hand, FDD is used for lower frequencies with two separate channels for UL and DL transmissions, reducing interference problems with large cells [21].

FDD is widely used, although it requires more spectrum than TDD. It includes unused spectrum for adequate channel separation and adheres to predetermined UL and DL network resource allocations. Therefore, TDD is more suitable for 5G network applications, particularly at high millimetre-wave bands. It improves spectrum management by allowing for asymmetric traffic and dynamic bandwidth allocation of high-band frequencies in dense 5G network deployments.

The ability to support multiple and scalable numerologies is one characteristic that distinguishes 5G communication systems. Radio requirements are thus defined for a subset of supported numerologies for each frequency band. Numerology is used to calculate the Sub Carrier Spacing (SCS), which is given by:

$$\Delta f_{subc[\mathrm{kHz}]} = 2^{\mu} f_{ref[\mathrm{kHz}]} \quad (1)$$

where:

- Δf_{subc} – SCS.
- μ – Numerology (integer number from 0 to 4).
- f_{ref} – Reference frequency of 15 kHz (subcarrier spacing when μ is 0).

To make TDD networks effective, 5G NR uses the 2^{μ} factor, ensuring that slots and symbols with various numerologies are aligned in time.

The numerology structures for 5G NR are illustrated in Table 2.2. The SCS ranges from 15 kHz to 240 kHz. The numerology is chosen based on the size of the cell and the frequency band. Large cells have a higher time dispersion at the receiver, so a larger CPx is required to compensate for the differences in performance. Since a wider subcarrier is less sensitive to phase noise, higher numerologies are used for higher frequencies [22]. Latency reductions in OFDM require reductions in the length of the OFDM symbols.

Table 2.2 – Frame structure characteristics associated with each numerology (extracted from [14, 23]).

Index	Δf [kHz]	Number of slots per frame (10 ms)	Number of slots per subframe (1 ms)	T_{slot} [ms]
0	15	10	1	1
1	30	20	2	0.5
2	60	40	4	0.25
3	120	80	8	0.125
4	240	120	16	0.0625

The DL and UL transmissions are organised into ten-millisecond frames, each having ten subframes of one millisecond. The regular slots have fourteen OFDM symbols with a normal CPx. Figure 2.3 illustrates the length of a slot in milliseconds, which is determined by the corresponding numerology, ranging from 1 ms when having an SCS of 15 kHz up to 0.0625 ms at 240 kHz [23].

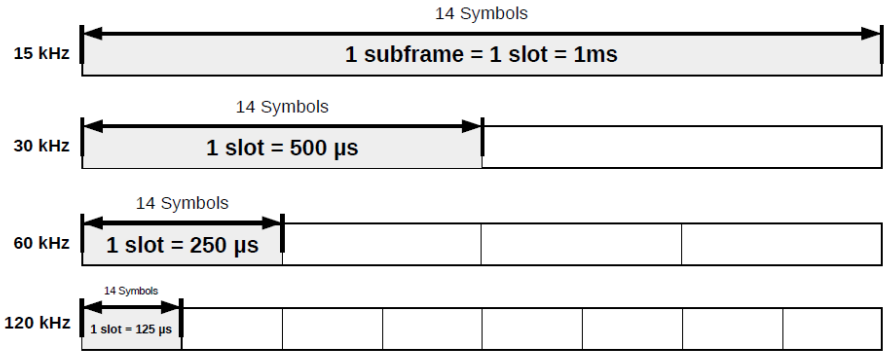

Figure 2.3 – 5G NR frame structure (extracted from [23]).

The slot is the primary transmission unit. On the other hand, it can be replaced by mini-slot-based transmissions to provide more agile and shorter units. The mini-slot can be of variable length and begin at any OFDMA symbol. The 3GPP standard specifies mini-slot sizes of 2, 4, or 7 symbols. One of the motivations for a mini-slot is to support URLLC traffic and fast transmission [24].

In NR, the Resource Block (RB) serves as the fundamental unit for managing the distribution of radio resources. The RB is assigned to users based on their QoS requirements and the network's available resources. An RB is a block of 12 subcarriers over which the transmissions are scheduled.

Besides the frame structure, Transmission Time Interval (TTI) is also a feature of 5G NR. This type of network is user-centric, and bandwidth parts can be employed to satisfy UE temporal requirements using dynamic lengths. TTI equals the symbol length times the number of symbols in time. Thus, a low number of symbols or short symbol lengths can reduce TTI for services that demand lower latencies. A more extended TTI increases spectral efficiency and performance. The TTI is typically set to 1 ms in 5G systems [23].

In practical use, there is a direct correlation between the subcarrier spacing, TTI, and the total number of subcarriers. Due to the short symbol duration, large subcarrier spacing is employed for low subcarrier frequencies, resulting in low latency and a lower TTI. Different TTIs enable flexible multiplexing of users

and services across the resources available, providing service-aware TTI multiplexing on the same frequency [23].

2.2 Network Slicing and Virtualisation

Software-Defined Networking (SDN) and Network Function Virtualisation (NFV) are complementary concepts that enable the virtualisation of network functions previously tied to hardware to run efficiently on cloud infrastructures.

SDN uses centralised control, enabling the network to manage and optimise its resources globally. On the other hand, NFV virtualises and packages network functions to decouple hardware and software. Therefore, a network function can be despatched as simple software to a service provider or network operator. Firewalls, data processing and IP address management are a subset of network services called Virtualised Network Functions (VNF). In typical physical facilities, each network service connects many VNFs [25].

The SDN standard layering architecture proposed by the Open Networking Foundation has three layers: infrastructure, control, and application. The application layer oversees maintaining the applications and software necessary to control the network. It supports various applications, including network monitoring, network setup and administration, and network automation. The control/orchestration layer links the infrastructure levels and applications and is also in charge of processing the application layers' instructions and passing them on to the networking components. The infrastructure layer comprises network devices and elements that regulate the network's forwarding and data-processing capabilities [14, 26].

SDN has four main advantages. Firstly, it provides high-performing granular network traffic control across multiple network Operators' devices. Network administrators can use network control to implement various Quality of Experience (QoE) and QoS policies at the application and network device levels. Secondly, network applications can benefit from centralised network intelligence to adapt to network conditions and provide a better user experience based on user needs. Thirdly, the network's flexibility increases because there is no need to configure individual devices for new capabilities and network services. Finally, network device autonomy improves network security and reliability.

The NFV infrastructure network transforms the network design, replacing physical equipment with network applications hosted on virtual machines [27]. The NFV architecture framework is mainly composed of four functional layers: Operations Support Systems (OSS)/ Business Support Systems (BSS), VNF, NFV Infrastructure (NFVI), and NFV Management and Orchestration (MANO). This flexible network function deployment enables network Operators to launch new network services more quickly on the same physical infrastructure. As a result, components may be created at any NFV-enabled device in the network, and their connections can be configured differently. Furthermore, dynamic scaling is essential for VNF performance based on current load and user requirements [28].

The increasing need for customisation, efficiency, flexibility, and improved performance in network infrastructure has led to the network slicing concept. Network slicing is based on dividing the physical

network into many independent virtual slices that supply various resources to different traffic types, modifying the network to satisfy the heterogeneous services that NR is expected to provide. It is implemented by integrating the two technologies mentioned above, SDN and NFV, which, when deployed together, advanced digital services [25].

Network slicing is impossible on NSA because it requires a 5GC to function correctly. The LTE is an anchor for smooth deployment due to the non-decoupling of UP and CP, which can maximise the QoS of served users but cannot perform resource allocation in slicing environments. As a result, UEs receive resources with the same priority value from the same traffic. This limitation stems from the fact that in LTE, resource allocation is accomplished by prioritising the service requested by UEs. This approach fails when it is considered that in 5G, different UEs may belong to different slices with different priorities. Therefore, such UEs should be managed by taking the priority of the slice they belong to into account and the priority of the service they require. As a result, UEs in 5G SA receive higher QoS than in LTE because different slices can meet the exact traffic requirement with different priority values [29].

2.3 C-RAN and MEC node

The 5G virtualisation concept introduces improved cloud and sophisticated edge computing to handle the increasing number of users and data traffic loads. The Cloud-RAN (C-RAN) is a radio-centralised architecture that uses cloud computing and real-time virtualisation technology to provide reliable services for next-generation wireless access networks. It provides recent data centre network technology, allowing for a high-reliability, low-latency, low-cost, and high-bandwidth interconnect network. It uses real-time virtualisation technology and open platforms based on cloud computing to support multi-technology environments and achieve dynamic shared resource allocation.

Added to this technology, MEC appeared to provide cloud computing capability, relocating the application's access to the cloud to the application's edge closer to mobile users [30]. Compared to traditional cloud computing, edge computing is a decentralised computational paradigm in which the network's edge can perform computationally intensive tasks.

The MEC functionality is supported only by 5G's SA architecture because 5G NSA architecture only allows for uniform service levels, preventing network slicing. C-RAN divides the node into the Remote Radio Head (RRH) and the Base Band Unit (BBU). The RRH is in charge of radio frequency transmission and is densified to increase network capacity and service quality in response to the application's ever-increasing demand. The transmitted and received RF signals are transmitted to the cloud via optical fibre (since it meets both the demanding latency and bandwidth requirements). The BBU is responsible for baseband signal and packet processing and is used to manage and control [31]. The link between RRH and BBUs is known as Fronthaul (FH), and data is sent through the enhanced Common Public Radio Interface (eCPRI). This protocol makes better use of bandwidth and is packet-based. Thus, it can be framed within Ethernet. It significantly benefits the FH network, enabling Ethernet connectivity instead of relying on fibre availability, depending on the functional split. The eCPRI interface is open, allowing Operators to mix and match vendor equipment. This communications network specification outlines the

main criteria for integrating transport, connection, and control communications. The general C-RAN architecture in Figure 2.4 points out the RRH, the BBU, and the FH and BH connections [32].

C-RAN architecture is used by Operators to address coverage and capacity issues, as well as network self-optimisation via software control and management via SDN. Implementing such an architecture improves network security and controllability [33].

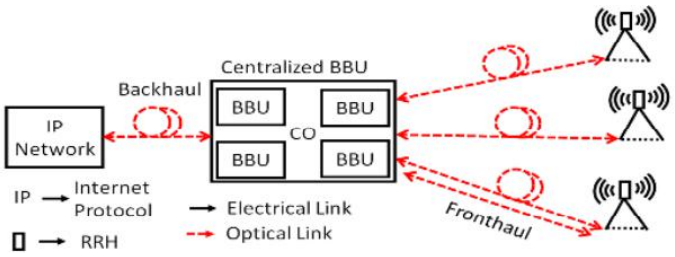

Figure 2.4 – C-RAN architecture (extracted from [32]).

Subsequently, the Open-Radio Access Network (O-RAN) architecture is being created to enable further growth of 3GPP RAN architecture in non-public networks, self-organised networks, and integrated access. O-RAN is based on C-RAN concepts and uses increasingly software-defined wireless communications and networking functionalities. It results from a distributed deployment into different functional entities closer to the edge. Instead of Operator-specific interfaces controlled by prominent industry participants, it defines an open architecture and interfaces allowing innovation at all tiers. Cellular network management is becoming more data-driven and defined by the interfaces for data collecting and general modules, dissemination, and processing.

In the O-RAN architecture, the functions from the 3GPP protocol stack will be split into several Centralised Unit (CU)/Distributed Unit (DU)/Radio Unit (RU) deployment options, including regional clouds or operator-specific locations. This implementation enables more functions to be executed locally in the DU closer to the user before being transferred to the CU, where processing capacity is more significant and can benefit from processing centralisation. Figure 2.5 illustrates the 5G NR O-RAN implementation. In this deployment, the RRH and BBU functions are split between the RU, DU, and CU nodes.

In parallel, the MEC node has been standardised to supplement cloud computing facilities by bringing computing resources closer to mobile users to achieve these requirements. The MEC node offers decentralised data, and the applications generate decentralised data, which is always more accessible to the users. Thus, mobile edge computing can be used in multiple locations, leading to low latency. The MEC architecture includes interconnected, layered, and deployable devices and systems. It combines the functional elements, providing a framework for dealing with dispersed environments, applications, and services [30].

There are three significant advantages of incorporating MEC into an existing cellular network. The first is offloading, in which the devices save energy by offloading time-consuming computing tasks. There is also decongestion, where processing is performed at a neighbouring BS instead of the central cloud, significantly reducing main network congestion and E2E delays. Finally, by extending computing resources to the network's edge, low latency allows packets to arrive faster, and there are fewer delays before the content flow begins. MEC networks are best suited for delay-sensitive applications, and lower latency translates into better QoE for users [35, 36].

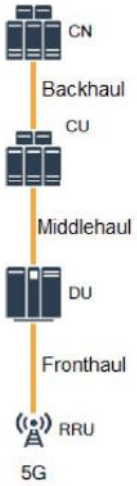

Figure 2.5 – 5G O-RAN implementation (adapted from [34]).

Edge computing provides users with various response services, particularly in intelligent manufacturing, automatic driving, and video monitoring. So even though edge computing is responsible for tasks within its scope, data processing is based on the local, and there is no need to upload to the cloud, ensuring data security by avoiding the risks brought by the network transmission process. Only local data is affected when the network is attacked [37]. However, it is difficult in MEC systems to identify, authenticate, and authorise devices and the data they create, maintaining at the same time low latency communications. Regarding associated costs, it does not require as much network bandwidth, so the load on the network bandwidth and the power consumption at the network's edge is reduced.

Through 5G and wired networks, the MEC node provides fixed-mobile coverage services. When C-RAN and MEC are deployed together, they represent a significant change for forwarding in the flexibility of the 5G framework. They improve service support and scalability by providing cloud computing at the edge and virtualisation.

2.4 Applications and Services

5G NR is being developed under the International Telecommunication Union (ITU) performance requirements. Table 2.3 illustrates the essential capabilities and indicative target numbers to provide initial high-level guidance for the more detailed International Mobile Telecommunications (IMT) 2020 requirements currently being developed. The importance of these specific capabilities varies depending on the use case or scenario, but all key capabilities are essential for most use cases.

Table 2.3 – Overview of technical performance requirements for IMT-2020 (extracted from [38]).

Parameter	Peak data rate [Gbit/s]	Peak Spectral Efficiency [bit/s/Hz]	User experience data rate [Mbit/s]	Area traffic capacity [Mbit/s/m^2]	UP latency [ms]	CP latency [ms]
Performance Requirement	10-20	10-30	50-100	10	1-4	20

With a diverse set of new use cases being one of the primary drivers for 5G, the ITU has defined three 5G use cases: eMBB, URLLC, and mMTC [10, 39]. The eMBB addresses human-centric data-driven use cases through massive MIMO and millimetre waves for multimedia content, services, and data access. The application scenario includes Virtual Reality (VR), mobile cloud computing, video monitoring, enhanced indoor and outdoor broadband, Augmented Reality (AR), and enterprise collaboration. In this way, it characterises systems with high capacity, coverage, and data rates.

The URLLC is used to support the delivery of critical communications and has stringent requirements for capabilities such as throughput, latency, and availability. Autonomous vehicles, remote patient monitoring, smart grids, telehealth, and industrial automation are a few examples.

Finally, the mMTC are distinguished by connected devices that transmit a low volume of non-delay sensitive data. The devices have long battery life. IoT, asset tracking, smart agriculture, smart cities, energy monitoring, smart home and remote monitoring are covered. NR supports UL and DL latencies in this use case and delivers error-free packets within low latency.

5G use cases can be classified into four classes: streaming, conversational, interactive and background [40, 41], inserted in Guaranteed Bit Rate (GBR) for real-time services or non-GBR (n-GBR) for non-real-time services, both characterised by Packet Error Rate (PER), Channel Quality Indicator (CQI), delay and priority parameters. Some standard use cases (critical and non-critical) are presented in Table 2.4.

Table 2.4 – NR class characteristics (extracted from [15]).

Class	**QCI**	**Priority**	**Delay [ms]**	**PER (10^{-n})**	**Service**
GBR	1	2	100	2	Voice (conversational)
	2	5	150	3	Video (streaming)
	4	4	300	6	Video (streaming live)
n-GBR	69	0.5	60	6	Mission Critical signalling
	70	5.5	200	6	Mission Critical data
	80	6.8	10	6	Low latency applications

The conversational class evaluates QoS tools such as telephony speech, voice-over-Internet protocol and video conferencing. Since the services are real-time conversation schemes, the required characteristics are provided by human perception. The latency must be low for the conversation to be possible to avoid an undesirable low-quality service.

Conversely, some transfer delay does not affect the streaming class. However, the E2E delay variation must be minimal to maintain the time relationship between audio and video. Since time-alignment applications correct minor variations at the receiving end of the stream, the maximum delay variation is

determined by the type of application that controls it. The preserved time relationship between the information entities is a real-time stream's fundamental property.

The interactive class is used when there is an interaction between the remote equipment and the user (machine or human). Such activities include server access, web browsing, and polling for measurement records. The end-request-response user's pattern distinguishes interactive traffic, being the request-response pattern and the preservation of payload content fundamental characteristics.

Lastly, the background class is used when a device sends and receives data files in the background, corresponding to a traditional data communication scheme in which the destination end-user does not expect data at a specific time. As a result, traffic is not time-sensitive and must be transferred transparently. Background fundamental characteristics include the destination not expecting data within a particular time frame and the preserved payload content [14, 34].

2.5 Private Networks

A 5G private network is a dedicated local area network that provides enhanced communication functionalities, unified connectivity, optimised services, and customised security within a particular area. Therefore, it is expected to provide agile solutions for effectively deploying and operating services with rigorous and diverse requirements [42].

5G private networks can be deployed as an SA or public network integrated mode, depending on the spectrum, infrastructure availability, network management, and access control level [43]. Figure 2.6 illustrates both types of 5G private network architectures. The SA 5G private network is deployed as an isolated and self-contained system that does not rely on a public 5G network and has its unique identifier and spectrum resources independent of the public network. It has a logical deployment of the E2E 5G system (radio access, transport, and CN domains).

The independent private network (SA mode) can be classified into two types:

- Independent private 5G Local Area Network (LAN) by the enterprise (totally private, local 5G frequency, no sharing): the enterprise deploys a private network (including UDM, 5GC CP, UPF, and 5G gNB) totally separated from the MNO's public network. The frequency is a local 5G frequency, not an MNO's licenced frequency. Enterprises keep the subscription and user information locally, controlling the network and data services.
- Independent private 5G LAN by the MNO (totally private, licensed frequency, no sharing): it has the same network design as the independent private 5G LAN by the enterprise. The main distinction is that it is created and operated by an MNO using its own licenced 5G frequency spectrum.

Although an SA 5G private network can function independently, some devices may occasionally require access to public network services. Therefore, a firewall connection between the private and public networks can be optionally established. Otherwise, the integrated private network is anchored on the 5G public network. Since public and private networks are not physically separated, compared to the SA deployment, this provides less customisation, self-control, and security. Due to its physical isolation, the

SA model allows for extensive customisation. Accurate self-control is theoretically possible but at a high cost [44].

The integrated private network can be classified into three types based on the degree of integration [42, 44].

- RAN and signalling sharing: the UDM, 5GC CP, and UPF are deployed, so network functions are handled locally. The spectrum and the 5G gNBs are shared across the public and private networks (RAN sharing). The MNO handles the network and the user control. Private network (private slice) and public network traffic are routed to the corresponding private UPF in the enterprise and UPF at the MNO's edge cloud, respectively.
- Network slicing (RAN and Core sharing): the UDM, CP, and UPF are installed on the MNO's edge cloud, and the 5G gNBs are deployed within the enterprise premises. Private and public networks share logically detached 5GC and RAN.
- RAN and CP sharing: dedicated UPF and 5G gNBs are incorporated inside the premises. UDM and 5GC CP are shared across public and private networks at MNO's edge cloud. The UDM, 5GC CP, and gNB are logically separated, whereas the UPF is physically isolated.

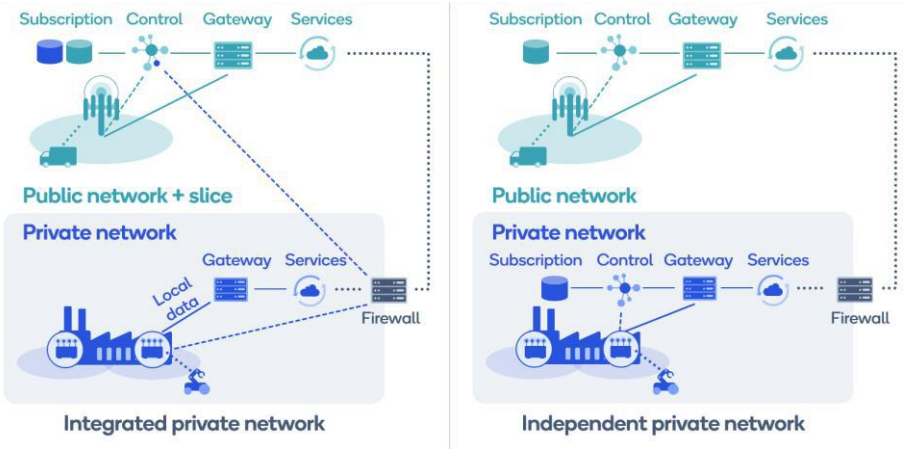

Figure 2.6 – 5G private network architecture (extracted from [43]).

The deployment of 5G private networks is contingent on spectrum availability, considering three options: the Licensed Spectrum, in which the MNO reserves a portion of its owned spectrum bands for private use. It allows minimal customisation for the Shared RAN and CP model but only for self-control. The Dedicated Private Spectrum, also known as Shared Spectrum, where the regulator provides a spectrum with high-performance certainty due to reduced interference, allowing 5G private networks to operate independently of public mobile network Operators. This spectrum option is being investigated in various global markets. The third option is the New Radio Unlicensed (NR-U) Spectrum, free of charge, currently allowing 5G private networks to expand rapidly. NR-U employs a Licence Assisted Access (LAA) approach, in which unlicensed spectrum access is only available when combined with licenced spectrum access. Carrier Aggregation and Dual Connectivity are the two modes of LAA. The licenced spectrum sends UL and CP signals in Carrier Aggregation mode, while the unlicensed spectrum manages the data plane DL, augmenting its capacity. Dual Connectivity mode allows data plane traffic in UL and DL to use unlicensed spectrum, while the CP uses licenced spectrum. NR-U supports both modes, with the

added benefit of an SA NR-U that operates in an unlicensed spectrum without requiring a licenced carrier. However, if not correctly managed, malicious jamming and external interference could cause service disruptions in some vertical industries. This specification permits mobile devices to access up to 400 MHz of unlicensed radio bandwidth in the DL and 100 MHz in the upload connection [45].

The requirements for a 5G private network must guarantee critical QoS parameters to avoid any degradation in the targeted use case. The private network needs the flexibility to include (and configure) add-on features to the 5G system to meet the customer's functional and performance requirements. Network control is also a requirement and represents the desire to retain certain network controls, such as configuration management of specific network functions and traffic flow policies. Data protection is also essential to ensure that unauthorised entities do not have access to sensitive data (e.g., operational data, subscriber data, and business-related data). As a result, security mechanisms (such as encryption and secondary authentication) are implemented, network functions are deployed on-premises, and redundancy is provided. Radio coverage in a specific geographical area is also required to ensure that radio signals are confined on-premises to avoid interference with public subscribers and to secure private communications further. It is critical to note that QoS is only guaranteed in areas where the enterprise requires coverage [4].

5G private networks are a relatively new technology on a global scale, with real-world deployments already underway. However, spectrum usage, cost, and a lack of knowledge can be limiting factors or challenges associated with the private deployment of 5G. Despite these challenges, 5G private networks are safe, fast and straightforward to manage, leading to the delivery of dependable voice and data services inside buildings or in remote locations. These networks can support various use cases from various industries [44].

2.6 State of the Art

According to [3, 46], 5G private networks for public safety and critical industrial applications are designed to assure service continuity even when unexpected and unwelcome events occur. This type of network deployment also ensures that critical civic functions and business operations communicate effectively, even when system elements fail due to external circumstances. As a result, 5G private network installations are increasing exponentially, leveraging network resources to generate secure, dependable, and scalable solutions. They are appropriate for all enterprises and traffic scenarios, even if the networks increase in complexity and volume. The installation can be done in private mode (i.e., on-premises) or hybrid mode (i.e., integrated public network) to regulate spectrum assets. Following [46], private networks must be robust, high-performing, and future-proof to enable business-critical and mission-critical activities. According to [3], spectrum ownership and management determine whether the deployment options are licenced, unlicensed, or shared. The QoS needs, and additional committed resources are analysed, leading to deployment locations strategically defined.

In [47], one of the essential characteristics of 5G private networks is the support of network slicing, which allows several virtual networks to be built within a single physical network. Each slice may be customised

with varied performance and security features, allowing organisations to customise the network to specific use cases and user groups.

According to [48], a military communications network is necessary to ensure the efficient and smooth conduct of military operations and is one of the key elements influencing combat capability. It must be fast, accurate, confidential and uninterruptible. However, it differs from a civil network, including the absence of dynamic changes in network topology, large-scale fixed infrastructure support, various propagation conditions and a complex electromagnetic environment. This type of network communications cannot rely on fixed infrastructure and be equipped with fixed BSs like the civil communication network. Therefore, this leads to different requirements for coverage area and multi-domain interconnection of land, sea, air and space. Unlike the civil network, which has a fixed CN plus an access one, the military communication network's topology changes dynamically. As a result, it must withstand high levels of electromagnetic interference while providing secure transmission with improved confidentiality and reliability to communicate in a combat environment characterised by changing terrain and severe weather.

Following [49], the key performance indicators of 5G are defined jointly by performance and efficiency requirements. In [48, 50], the military application, the reliability requirements of executing tasks, the priority of military tasks and the security requirements of military communication networks in a high-conflict environment are all considered. As a result, regarding [51], the performance indicators for 5G military applications are classified into eight categories: priority, delay, user rate, reliability, mobility, connection density, energy efficiency and security classification. The priority of 5G network slice scheduling resources can be determined based on the importance of military tasks, which can be dynamically adjusted based on the task process or environment. This parameter is associated with the E2E latency, requiring higher standards for the unmanned combat platform's remote-control service.

Regarding reliability, it can provide services for specific military tasks under specified conditions and functions. In the case of user rate, it is necessary to guarantee user speed (mobility) under actual load conditions associated with the highest mobile rate, supported under specific QoS and seamless transmission conditions. The connection density corresponds to the total number of online terminals supported per unit area. The terminal communicates with a specific Out of Service level, typically used in military material support scenarios involving massively distributed and interconnected sensors. In the case of security classification, it refers to a military application's level of security, where services in a physical network are logically isolated based on their security level. Lastly, energy efficiency corresponds to the amount of data received and sent per unit of energy consumed on both the network and terminal sides. It is primarily for the IoT, such as landing operations and offshore far from command posts [51].

[52] defends that a 5G military network must be built to provide a differentiated and customised network to improve military efficiency and meet the requirements of diverse military application scenarios. That is to create an exclusive, secure, low-cost and customised network. According to [48], four schemes are applied to 5G private military networks: a 5G military private network with an E2E public network, a 5G military private network completely isolated from the public network, a 5G military private network

sharing the CP with a public network and with isolated UP, and a 5G military private network sharing with a public network but deploying edge computing.

According to [51], the private military network is associated with high security. Thus, a private network sharing with a public network but with an edge computing scheme is the closest to the desired requirements for military communications [48]. In this deployment scenario, the MEC node is installed at the private network's edge, providing data forwarding paths between the wireless access network and the CN and implementing local data flow unloading. The MEC data determines the destination IP address of BS packet data. If the IP data packet is local, it is routed to the internal private network. As a result, private and public network traffic can be separated to ensure the security of private network data. The cost of this deployment is significantly reduced because the UP is not deployed in the private network. Under certain security guarantees, daily communication on the public and private communication on the private networks can be realised [48].

The scheme described in [51] applies to logistics support scenarios, such as intelligent military infrastructures. Unclassified information, such as short messages and daily calls, can be transmitted on the public network.

According to [50], one of the main applications of 5G private networks in the Air Force is enhanced Intelligence, Surveillance and Reconnaissance (ISR) Grid and drone development. These types of applications are introduced in the concept of Non-Terrestrial Networks (NTN). 5G NTNs extend the reach of 5G NR technology and its benefits to non-terrestrial platforms. Without any intermediate protocol or technology conversion, an airborne 5G NR architecture should enable MNOs to provide 5G-based services in locations where terrestrial networks are unavailable. Aircraft and low-Earth orbit satellites are the most promising vehicles due to their shorter propagation delay. This way, 5G NTNs may open up new tactical application possibilities.

Following [48, 52], the 5G NTN architecture specification is not a top priority in 5G standardisation and is still far off. It may provide application services to a naturally underserved joint operations area (regarding supporting communications infrastructure) via airborne or satellite-based 5G systems and opportunities to extend tactical communications. For example, aircraft-based 5G NTN systems could illuminate a tactical joint operations area. Other applications (e.g., force tracking and intelligence) and broadband communications could be provided to mobile troops on the ground while connecting to distant parent tactical Head Quarters [52].

Chapter 3

Model and Simulator Description

This chapter concerns the description, proposal, implementation, and assessment of the model for analysing the parameters selected to determine the most adequate 5G type of private network. The first section describes the theoretical model's objectives and assumptions. Subsequently, the implementation of the developed model is explained, with two detailed flowcharts showing the approach taken in the simulation. The chapter culminates with an assessment of the model's results through comparison with data collected from previously implemented systems and literature.

3.1 Model Overview

The thesis aims at developing a model capable of analysing the feasibility of implementing 5G private networks in the Portuguese Air Force infrastructures. The model is intended to adapt to the network's characteristics and the users' profile, with service differentiation concerning the performance parameters assigned to the network requirements. The User's Manual is in Annex A. Figure 3.1 presents an overview of the model, including the input and output parameters.

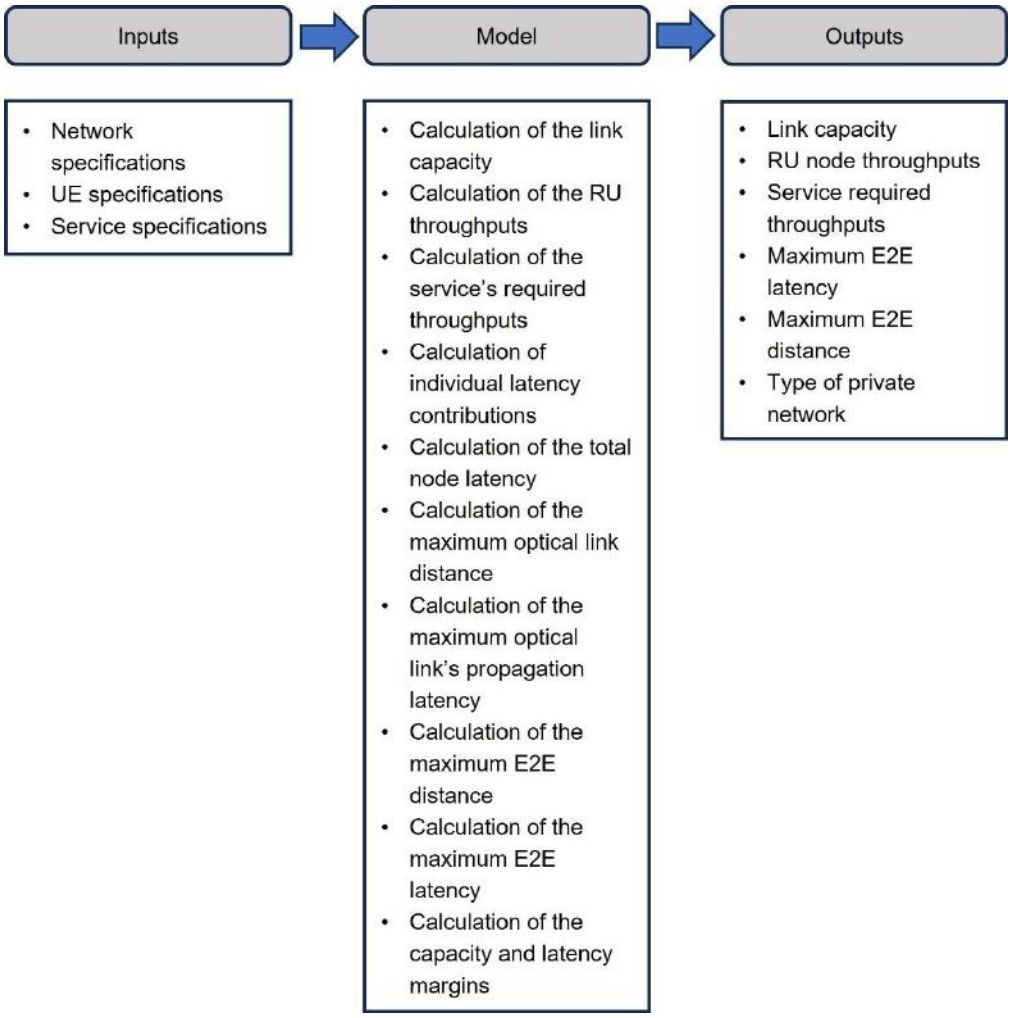

Figure 3.1 – Model overview.

The thesis considers the model approach of [14] to calculate the outputs corresponding to the initial latency contributions, total node latency, 5G node throughputs, and the services required throughputs applied to the three Portuguese Air Force scenarios. The scenarios involve an Airbase, a Wide Area Multilateration (WAM) System and a UAV Remote-Control Squadron. The Airbase is a restricted area with indoor and outdoor UEs. The WAM System has GSs distributed over a wide area, with air and ground UEs, and the Squadron's primary focus are the UAVs, the UEs to be analysed. The detailed characterisation of each scenario is presented in Section 4.1.

The model inputs are grouped in parameters associated with the network, the UEs and the services. These parameters are saved into variables and used to calculate the outputs. Network specifications

are referent to all the variables related to the network required to calculate the total node latency. These variables are associated with the scenario environment and are introduced by the programme user. Some parameters are explicitly associated with the RU node, influencing the calculated throughputs. Therefore, these specifications are divided into three main groups: the general parameters, the network structure parameters related to the service, and the RU node specification parameters.

The general network structure specifications, presented in Table 3.1, are introduced based on the architecture and network characteristics. The FH, MH, BH and Transport links are fixed parameters.

Table 3.1 – General network structure parameters.

Network Architecture	The network architecture.
MEC Specification	The MEC node deployment option.
FH Link	The FH splitting option.
MH Link	The MH splitting option to determine the MH link capacity.
BH Link	The BH link capacity.
Transport Link	The TL capacity.

The network parameters associated with the service are presented in Table 3.2. The initial link type, which can be UL, DL or both, influences the RU node throughputs because it dictates the Overhead ratio used in the communication. Each latency adaptation parameter, presented in Annex B, varies between 0 and 1, indicating the service performance's responsiveness to the latency variation introduced by the network structure. Therefore, a low value indicates that the service is more sensitive to latency changes. In contrast, a high value means that significant variations are required to trigger corrective actions or adjustments in the performance of the service.

Table 3.2 – Network parameters associated with the service.

Initial Link Type	The initial link type for each service (UL, DL or both).
Packet Size	The packet size of the service.
Latency Adaptation Parameter	The responsiveness of the service to latency variations in the network structure.
Priority	The priority of the service.

The RU node parameters, presented in Tables 3.3 and 3.4, are used to calculate the RU node throughputs. In this group, only the CQI value is a variable factor; the remaining are selected to achieve the throughputs that reflect the closest performance in a real-world scenario of each service.

Table 3.3 – RU node specification parameters.

MIMO Layers	The number of MIMO layers.
Numerology Parameter	The numerology parameter to determine the RU throughputs.
Bandwidth	The radio node bandwidth that defines the number of RBs.
CQI Value	The CQI determines the R_{max} and the modulation order.
DL Scaling Factor	The parameter that scales the RU throughput.

Table 3.4 – (contd.) – RU node specification parameters.

Frame Structure	The DL percentage frame.
Average Factor	The factor that accounts for the throughput losses.

The UE specifications in Table 3.5 correspond to the inputs associated with the network usage profile. The parameters account for the service selected, the number of users connected to each node and their percentage associated with each service type (service mix). These parameters are used to calculate the service-required throughputs. The distances between the users and the RU node are also defined.

Table 3.5 – UE specifications.

Distance	The distance between the UEs and the connected RU node.
Service	The service selected to be analysed.
Number of Users	The number of users connected to each node.
RU Service Mix	The percentage of total UEs that are using a service.
DU Service Mix	The percentage of total UEs connected to the DU node that are using a specific service. It covers all the RU nodes that are connected.
CU Service Mix	The percentage of total UEs connected to the CU node that are using a specific service. It covers all the DU nodes that are connected.

Table 3.6 presents the service specification parameters corresponding to each service required E2E latency and data rate requirements. The list of all service requirements is presented in Annex C.

Table 3.6 – Service specifications.

Required E2E latency	The required E2E latency of the services.
Data rate	The data rate of the services.

The outputs are separated into two groups: the latencies, throughputs and capacities outputs and the type of private network output, resulting from the margins values applied to the RU node throughputs and the E2E latency required in each system scenario. The outputs are presented in Tables 3.7 and 3.8.

Table 3.7 – Model outputs.

Total Node Latency	The sum of the queuing, transmission and processing latencies. It cannot exceed the maximum E2E latency.
Link Capacity	It is used to dimension the network parameters to achieve lower latencies. It also dictates the processing capacity of the nodes.
RU Node Throughputs	The data rates provided by the RU node.
Maximum E2E Distance	It estimates the maximum link lengths to achieve the required latency.

Table 3.8 – (contd.) – Model outputs.

Maximum E2E Latency	Results from the sum of all latency contributions depending on the network structure.
Type of Private Network	Define the best type of network after calculating the latency and throughputs based on the margins applied.

3.2 Model Development

3.2.1 Architecture Options

The 5G link network generally consists of an FH, an MH, and a BH. However, the architecture can be deployed differently, leading to different latency contributions from the possible connections. The RU, DU, and CU nodes can be collocated in various configurations, and the latency impact varies depending on the approach used. Therefore, understanding how MEC nodes can be added and placed in these different architecture structures is crucial to decreasing the latency contributions that impact E2E communications.

The 3GPP defines four network deployment scenarios for 5G O-RAN [14, 34]:

- Independent RU, DU, and CU nodes deployment, in which the FH, MH, and BH links are present in the network. This approach contributes to propagation latency because it considers all links. In this case, the distance between RU and DU can reach 10 km, whereas the distance between DU and CU can range from 20 km to 40 km.
- Collocated DU and CU nodes and independent RU node deployment, where the MH link is absent from the architecture.
- Collocated RU and DU and independent CU deployment, with no FH link. In this type of architecture, the latency can reach a minimum value if the MEC node is installed between the RU and the DU.
- Collocated RU, DU and CU deployment. In this case, all network nodes are part of a single one.

The O-RAN architecture has the characteristic of distributing baseband processing among logical nodes to reduce the CN transmission and processing delay. 3GPP specifies several options for functional splits between nodes. A functional split determines how many functions are left locally at the BS site and how many are centralised at a high-processing-power CN. Each split defines how the logical nodes interact with one another and the exact number of operations each performs. Figure 3.2 represents the optional splitting points.

The splitting options correspond to the division of functions and process tasks between network elements. These are based on the type of functionalities and respective throughput applied to each node, i.e., on the FH link, the most common splitting options applied are the Splitting Option 6, 7.1, 7.2, or 7.3, and in the MH link, the Splitting Option 2 [14, 34], to optimise different aspects of network performance, such as latency, bandwidth efficiency and flexibility. Splitting Options 7.1, 7.2 and 7.3 are variants of Splitting Option 7 and can be used independently in the UL and DL.

Splitting Option 1 sets the highest demands on the FH link with high data rates and severe latency constraints. It is used in scenarios where fibre is economically feasible, such as in urban areas or where Operators have access to it. Conversely, Splitting Option 8 introduces all baseband processing into the RU node, making it more complex than Splitting Option 1. However, because the complete protocol stack resides in the RU node, the FH network requirements of Splitting Option 8 are substantially simpler. As a result, additional processing is required before data can be sent between the RU and DU nodes, resulting in substantially lower bit rates and larger latency tolerances on the FH network. The higher the split level, being Splitting Option 8 the highest level, the lower the demands on the FH link [53].

The 5G architecture currently supports Splitting Option 7.2 for networks with high capacity and reliability requirements [14]. The Operators selected this option because it leads to a relatively simple RU node with size and power consumption that supports network densification, facilitating the developing neutral host market. Thus, in this thesis, this splitting option is studied for all cases (critical and non-critical) to optimise its implementation. In the development analysis, the type and knowledge of each split function are irrelevant to the study, just that the number varies according to the type of splitting option chosen.

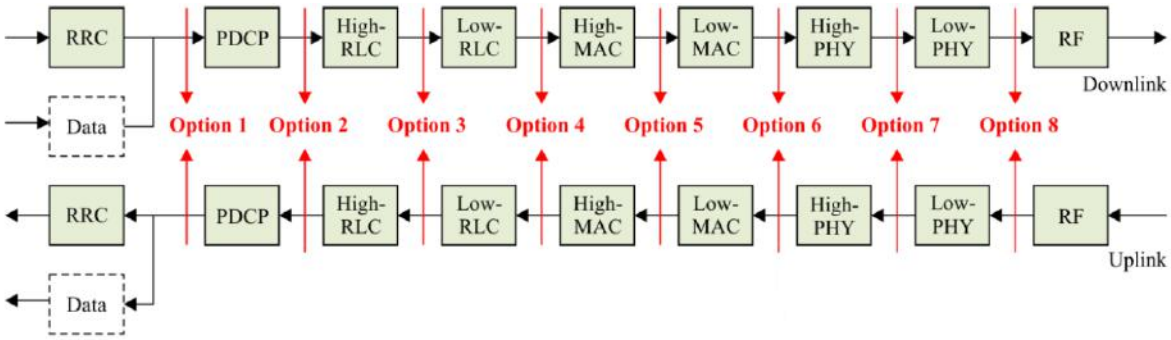

Figure 3.2 – 3GPP optional splitting points (adapted from [53]).

In the military context, where services often require very low latency and are mostly considered critical, the type of architecture can have significant implications for the effectiveness and reliability of the communication systems. Each architecture option has advantages and disadvantages aligned with the military organisation's specific operational and mission objectives.

Therefore, the independent RU, DU and CU nodes deployment is the most adequate option for analysing latency and coverage of a network, especially when these factors are critical considerations. Each component operates separately, making it easier to measure latency introduced at different stages of the communication process. Thus, each component can be analysed individually, providing insights into where latency may be introduced or where improvements are required, which is crucial for optimising applications. Regarding the coverage assessment, the independent deployment allows for precise coverage analysis. By varying the positioning and configuration of the RUs, DUs and CUs nodes, it is possible to assess coverage in different areas, enabling network planners to optimize it for specific mission requirements.

Therefore, by independently analysing latency and coverage, military organisations can make data-driven decisions on network optimisations and infrastructure investments. Thus, this deployment is close

to real-world network deployment, where the RU, DU and CU nodes often operate independently, leading to results that highly represent actual network performance [53]. Since all network contributions are considered, this thesis uses the independent RU, DU and CU architecture in the scenarios simulation.

The MEC node is also part of the network architecture and can be deployed in various locations along network links. A MEC node deployment scenario to decrease CN transmission and processing delay is required to apply in low-latency communications. Instead of travelling to the CN, which might be hundreds of kilometres distant, the information is directed to the nearest MEC node to be processed and to fulfil the reduced latency requirement of numerous 5G applications.

The three possible MEC node deployment options for 5G are presented in Figure 3.3. Installing the MEC node between the RU and the DU (Option RU-DU) is the most effective approach in reducing latency and optimising the FH capacity. However, ensuring this deployment is not always possible because the MEC node may be connected to a specific RU node in a network architecture and to a DU or CU node in another. Similarly, installing the MEC node between the DU and the CU (Option DU-CU) presents a viable alternative because the MH link often has long lengths (20 km to 40 km), and the MEC technology may be deployed near the DU, lowering the propagation delay associated with this deployment. Finally, installing the MEC node between the CU and the Core (Option CU-Core) reduces the CN's processing delay and the contribution of the BH link length in propagation latency. However, it is not optimal because there are still three nodes between the UE and the MEC node, and the CU is a point of traffic aggregation because many DUs are connected to it. The 5G architecture can also deploy the MEC node between a collocated RU-DU, a collocated DU-CU, or collocated RU-DU-CU nodes. This thesis does not consider collocated options for the reasons given above.

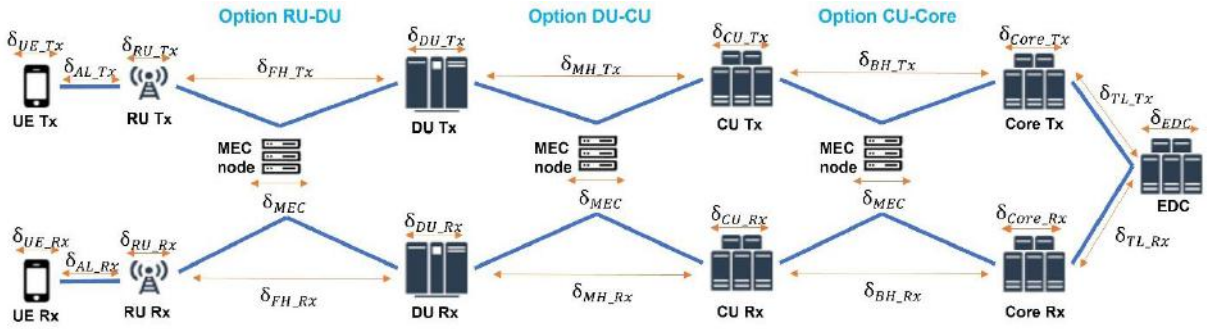

Figure 3.3 – MEC node installation options for 5G architecture (adapted from [14]).

3.2.2 Latency Contributions

The transmission, propagation, queuing, and processing are the primary E2E latency contributions. These contributions are converted into the following several mathematical expressions that lead to the developed model [14, 54]:

$$\delta_{UE\_Tx_{[\mathrm{ms}]}} = \delta_{UE\_Proc_{[\mathrm{ms}]}} + \delta_{UE\_Trans_{[\mathrm{ms}]}} \tag{3.1}$$

$$\delta_{UE\_Rx_{[\mathrm{ms}]}} = \delta_{UE\_Proc_{[\mathrm{ms}]}} \tag{3.2}$$

$$\delta_{RU\_Tx_{[\mathrm{ms}]}} = \delta_{RU\_Rx_{[\mathrm{ms}]}} = \delta_{RU\_Proc_{[\mathrm{ms}]}} + \delta_{RU\_Queu_{[\mathrm{ms}]}} + \delta_{RU\_Trans_{[\mathrm{ms}]}} \tag{3.3}$$

$$\delta_{DU\_Tx_{[\mathrm{ms}]}} = \delta_{DU\_Rx_{[\mathrm{ms}]}} = \delta_{DU\_Proc_{[\mathrm{ms}]}} + \delta_{DU\_Queu_{[\mathrm{ms}]}} + \delta_{DU\_Trans_{[\mathrm{ms}]}} \tag{3.4}$$

$$\delta_{CU\_Tx_{[\mathrm{ms}]}} = \delta_{CU\_Rx_{[\mathrm{ms}]}} = \delta_{CU\_Proc_{[\mathrm{ms}]}} + \delta_{CU\_Queu_{[\mathrm{ms}]}} + \delta_{CU\_Trans_{[\mathrm{ms}]}} \tag{3.5}$$

$$\delta_{Core\_Tx_{[\mathrm{ms}]}} = \delta_{Core\_Rx_{[\mathrm{ms}]}} = \delta_{Core\_Proc_{[\mathrm{ms}]}} + \delta_{Core\_Trans_{[\mathrm{ms}]}} \tag{3.6}$$

$$\delta_{EDC_{[\mathrm{ms}]}} = \delta_{EDC\_Proc_{[\mathrm{ms}]}} + \delta_{EDC\_Trans_{[\mathrm{ms}]}} \tag{3.7}$$

$$\delta_{MEC_{[\mathrm{ms}]}} = \delta_{MEC\_Proc_{[\mathrm{ms}]}} + \delta_{MEC\_Trans_{[\mathrm{ms}]}} \tag{3.8}$$

where:

- $\delta_{UE/RU/DU/CU/Core\_Tx}$ – Latency on the transmitter side.
- $\delta_{UE/RU/DU/CU/Core\_Rx}$ – Latency on the receiver side.
- $\delta_{UE/RU/DU/CU/Core/EDC/MEC\_Proc}$ – Processing latency.
- $\delta_{UE/RU/DU/CU/Core/EDC/MEC\_Trans}$ – Transmission latency.
- $\delta_{RU/DU/CU\_Queu}$ – Queuing latency.
- δ_{EDC} – Latency of the EDC node.
- δ_{MEC} – Latency of the MEC node

In a packet-switched network, transmission latency corresponds to the time delay between the initiation of a data transfer and the actual reception at the destination. Thus, the latency-associated results from the link's data rate do not depend on the distance between the two nodes. This delay is proportional to the packet's size, and the expression is given by [55]:

$$\delta_{Trans_{[\mathrm{ms}]}} = \frac{8D_{[\mathrm{Bytes}]}}{R_{[\mathrm{Gbits/s}]}} \times 10^{-6} \tag{3.9}$$

where:

- δ_{Trans} – Transmission latency.
- D – Packet size.
- R – Data rate provided by the link.

Propagation latency is the time it takes for the signal to travel through the link. Contrary to the later latency, this one is primarily determined by the velocity of the signal in the link and the distance between the signal's origin and destination. The implementation of each link can be done within an optical link or a radio link, with a signal velocity of 2.14×10^8 m/s and 3×10^8 m/s, respectively. The thesis considers that the FH, MH and BH links are implemented each one within an optical link. The expression used to calculate this latency contribution is given by [55]:

$$\delta_{Prop_{[\mathrm{ms}]}} = \frac{d_{[\mathrm{m}]}}{v_{[\mathrm{km/s}]}} \tag{3.10}$$

where:

- δ_{Prop} – Propagation latency.
- d – Distance between the origin and destination of the signal.
- v – Velocity of the signal on the link.

Processing latency is the time a node takes to process a data packet. This latency includes time for error checking, scanning the packet header, and searching for the link to the next node, depending on the destination address. Thus, it depends on the functions assigned to the node. The node processing latency is generally minimal, but it is crucial to evaluate the E2E latency of critical services. The delay values are usually fixed and determined by the UE and gNB capacities. The processing latency of the External Data Centre (EDC) or between the CN and the EDC is not considered.

The model calculates each node's processing latency by analysing the number and type of assigned radio functionalities. In the UE, the processing delay is related to the TTI, corresponding to the time one packet takes to be transmitted to the air interface since the process is done at the packet level and not in a specific time frame. In this approach, each TTI corresponds to 14 OFDM symbols. Therefore, increasing the data rate at the packet level (more bits to accommodate) makes packet processing slower. The processing latency at the UE depends on the respective transmission latency and the processing delay ratio, which is related to the SCS. The SCS channel size has a significant influence on URLLC outage latency. According to [14], the most indicated SCS to use at 5G communications associated with UE processing latency ratio is presented in Table 3.9.

Table 3.9 – 5G UE processing latency ratio (adapted from [14]).

SCS [kHz]	30
$\boldsymbol{\rho_{UE}}$	$\frac{2}{14}$

The processing latency in the UE is given by (3.11). It is used (3.9) to determine the transmission latency in the UE, corresponding usually to 1 ms.

$$\delta_{UE\_Proc_{[\mathrm{ms}]}} = \delta_{UE\_Trans_{[\mathrm{ms}]}} \ \rho_{UE} \tag{3.11}$$

where:

- δ_{UE_Proc} – UE node processing latency.
- ρ_{UE} – Latency processing ratio of the UE.
- δ_{UE_Trans} – UE transmission latency.

According to [34], the network architecture does not affect the processing latency because the nodes processing packets have the same functions when the same functional split is selected. A functional split assigns to different nodes different processing capabilities, resulting in a variety of processing latency accumulation along the network. In the case of the remaining nodes (RU, DU, CU and Core), it is necessary to consider an adaptation parameter to determine the processing latency.

The processing latency of the RU, DU, and CU nodes is directly proportional to the transmission latency at the UE, the ratio of functionalities associated with the respective node, and a parameter that adapts the processing resources. Table 3.10 presents the required processing ratios to calculate the processing delays of the nodes. The ratios are assigned according to the distribution of functionalities between the RU and CU nodes. The Splitting Option 7.2 corresponds to a transition option, has eleven processes between the RU and DU nodes, and the CU node always keeps two functionalities (RRC (Radio Resource Control) and PDCP (Packet Data Convergence Protocol)).

The RU node processing latency is given by:

$$\delta_{RU\_Proc_{[\mathrm{ms}]}} = \delta_{UE\_Trans_{[\mathrm{ms}]}} \ \rho_{RU} \ \rho_{lat} \tag{3.12}$$

where:

- δ_{RU_Proc} – RU node processing latency.
- ρ_{RU} – Ratio of functionalities assigned to the RU node.
- ρ_{lat} – Latency adaptation parameter.

Table 3.10 – RU, DU and CU processing latency ratios for Splitting Option 7.2 (adapted from [14]).

$\boldsymbol{\rho_{RU}}$	$\frac{19}{11}$
$\boldsymbol{\rho_{DU}}$	$\frac{58}{11}$
$\boldsymbol{\rho_{CU}}$	2

The DU node processing latency is given by:

$$\delta_{DU\_Proc_{[\mathrm{ms}]}} = \delta_{UE\_Trans_{[\mathrm{ms}]}} \ \rho_{DU} \ \rho_{lat} \tag{3.13}$$

where:

- δ_{DU_Proc} – DU node processing latency.
- ρ_{DU} – Ratio of functionalities assigned to the DU node.

The CU node processing latency is given by:

$$\delta_{CU\_Proc_{[\mathrm{ms}]}} = \delta_{UE\_Trans_{[\mathrm{ms}]}} \rho_{CU} \ \rho_{lat} \tag{3.14}$$

where:

- δ_{CU_Proc} – CU node processing latency.
- ρ_{CU} – Ratio of functionalities assigned to the CU node.

The CN processing latency depends on the network load and the number of intermediate switching process nodes. Fixed values are typically used in the latency introduced by the transport network and CN. According to [56], the one-way CN processing latency is 200 µs for NSA networks and 100 µs for SA networks, respectively, while the delay induced in the link between the CN and the application server is 5.4 µs. It is used the expression from [14] to determine the CN processing latency:

$$\delta_{Core\_Proc\ [\mathrm{ms}]} = \frac{4}{2385} D_{[\mathrm{Bytes}]} + \frac{469}{477} \quad (3.15)$$

where:

- δ_{Core_Proc} – CN processing latency.

Regarding the latency associated with the MEC node and the EDC, it is necessary to consider that processing latency increases linearly with the decrease of the processor frequency. The processing frequency for the EDC is approximately 3 GHz, and for the MEC node, 1 GHz. Therefore, the approach in [14] relates the latency generated in the MEC node to approximately one-third of the EDC's latency.

The expression to determine the MEC node processing latency (assuming the processing of a single functionality) is given by:

$$\delta_{MEC\_Proc_{[\mathrm{ms}]}} = 4 \times 10^{-5} D_{[\mathrm{Bytes}]}\ \rho_{func} \quad (3.16)$$

where:

- δ_{MEC_Proc} – MEC node processing latency.
- ρ_{func} – Number of functionalities executed by the MEC node.

The expression to determine the EDC processing latency is given by:

$$\delta_{EDC\_Proc_{[\mathrm{ms}]}} = 1.33 \times 10^{-5} D_{[\mathrm{Bytes}]} \quad (3.17)$$

where:

- δ_{EDC_Proc} – EDC node processing latency.

Queuing latency is the time a packet or data unit waits in a queue before it can be transferred or processed. It happens in networks when data packets must wait in a buffer before being transferred. This delay can significantly influence network performance by increasing latency, decreasing throughput, and even causing packet loss. The size of the buffer, the rate of incoming traffic, and the processing capability of the network devices are all elements that might contribute to queueing delay. In general, larger buffers can help minimise queueing latency by allowing packets to wait before being forwarded. Excessive buffer size, on the other hand, might result in increased delay and jitter. Therefore, implementing QoS systems that prioritise some types of traffic over others is one technique to eliminate queueing delays. Real-time traffic, such as audio and video, may be prioritised over non-real-time traffic, such as email and file transfers. Even when the network is congested, this can assist in guaranteeing that critical traffic is transmitted with minor delay. In this model, the Core's processing capacity is adjusted to network congestion, and the queuing delay is only considered in the RU, DU, and CU nodes. The queuing delay in a specific node is calculated by accounting for packets that arrive in the node and belong to a service with the same or higher priority than the considered reference user service. In this model, the simulated traffic determines the queuing delay for the scenarios based on the number of users connected to a network node at a given moment. The DU and CU traffic indicate the aggregation of primary network nodes, e.g., the CU nodes' traffic represents traffic from numerous aggregated DU nodes.

The queuing delay is calculated using the following expression:

$$\delta_{Queu_{[\mathrm{ms}]}} = 10^3 \sum_{p=1}^{M_{p,serv}} \frac{8D_{serv,p[\mathrm{Bytes}]}}{R_{\max\,[\mathrm{bps}]}} \tag{3.18}$$

where:

- δ_{Queu} – Queuing latency.
- $D_{serv,p}$ – Packet size for a specific service with priority *p*.
- $R_{\max}$ – Maximum capacity offered by the link.
- $M_{p,serv}$ – Number of users connected to the node and utilising services with a higher or equal priority than the examined service.

3.2.3 Network Structure Contributions

The approach used in [14] divides the E2E latency computation into multiple segments. The division consists of separating the node latency contributions from the propagation ones. In this model, the propagation latency contribution of the optical links is assumed to be 0 ms in the expression (3.24) to compute the maximum E2E latency. Given this, the margin between the required E2E latency, and the remaining latency contributions (total node latency plus the ALs propagation latencies) is calculated to determine the network's maximum optical link length, which can be deduced from the expression (3.26).

The MEC node deployment is studied according to the options presented in Section 3.2.1. In order to achieve the E2E latency requirements associated with the respective services, all options are analysed, including the network architecture without the MEC node. This technology has a significant advantage in allowing data packets to be transmitted to another UE in the network to update information. Therefore, the data packet does not have to return to the same UE that started the connection, significantly reducing the E2E latency.

The total node latency for the 5G architecture without an MEC node deployment is computed using the following expression:

$$\begin{aligned}\delta_{Total\_node_{[\mathrm{ms}]}} = {} & \delta_{UE\_Tx_{[\mathrm{ms}]}} + \delta_{RU\_Tx_{[\mathrm{ms}]}} + \delta_{DU\_Tx_{[\mathrm{ms}]}} + \delta_{CU\_Tx_{[\mathrm{ms}]}} + \delta_{Core\_Tx_{[\mathrm{ms}]}} + \delta_{EDC_{[\mathrm{ms}]}} \\ & + \delta_{Core\_Rx_{[\mathrm{ms}]}} + \delta_{CU\_Rx_{[\mathrm{ms}]}} + \delta_{DU\_Rx_{[\mathrm{ms}]}} + \delta_{RU\_Rx_{[\mathrm{ms}]}} + \delta_{UE\_Rx_{[\mathrm{ms}]}}\end{aligned} \tag{3.19}$$

where:

- δ_{Total_node} – Total node latency.

According to the architectures that consider the installation of an MEC node, the first consists of deploying the MEC node between the CU and Core nodes, the second between the DU and CU nodes and the third between the DU and RU nodes. The total node latencies are given by (3.20), (3.21) and (3.22), respectively.

$$\begin{aligned}\delta_{Total\_node_{[\mathrm{ms}]}} = {} & \delta_{UE\_Tx_{[\mathrm{ms}]}} + \delta_{RU\_Tx_{[\mathrm{ms}]}} + \delta_{DU\_Tx_{[\mathrm{ms}]}} + \delta_{CU\_Tx_{[\mathrm{ms}]}} + \delta_{MEC_{[\mathrm{ms}]}} + \delta_{CU\_Rx_{[\mathrm{ms}]}} \\ & + \delta_{DU\_Rx_{[\mathrm{ms}]}} + \delta_{RU\_Rx_{[\mathrm{ms}]}} + \delta_{UE\_Rx_{[\mathrm{ms}]}}\end{aligned} \tag{3.20}$$

$$\delta_{Total\_node_{[\mathrm{ms}]}} = \delta_{UE\_Tx_{[\mathrm{ms}]}} + \delta_{RU\_Tx_{[\mathrm{ms}]}} + \delta_{DU\_Tx_{[\mathrm{ms}]}} + \delta_{MEC_{[\mathrm{ms}]}} + \delta_{DU\_Rx_{[\mathrm{ms}]}} + \delta_{RU\_Rx_{[\mathrm{ms}]}} + \delta_{UE\_Rx_{[\mathrm{ms}]}} \quad (3.21)$$

$$\delta_{Total\_node_{[\mathrm{ms}]}} = \delta_{UE\_Tx_{[\mathrm{ms}]}} + \delta_{RU\_Tx_{[\mathrm{ms}]}} + \delta_{MEC_{[\mathrm{ms}]}} + \delta_{RU\_Rx_{[\mathrm{ms}]}} + \delta_{UE\_Rx_{[\mathrm{ms}]}} \quad (3.22)$$

Regarding the total propagation latency, the model considers the optical links and ALs as a contribution. The general expression is given by:

$$\delta_{Total\_prop_{[\mathrm{ms}]}} = \delta_{AL\_Tx_{[\mathrm{ms}]}} + \delta_{FH\_Tx_{[\mathrm{ms}]}} + \delta_{MH\_Tx_{[\mathrm{ms}]}} + \delta_{BH\_Tx_{[\mathrm{ms}]}} + \delta_{TL\_Tx_{[\mathrm{ms}]}} + \delta_{TL\_Rx_{[\mathrm{ms}]}} + \delta_{BH\_Rx_{[\mathrm{ms}]}} + \delta_{MH\_Rx_{[\mathrm{ms}]}} + \delta_{FH\_Rx_{[\mathrm{ms}]}} + \delta_{AL\_Rx_{[\mathrm{ms}]}} \quad (3.23)$$

where:

- δ_{Total_prop} – Total propagation latency.
- $\delta_{AL/FH/MH/BH/TL\_Tx}$ – Propagation latency on the transmitter side.
- $\delta_{AL/FH/MH/BH/TL\_Rx}$ – Propagation latency on the receiver side.

The model divides the computation of the maximum E2E latency into two terms, one corresponding to the latency at the nodes and the other to the maximum propagation latency resulting from the link's lengths. However, only the lengths of the FH, MH and BH optical links are estimated because the AL lengths are calculated as individual latency contributions. Once the two terms are determined, the maximum E2E latency is computed using the following expression:

$$\delta_{Max\_E2E_{[\mathrm{ms}]}} = \delta_{Total\_node_{[\mathrm{ms}]}} + \delta_{Total\_prop_{[\mathrm{ms}]}} \quad (3.24)$$

where:

- δ_{Max_E2E} – Maximum E2E latency.

As an example, if a MEC node is deployed between a DU and CU node, the maximum E2E latency is given by:

$$\delta_{Max\_E2E_{[\mathrm{ms}]}} = \delta_{UE\_Tx_{[\mathrm{ms}]}} + \delta_{AL\_Tx_{[\mathrm{ms}]}} + \delta_{RU\_Tx_{[\mathrm{ms}]}} + \delta_{FH\_Tx_{[\mathrm{ms}]}} + \delta_{DU\_Tx_{[\mathrm{ms}]}} + \delta_{MEC_{[\mathrm{ms}]}} + \delta_{DU\_Rx_{[\mathrm{ms}]}} + \delta_{FH\_Rx_{[\mathrm{ms}]}} + \delta_{RU\_Rx_{[\mathrm{ms}]}} + \delta_{AL\_Rx_{[\mathrm{ms}]}} + \delta_{UE\_Rx_{[\mathrm{ms}]}} \quad (3.25)$$

The maximum optical link length is determined considering the latency margin without accounting for the propagation latency corresponding to the optical links. It is obtained using the required E2E latency of the service, excluding the total node latency and the ALs propagation latency contributions. The following expression uses a 1.67 factor to justify the non-straight line installation of the optical fibres.

$$d_{Max\_optical\ [\mathrm{km}]} = \left(\delta_{service\ [\mathrm{ms}]} - \delta_{Total\_node\ [\mathrm{ms}]} - \delta_{AL\_Tx_{[\mathrm{ms}]}} - \delta_{AL\_Rx_{[\mathrm{ms}]}}\right) \frac{v_{[\mathrm{km/s}]}}{1.67} \times 10^{-3} \quad (3.26)$$

where:

- $d_{Max\_optical}$ – Maximum optical link length.
- $\delta_{service}$ – Required latency associated with the chosen service.

The result of (3.26) enables determining, using (3.10), the maximum propagation latency associated with the optical links to ensure the service's E2E latency requirement. Therefore, the total propagation is given by:

$$\delta_{Total\_prop_{[\mathrm{ms}]}} = \delta_{Max\_optical_{[\mathrm{ms}]}} + \delta_{AL\_Tx_{[\mathrm{ms}]}} + \delta_{AL\_Rx_{[\mathrm{ms}]}} \quad (3.27)$$

where:

- $\delta_{Max\_optical}$ – Maximum optical link propagation latency.

The maximum E2E distance takes into account the ALs length and the maximum optical link length, given by the following expression:

$$d_{Max\_E2E_{[\mathrm{km}]}} = d_{Max\_optical\ [\mathrm{km}]} + d_{AL\_Tx_{[\mathrm{km}]}} + d_{AL\_Rx_{[\mathrm{km}]}} \quad (3.28)$$

where:

- d_{AL_Tx} – AL link length on the transmitter side.
- d_{AL_Rx} – AL link length on the receiver side.

The E2E distance results from the contributions of the link lengths in the network and is obtained by the following expression:

$$\begin{aligned} d_{E2E\ [\mathrm{km}]} = {} & d_{AL\_Tx_{[\mathrm{km}]}} + d_{FH\_Tx_{[\mathrm{km}]}} + d_{MH\_Tx_{[\mathrm{km}]}} + d_{BH\_Tx_{[\mathrm{km}]}} + d_{TL\_Tx_{[\mathrm{km}]}} + d_{TL\_Rx_{[\mathrm{km}]}} \\ & + d_{BH\_Rx_{[\mathrm{km}]}} + d_{MH\_Rx_{[\mathrm{km}]}} + d_{FH\_Rx_{[\mathrm{km}]}} + d_{AL\_Rx_{[\mathrm{km}]}} \end{aligned} \quad (3.29)$$

where:

- d_{E2E} – E2E distance.
- $d_{FH/MH/BH/TL\_Tx}$ – Link lengths on the transmitter side.
- $d_{FH/MH/BH/TL\_Rx}$ – Link lengths on the receiver side.

Estimating the length of each link depends on the organisation's requirements. The usual link length ranges are shown in Table 3.11.

Table 3.11 – Network reach requirements (adapted from [57]).

Link	Range [km]
FH	[1,20]
MH	[20,40]
BH	[1,10]

3.2.4 RU Node Throughputs

The capacity offered by a 5G FDD network depends on several factors, such as channel bandwidth, modulation scheme, MIMO technology, and network load. According to 3GPP TS 38.306, the capacity of the 5G FDD radio link correspondent to a single carrier is calculated using the following expression:

$$R_{FDD\ [\mathrm{Mbits/s}]} = \frac{v_{Layers}\ \ Q_{m\ [\mathrm{bits/symbol}]}\ f_s\ R_{code\_max}\ \left(\frac{12\ N_{PRB\ [\mathrm{RBs}]}^{B,\mu}}{T_{s\ [\mathrm{s}]}^{\mu}}\right)\ (1-O)}{10^6} \quad (3.30)$$

where:

- R_{FDD} – Capacity of the 5G FDD radio link.
- v_{Layers} – Number of layers, dependent on the MIMO system implemented. The maximum number of DL layers is 4, and for UL layers, it is determined by the number of transmitting antennas at the terminal. However, in this thesis, the maximum number of UL layers considered is 8.
- Q_m – Average modulation order (2 for Quadrature Phase-Shift Keying (QPSK), 4 for 16-Quadrature Amplitude Modulation (QAM), 6 for 64-QAM and 8 for 256-QAM).
- f_s – Scaling factor (1, 0.8, 0.75 or 0.4), which is related to the upstream and downstream ratio of the frame structure. Due to the handover process, it is defined per band or band combination and is relevant in UE high or medium mobility situations.
- R_{code_max} – Maximum coding rate is a constant dependent on the modulation order. It represents the ratio of the number of information bits to the total number of coded bits transmitted over the air interface, indicating how much redundancy is added to the data to ensure a reliable transmission. The CQI allows the selection of an appropriate coding rate. The higher the CQI, the higher the data rate. The maximum is $\frac{948}{1024}$ for 256-QAM, which can be approximated to 0.9. The best coding rate values for the respective modulation are $\frac{449}{1024}$ for QPSK, $\frac{616}{1024}$ for 16-QAM, and $\frac{873}{1024}$ for 64-QAM. The constants are present in Annex D.
- $N_{PRB}^{B,\mu}$ – The maximum number of physical RB allocations in bandwidth B with numerology μ, where B is the UE-supported maximum bandwidth in a given band or band combination. The respective values are presented in Table 3.12.
- T_s^{μ} – The average subframe OFDM symbol duration in a subframe for a numerology μ, which is related to the SCS.
- O – The Overhead for control channels is related to the bandwidth required to transmit the packet. It is affected by the frequency and MIMO technology. Table 3.13 presents the Overhead ratios of the control channel relative to the total transmitted data. On average, about 8% correspond to the transmitted data on the UL and 14% of the DL control channel. The simulated band is centred at 3.6 GHz, corresponding to the FR1 band.

The Overhead concept in 5G networks refers to the additional data transmitted alongside the user's data to guarantee a stable and efficient connection. This extra data contains control information, error correction codes, and synchronisation signals required for the network to function effectively. Therefore, adopting sophisticated modulation methods and MIMO antenna systems, which need more signalling information than earlier generations of wireless networks, is one of the primary causes of implementing Overhead in 5G networks.

Table 3.12 – Maximum number of RBs for each transmission bandwidth and SCS for FR1 (extracted from [14]).

	Number of RBs													
SCS	**Bandwidth [MHz]**													
[kHz]	5	10	15	20	25	30	40	50	60	80	90	100	200	400
15	25	52	79	106	133	160	216	270	N/A	N/A	N/A	N/A	N/A	N/A
30	11	24	38	51	65	78	106	133	162	217	245	273	N/A	N/A
60	N/A	11	18	24	31	38	51	66	79	107	121	132	264	N/A
120	N/A	N/A	N/A	N/A	N/A	N/A	N/A	32	N/A	N/A	N/A	66	132	264

Table 3.13 – Overhead for control channels in 5G (extracted from [14]).

5G Band	**UL**	**DL**	**Average Overhead**
FR1	0.08	0.14	0.11

Overall, the transmission bandwidth in 5G can vary from 5 MHz to 400 MHz, and the modulation scheme used is mainly QAM, which allows for higher data rates [58]. Nowadays, in Portugal, the frequencies allocated for NR are 0.7 GHz and 3.6 GHz, and the respective bandwidths are 10 MHz and 100 MHz [14].

In 5G TDD mode, the structure of the slot determines how much time is allocated for UL and DL transmissions. The slots can be adjusted based on the number of symbols assigned to the UL and DL, which is related to the traffic demand allocated to the respective transmissions and, therefore, the system's throughputs. A flexible frame structure can be applied, enabling dynamic resource distribution to diverse users. The frame structure comprises sub-frames, which can be further subdivided into slots. The length and number of slots in a sub-frame can be dynamically changed based on traffic demands, enabling more efficient resource utilisation and higher throughputs. The updated periodicity pattern could be either per slot or aggregated slots.

For a dynamic TDD deployment, it is first considered that the UEs are evenly distributed across the RU nodes and then to the following nodes, depending on the type of service. The nodes dynamically match their transmission links to the sporadic traffic arrivals. Then, the number of DL and UL symbols that best satisfy the specific link selection criteria is chosen. In order to select between UL and DL, a buffered traffic ratio is defined, depending on the aggregated buffer traffic size DL and UL. The expression to calculate the buffered traffic ratio is given by [59]:

$$b_c = \frac{Z_c^{DL}}{Z_c^{DL} + Z_c^{UL}} \tag{3.31}$$

where:

- b_c – Buffered traffic ratio.
- Z_c^{DL} – Aggregated buffered traffic size in DL.
- Z_c^{UL} – Aggregated buffered traffic size in UL.

The lower the ratio, the larger the buffered UL traffic flow, and consequently, the slot types with a high UL symbol density are chosen. If there are no new packet arrivals or buffered traffic, the RU nodes

revert to a default slot configuration with an approximate number of DL and UL symbol shares. Usually, the 5G system considers 57% of framing for DL and 43% for UL. Notably, this frame structure is not typical, but [14] claims that NR will feature a flexible frame structure regime that might lead to this frame split. However, the nodes do not schedule any UEs. As a result, they quickly adjust to the accumulating buffered traffic, balancing DL and UL TDD queuing performance. If necessary, flexible subframes can be used by dynamically adjusting the duration of UL and DL transmissions, allowing the network to allocate more resources to areas with high traffic demand while minimising interference in areas with low traffic demand [59].

In this dynamic deployment, the expression to determine the throughput is based on the 5G FDD mode but considering the time division. It also considers the losses applied to the link due to signal attenuation, interference, and noise, which leads to an actual throughput lower than the theoretical one. Thus, the average throughput of the radio in 5G UL in TDD can be calculated by the following expression:

$$R_{TDD/UL\,[\text{bits/s}]} = R_{FDD\,[\text{bits/s}]}\ F_{UL}\ A_f \tag{3.32}$$

where:

- $R_{TDD/UL}$ – Average throughput of the radio in 5G UL in TDD.
- F_{UL} – Percentage of the slot reserved for the UL.
- A_f – Average factor that accounts for 5G system throughput losses.

By applying the same approach, the average throughput of the radio in 5G DL in TDD can be calculated using the following expression:

$$R_{TDD/DL\,[\text{bits/s}]} = R_{FDD[\text{bits/s}]}\ F_{DL}\ A_f \tag{3.33}$$

where:

- $R_{TDD/DL}$ – Average throughput of the radio in 5G DL in TDD.
- F_{DL} – Percentage of the slot reserved for the DL.

TDD is often selected in densely populated regions with significant UL and DL data traffic demands. It is so that the UL/DL ratio may be changed with more flexibility based on traffic demand while using TDD.

The required service throughput in the RU node results from the sum of all data rates of the services ensured by the respective node. The following expression is used to calculate the RU's required throughputs on both the receiver and transmitter sides:

$$R_{u\,[\text{Mbits/s}]} = \sum_{1}^{N_u} R_{s\,[\text{Mbits/s}]} \tag{3.34}$$

where:

- R_u – RU node required throughput.
- N_u – Number of users connected to the RU node.
- R_s – Data rate of the services offered by the RU node.

3.2.5 Link Capacity

The interfaces between nodes are designed to specify their capacities, and the process is developed with the functional split of network functionalities. The link capacities for the reference scenarios are presented in Annex E. In the thesis, Splitting Option 7.2 is used for the FH link and Splitting Option 2 for the MH link. The BH is required to transport data between network segments. It does not involve splitting options related to baseband processing because it serves different purposes in the overall network architecture.

In Splitting Option 7.2, the DU node includes the precoding (increases the data rate and reduces the error rate in the communication system) and the resource element mapper (assigns each data symbol to a specific resource element based on its modulation scheme, coding rate, and channel conditions). The FH link is responsible for transporting subframe symbols. This results in a slightly lower FH link bitrate, a more complex DU node, and less shared processing in the CU node. It is the first considered option where the link capacity becomes variable [60]. The FH link capacity for Splitting Option 7.2 in the UL and DL is specified by:

$$R_{Op.7.2\,[\mathrm{Mbps}]} = \left(2000_{[\mathrm{s}^{-1}]}\ N_{SC}\ \ N_{SY\,[\mathrm{symbols}]}\ \ N_{Q\,[\mathrm{Mbits/symbol}]}\ \ N_A\right)\ \mu_s + D_{MAC_{info}\,[\mathrm{Mbits}]} \tag{3.35}$$

where:

- $R_{Op.7.2}$ – FH link capacity for Splitting Option 7.2.
- N_{SC} – Number of subcarriers used in the system.
- N_{SY} – Number of symbols in the system.
- N_Q – Bit width.
- N_A – Number of antenna ports.
- μ_s – Subcarrier utilisation (load).
- $D_{MAC_{info}}$ – Maximum amount of data transmitted over the wireless network.

Splitting Option 2 is provided by the 3GPP as a feasible split to define the MH link capacity in the NR system. The PDCP and RRC are centralised in the CU node, while the remaining functions are done locally in the DU node. As a result, the traffic is separated into numerous flows that may be routed to different access nodes, enabling multi-connectivity. This division has limited potential for coordinated scheduling. However, this is likely to be compensated by beamforming. An advantage of this split is the benefit of centralisation and a more extensive capability for coordination of mobility and handover operations. The MH link capacity for Splitting Option 2 in the UL and DL is specified by:

$$R_{Op.2\,[\mathrm{Mbps}]} = R_{p\,[\mathrm{Mpbs}]}\left(\frac{B_{[\mathrm{MHz}]}}{B_{c\,[\mathrm{MHz}]}}\right)\left(\frac{N_L}{N_{L,c}}\right)\left(\frac{\log_2 M}{\log_2 M_c}\right) + R_{c\,[\mathrm{Mbps}]} \tag{3.36}$$

where:

- $R_{Op.2}$ – MH link capacity for Splitting Option 2.
- R_p – Peak rate.
- B – System bandwidth.
- B_c – Bandwidth for control signals.

- N_L – Number of layers in the system.
- $N_{L,c}$ – Number of layers for control signalling.
- M – Modulation order.
- M_c – Modulation order for control signals.
- R_c – Signalling rate.

The BH link (which connects the CU and the Core) and the TL (which connects the Core and the EDC) have typical interface capacities, which means there is no specific splitting option associated with it [53]. The respective capacity values are presented in Table 3.14.

Table 3.14 – Typical BH link and TL network capacities (adapted from [14, 53]).

Link	Link Capacity [Gbps]
BH	25
Transport	>100

3.2.6 Radio Link Length

The antenna's type and sensitivity, the UE's transmit power, and the location in which it is installed are some variables that affect an antenna's coverage area, defined by the respective range and directionality. In the context of the scenarios to be analysed, the range of an antenna is the maximum distance at which it can reliably receive signals from the UE. The model considers the target-sensor pair communication in Line of Sight (LoS) and takes the approach from [61] to determine the maximum AL length for airborne UEs. The propagation model adopted is the Effective Earth's Radius Model, which considers the first Fresnel ellipsoid with a clearance of 100% and is applied to low flight-level altitudes. The model from [61] was developed to analyse the performance of WAM systems, taking a cumulative radio coverage estimation to determine the accuracy of the aircraft location.

Since assessing LoS coverage for a target-sensor pair is computationally expensive, a first-order estimation for the coverage area ignores the terrain profile. It only considers a smooth spherical Earth to prevent needless calculations for points outside this area. The radius of this circular coverage region determines the maximum connection length. The effective Earth radius does not consider the atmospheric refraction, leading to the factor $k = 1$. Thus, the maximum propagation distance of the radio link in LoS, also known as radio horizon distance, is given by (3.39). The variables r_A and r_{GS} in (3.37) and (3.38) depend on the height of the aircraft and the GS above the Mean Sea Level (MSL), respectively. The following expressions define these variables:

$$r_{A\,[\mathrm{km}]} \triangleq R_{e\,[\mathrm{km}]} + h_{A,MSL\,[\mathrm{km}]} \tag{3.37}$$

$$r_{GS\,[\mathrm{km}]} \triangleq R_{e\,[\mathrm{km}]} + h_{GS,MSL\,[\mathrm{km}]} \tag{3.38}$$

where:

- r_A – Effective distance of the aircraft's antenna to the Earth's centre.
- r_{GS} – Effective distance of the GS's antenna to the Earth's centre.
- R_e – Effective Earth radius (6 371 km).

- $h_{A,MSL}$ – Aircraft height above MSL.
- $h_{GS,MSL}$ – GS height above MSL.

The calculation of the radio horizon distance is given by:

$$d_{RH\,[\mathrm{km}]} = \sqrt{r_{A\,[\mathrm{km}]}{}^2 - R_{e\,[\mathrm{km}]}{}^2} + \sqrt{r_{GS\,[\mathrm{km}]}{}^2 - R_{e\,[\mathrm{km}]}{}^2} \tag{3.39}$$

where:

- d_{RH} – Radio horizon distance.

Although the radio horizon distance is used in simulation, considered the longest distance to establish communication, the radio path length corresponds to the signal's physical distance from the transmitter to the receiver. Therefore, radio path distance is smaller than the radio horizon distance since it encounters obstacles, which leads to signal attenuation. Thus, the maximum LoS distance is a theoretical result and does not account for losses. The radio link calculation is only applied to scenarios involving a distance between the UE and the RU node in the order of tens of kilometres.

3.3 Model Implementation

The model implementation used in this thesis is divided into two parts, and results are obtained through MATLAB. The first part estimates the maximum E2E latency and the maximum E2E distance. The programme starts by calculating the links' capacities, the radio node's throughputs, and the required throughputs of the respective services. These calculations are based on a specific service mix (Annex F) applied to the transmitter and receiver sides of the RU, DU and CU nodes. In this model, the sum of the data rates of the services does not exceed the respective node's capacity.

Then, the initial latency contributions are computed, corresponding to the UE processing, the UE transmission and the AL propagation latencies on the transmitter and receiver sides, different for all network structures. The individual contributions are calculated based on the input parameters associated with each type of 5G architecture. These contributions depend also on the MEC node deployment option (None, RU-DU, DU-CU or CU-Core) selected.

After this code segment, the programme calculates the total node latency, which results from the sum of the latency contributions applied to all nodes. Afterwards, the latency referent to the network architecture without the optical links (FH, MH and BH links) is computed. The optical link lengths are estimated to structure the network to ensure the latency requirements of the services, leading to the calculation of the maximum optical link length, which corresponds to the total maximum distance between nodes computed for each network architecture option. Then, the obtained results are used to compute the propagation latency associated with the optical link lengths.

The maximum distance the MEC node can be installed depends on the sum of the maximum optical link's length and the AL's length on the transmitter and receiver sides. The maximum E2E latency is determined by summing the total node and the total propagation latency. Therefore, it is calculated considering the contribution of all types of links and nodes.

The flowchart model applied to this part of the programme is presented in Figure 3.4. In this thesis, the part of the model developed by [14] to compute the capacities, throughputs, and the initial, individual and total node latency contributions is in coloured blocks. The remaining blocks have been developed to analyse the network contributions following a different approach than the previous reference.

Regarding the second part of the model, the required E2E latency and the UL and DL RU node throughputs (output from the flowchart of Figure 3.4) are used to calculate the margin values applied to each scenario, depending on the type of service (critical or non-critical). The main objective is to deploy an integrated private network whenever possible. Thus, the conditions applied to determine the type of private network differ based on this first service classification. In the case of critical services, for safety and insurance purposes, it is considered a margin of 10% regarding the maximum E2E latency and a margin of 50% regarding the throughputs of the RU node. Therefore, the condition to adopt an integrated private network considers the service's throughput to be less than 50% of the UL and DL throughput of the RU node and the maximum E2E latency to be less than 90% of the latency required by the service.

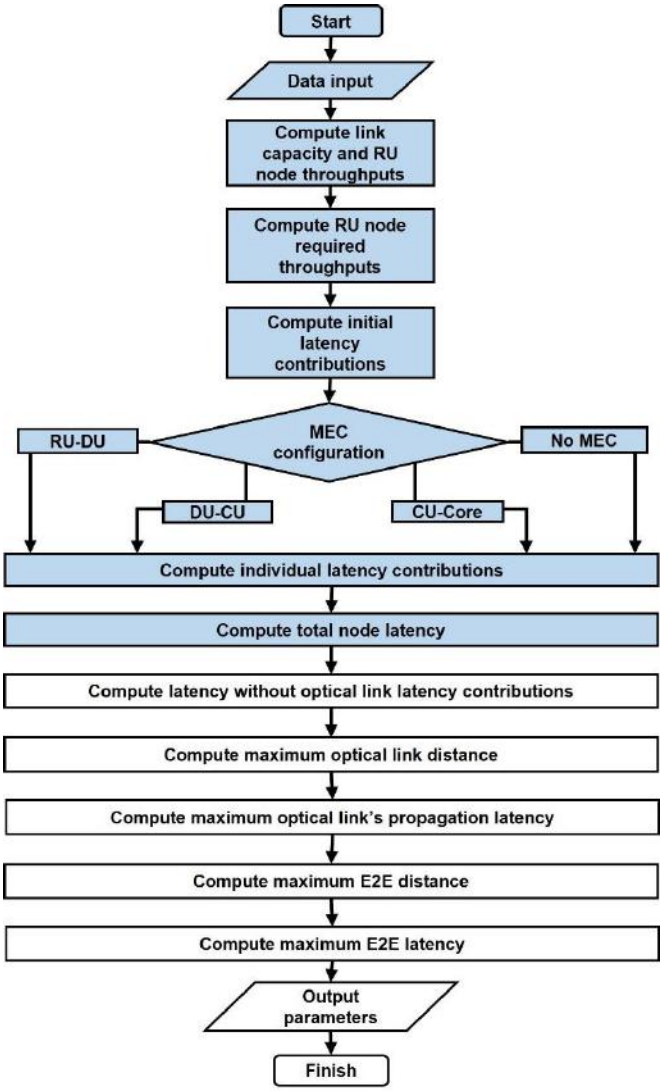

Figure 3.4 – Flowchart model of the maximum E2E latency and maximum E2E distance (adapted from [14]).

Although latency and throughput requirements for non-critical services may be less restrictive, they are essential to provide a positive user experience. Considering that slight delays might not significantly impact the operation, maintaining an appropriate level of latency and capacity for delivering uninterrupted and responsive services is necessary. In this way, to adopt an integrated private network, the service's throughputs has to be less than 70% of the throughputs of the RU node and the maximum E2E latency less than 95% of the latency required by the service. The conditions implemented result from references to military operation services under daily conditions. Figure 3.5 represents the flowchart model of the second part of the programme.

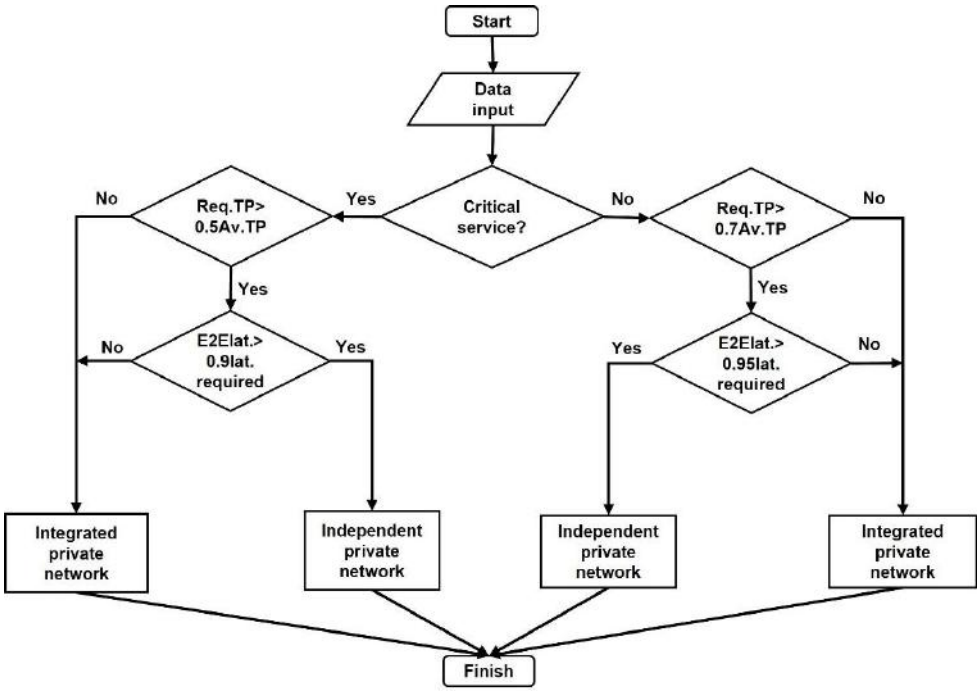

Figure 3.5 – Flowchart model of the type of private network.

3.4 Model Assessment

The accuracy of the experimental results depends on the validation and evaluation of the model applied during simulations. Several steps are taken into account during the implementation process to ensure the proper operation of the network simulator. The expressions are implemented as separated code functions, and the response of the individual functions to several inputs is registered. It should be noted that when analysing the model's results, it is crucial to conduct a careful and critical approach, i.e., the circumstances in which the model is created and the limitations applied to produce reliable results should be considered. Table 3.15 presents the model assessment in eleven phases.

The model assessment starts by validating the input files. Each file contains different input parameters depending on the chosen type of UE, service and network specification. Therefore, to calculate the latency contributions, the capacities and the required throughputs, it is necessary to verify if the input parameters are correctly saved in the programme variables. This phase is validated by simulating the code segment that saves the numerical values to the respective parameters.

The second phase consists of four main parts. The first part validates the RU node throughputs and the FH and MH links capacities, which impact the queuing latency on the transmitter and receiver sides. The results are valid compared to the ones obtained by [57]. The second part validates the network functionalities vector, influenced by the Splitting Option 7.2. The third part consists of validating the user data vector created by the numerical values introduced by the user programme. Then, the fourth part, considered the most important, validates the RU throughput vector on the UL and DL sides, which is used to calculate the latency contributions. This last part depends on the scenario that is being analysed. Therefore, the number of RU nodes used in the link communication influences the service required throughputs. Two vectors of required throughputs are created if more than one RU node is used. Thus, two functions are developed: one responsible for calculating the required throughputs of the RU node in UL and DL on the transmitter side, and the other responsible for the same calculations on the receiver side but for another RU node. Afterwards, the vectors are validated based on the link type (UL, DL or both) and service mix associated with each RU node.

Table 3.15 – Model assessments empirical tests.

Test ID	Description
1	Validation of the input files. Each file contains different input parameters depending on the chosen type of UE, service and network specification.
2	Validation of: • The RU node throughputs, and FH link and MH link capacities vectors. • The network functionalities vector. • The user data vector. • The RU required throughputs vector. Check if the vectors are correctly created and filled according to the programme inputs.
3	Collection and validation of the initial latency contributions results.
4	Validation of the initial latency contributions with an independent RU, DU and CU nodes architecture and without including the MEC node.
5	Validation of the initial latency contributions associated with each MEC node deployment option.
6	Validation of the total node latency, the latency without the optical link latency contributions, and the maximum optical link length according to the programme parameters in each scenario.
7	Validation of the maximum optical link's propagation latency.
8	Validation of the maximum E2E distance and maximum E2E latency.
9	Validation of the margins established for each type of service (critical or non-critical).
10	Validation of the model's performance in choosing the type of private network as a function of the required throughputs, RU node throughputs, and E2E latency.
11	Validation of the output parameters according to the values introduced by the user programme and the parameters used to achieve the expected results.

The third phase consists of collecting and validating the initial latency calculations' results, which are used to compute the individual latency contributions. Different services are used to validate the

transmission latency of the UEs. Each service has associated a different packet size and link data rate. The results are valid compared to the theoretical results obtained using (3.9). Regarding the ALs propagation latencies, as expected, the distance variation between the UE and the RU node leads to a linear response of the latency, i.e., the longer the distance from the UE to the RU node, the higher the latency associated with the ALs. Both results are confirmed with the results obtained by [14].

The fourth phase validates the latency contributions of the network with an independent RU, DU and CU node architecture. This architecture type is selected to validate the processing, transmission and queuing latency because it accounts for all the network contributions. The calculations include all the previously validated results. The transmission latency is directly related to the packet size and the service's data rate, validated using the results obtained in the third phase. The processing latency is associated with the node's number and functionalities. As expected, as this number increases, the processing latency increases simultaneously. The link capacity and the selected service mix applied influence each node's queuing latency. As expected, an increase in the throughput associated with a network node increases the queuing latency in that node.

The fifth phase of the assessment consists of validating the processing, transmission and queuing latencies associated with the MEC node deployment option. In this case, it is necessary to consider that the packet service does not proceed to the following node, which means that the link latency decreases, but the processing latency increases. It is also necessary to consider the link that interconnects the previous node and the MEC node, which is influenced by the capacity associated. Thus, it is expected to verify a linear shape, i.e., as the packet size increases, the processing latency in the MEC node increases at the same rate. These results are validated based on the ones obtained by [14]. Therefore, it is possible to verify that the processing latency is higher when an MEC node is used than when the data travels up to the EDC with the same packet size.

The sixth phase is performed by checking the total node latency, resulting from the sum of the latency contributions validated in the previous assessment phases. The obtained results are a confirmation of the theoretical values. When analysing the scenario service mix, the validation process takes the three MEC node deployment options and the respective service. In this thesis, the links that connect the nodes are optical fibre. Service 1 validates the maximum optical link distance considering the three possible MEC node deployment options and the no-deployment, i.e., the independent RU, DU and CU node architecture.

The seventh phase consists of validating the maximum optical link's propagation latency. It is possible to verify that the propagation latency increases at the same rate as the maximum optical link length.

The eighth phase validates the maximum E2E distance. The results are obtained using the variables validated in the previous phases.

The nineth phase consists of validating the results obtained for the margins applied according to the type of service (critical or non-critical). The two service types are used to verify and validate the results according to the values obtained theoretically.

The tenth phase consists of validating the model's performance in choosing the type of private network as a function of the required throughputs, RU node throughputs, the required E2E latency, and the margins established based on these results. The margins depend on the type of service. The validation is performed using two services, one from a critical and the other from a non-critical scenario.

The eleventh phase consists of verifying the output parameters according to the values introduced by the user programme and the parameters used to achieve the expected results. These outputs align with the theoretical results obtained during the above phases.

Chapter 4

Results Analysis

This chapter presents a description of the scenarios and an analysis of the results.

4.1 Scenarios Description

The study is based on three main scenarios. These scenarios include services with different radio characteristics classified as critical and non-critical. The services are applied to emergency, contingency, security, control, surveillance, and reconnaissance operations. Table 4.1 presents the simulated systems with the respective services.

Table 4.1 – Scenarios with respective simulated systems and services.

Scenario	Simulated Systems	Simulated Services
Airbase	Security and Control	Internal Control Manipulations
		Video Streaming
		Sensor Motion Detection
	Flight Simulators	Remote Control
		Virtual Reality
WAM System	Weather Monitoring	Video Streaming
		Remote Controlled Sensors
	Air Traffic Control	Network-Based Sensor Sharing
Squadron	Remote-Controlled UAVs	External Control Manipulations
		Video Streaming
		Telemetry Link

In order to characterise the case studies, it is considered that the network structure in Portugal has the same robustness as the distribution of the population density. Thus, most RU nodes are concentrated in the coastal area, and the respective locations are estimated from [40].

The region of Lisbon has an average density of 948 inhabitants/km^2, 639 RU nodes, 55 CU nodes and 1 CN deployed [14]. Therefore, the values used for simulation consider the referenced number of BSs assigned to the Lisbon region. However, in the Squadron scenario, a reduction of approximately 85% in the number of RU nodes is considered since the population density is about 146.1 inhabitants/km^2. Despite that, the 55 CU nodes and 1 CN are maintained. This estimation results from the fact that the Alenquer region, where the Squadron is inserted, is located 50 km from Lisbon. In an independent 5G RU, DU and CU node architecture, the distance between a RU and a DU node can reach 10 km, and between a DU and a CU node, it can range from 20 km to 40 km [40].

The Airbase scenario is selected to analyse the viability of implementing Security and Control Systems and testing the performance of the Flight Simulators. The Security and Control Systems are installed inside the infrastructures and in the peripherical area. Thus, Remote Control Commands, Video Streaming in Closed-Circuit Television (CCTV) and Sensor Motion Detection are performed. Regarding the Flight Simulators, Remote Control Commands and Virtual Reality are used. The Airbase scenario studies the possibility of implementing these services, considering an average of 400 people working daily in the facilities. The Security and Control services have a latency requirement of 4 ms. These services are provided by 50 CCTV cameras and 52 network-based sensors. The Training and Mission Planning Department has 2 Flight Simulators, and the services provided are non-critical with a latency requirement of 4 ms.

Due to the attenuation, high user density and redundancy, deploying 4 RU nodes in an area close to the facilities of the Airbase is considered to ensure the achievement of the requirements. Airbase N.º6, located in Montijo, is used as an illustrative example. The deployments are presented in Figure 4.1.

The WAM System studies the possibility of using a 5G private network to determine the position of an aircraft by measuring the Time Difference of Arrival (TDOA) of signals transmitted from multiple known locations and collecting data from the environment used for weather monitoring. Three reference GSs are required to determine a precise location in two-dimensional space. The Portuguese WAM System consists of 23 GSs, and the management of the services is performed using Video Streaming and Network-Based Sensor Sharing. Because the GSs are distributed throughout the north-centre country area, allocating them all to a single RU node to determine the network's radio characteristics is impossible.

Figure 4.1 – Estimated deployment of RU nodes around the Airbase N.º6 – Montijo.

Therefore, in the thesis, it is considered that each RU node is allocated to 3 GSs, as represented in Figure 4.2, leading to the necessity of having more than 1 RU node to allocate all the GSs. The number of aircraft per GS is variable and depends on the traffic in the region. However, an average of 20 aircraft per GS is considered. It is a non-critical scenario with a latency requirement of 8 ms.

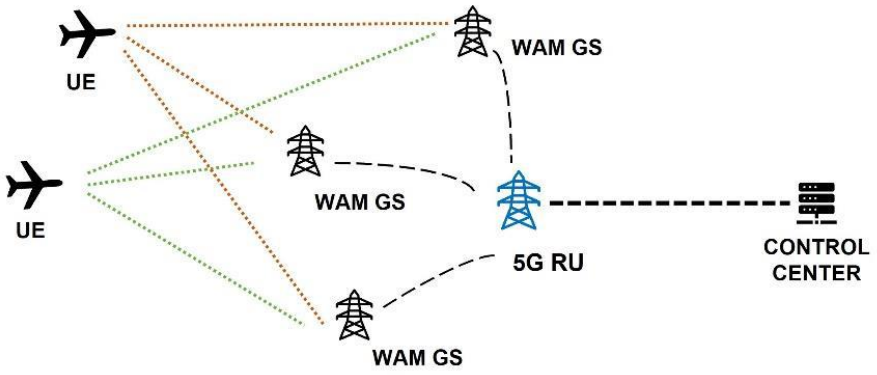

Figure 4.2 – WAM System interaction with 5G RU node and Control Centre.

In the 991 Squadron scenario, the study of implementing a 5G private network in Remote-Controlled UAVs is performed using External Control Manipulations, High-Quality Video Streaming and Telemetry Link services. The scenario specification consists of 3 operational UAVs, as represented in Figure 4.3, with a latency requirement of 0.5 ms, thus, considered an extremely critical scenario. Each UAV has two remotely controlled Pan-Tilt-Zoom cameras, providing flexibility in capturing shots from different angles. It is also equipped with three sensors. Due to the flight velocity and possible network congestion, it is necessary to ensure that these requirements are achieved to perform the attributed mission correctly. It is also considered that 400 people are working daily on the Airbase where the 991 Squadron is inserted.

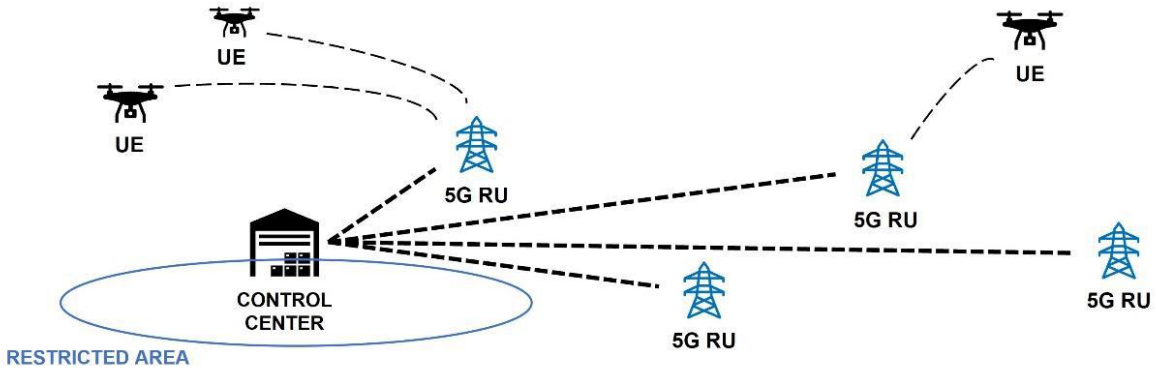

Figure 4.3 – UAV interaction with 5G RU node and Control Centre.

The reference scenarios are analysed based on each service's 5G radio characteristics. Thus, the following study provides the required UL and DL throughputs in each link for each scenario and the DL and UL RU node throughput on both the transmitter and receiver sides. This information is provided in graphs, where the margin used for selecting the most suitable type of private network is also highlighted. The choice of each CQI results from analysing and comparing the scenarios of this thesis with the ones presented in [14]. Depending on the requirements, environment and user traffic, the most appropriate CQI values were selected according to the scenario specifications.

The most adequate MEC node deployment option is also analysed to guarantee that the maximum E2E latency, calculated using (3.24), is not exceeded, as well as the margin applied to the RU node throughputs, making it possible to determine whether the UL and DL throughputs required by each service are above or below the respective value.

The maximum E2E distance, which corresponds to the maximum link length (transmitter plus receiver length contributions) to keep the E2E latency below the maximum required value, is a critical parameter when analysing the systems' redundancy. It is influenced by the MEC node deployment option, like the maximum E2E latency, and calculated using (3.28). However, when considering this distance, it must be taken into account that the RU node coverage distance can vary from a few hundred meters when using millimetre wave frequency bands to several kilometres when using a lower frequency band.

According to [1], no specific coverage distances are associated with a frequency band because the values depend on real-world factors, such as the RU node density, repeater cells, and terrain obstacles.

In this thesis, the scenario analysis considers the maximum distance the MEC node can be deployed and the adequate cell type to use as a function of the frequency bands allocated to 5G in Portugal and the millimetre wave bands (future deployment). The communication link between the RU node and the UEs is considered wireless for all scenarios.

Therefore, the RU node coverage distance can vary between 0.1 km to 30 km, depending on the cell type: macrocell, microcell, picocell and femtocell [18], and the frequency band used. The cell coverage required is estimated based on the scenario to be analysed and the environmental conditions (outdoor or indoor).

The Airbase scenario is mainly characterised as an indoor hotspot with a high stationary UE density. In this case, it is necessary to have RU nodes placed to ensure the service's data rate and latency requirements inside the infrastructures. The outdoor UEs account for a small percentage of the total users, leading to deploying RU nodes with different characteristics requiring a more extensive coverage radius.

The WAM system covers a large geographical area. Therefore, deploying outdoor RU nodes with antenna towers is essential to achieve the required coverage and latency. In this scenario, the UEs can move at more than 500 km/h. Therefore, the coverage radius depends on factors such as the altitude at which the aircraft is being tracked, the desired accuracy, and the regulatory requirements associated with the outdoor environment.

In the case of the 991 Squadron, a network structure with the same characteristics as the Airbase should be considered. However, the scenario is carried out inside and outside the premises, not inside the infrastructure. Therefore, when analysing the environment inside the premises, the RU nodes can be deployed around the facilities to provide localised coverage. These RU nodes must be suitable to ensure the take-off, landing, or conducting of training and surveillance missions near the Airbase where the 991 Squadron is deployed. If the mission extends beyond the facilities, RU nodes with more extensive coverage areas must be considered to operate over longer distances.

Table 4.2 presents the selection of the cell type associated with the above scenario's requirements. The choice is based on [18] considering the characteristics of each cell's type. It should be noted that the cell's maximum coverage distance depends also on the type of frequency used, which means that it may be lower than the value presented for each scenario. The coverage distance decreases as the frequency band increases. Therefore, the coverage distance used in the analysis is an estimation. It should be noted that each type of cell represents a specific geographic area covered by an RU node.

Splitting Option 7.2 is the only splitting option implemented and used in the simulations of this thesis. According to [14], the remaining options have led to similar E2E latency results regarding the same network radio parameters. Thus, analysing the splitting option is not crucial to deciding the most adequate type of private network.

Table 4.2 – Cell type associated with the scenario's requirements.

	Simulated Systems	Cell Type	Maximum Cell Coverage [km]	Location
Airbase	Security and Control Systems	Macrocell	30	Outdoor
		Picocell Microcell	0.2 2	Indoor
	Flight Simulators	Femtocell	0.1	Indoor
WAM System	Weather Monitoring	Microcell	2	Outdoor
	Air Traffic Control	Macrocell	30	Outdoor
Squadron	Remote-Controlled UAV	Picocell Microcell	0.2 2	Indoor Outdoor
		Microcell Macrocell	2 30	Outdoor

4.2 Airbase Scenario

4.2.1 Security and Control services

In the Airbase scenario, there are indoor and outdoor UEs. The data packets in the UL and DL are transmitted and received by the same RU node. Thus, the first consideration is installing an RU node near the Airbase facility's perimeter. The installation is analysed from four different sites. Therefore, the distance between the UEs and the RU node used in simulations corresponds to the distance from the deployment that is farthest away. The simulation is carried out initially with the RU nodes outside the Airbase premises to test whether installing an integrated private network is possible, which is the primary purpose.

Using the example of the Airbase N.º6, it is considered that the RU node is estimated to be located about 2 km from the Control Centre, where the operators view real-time data, make decisions and take actions based on information received from sensors and cameras. For outdoor UEs, the RU node is located 4 km away. Regarding the radio characteristics, a CQI of 8 is used for the Security and Control Systems since it ensures enough radio channel quality between the UEs and the Control Centre. Despite being a critical scenario, it is necessary to balance the benefits of higher modulation orders with the need for reliability and robustness of the services, even at the expense of data rate.

According to Figure 4.4, 5G provides enough throughput in both UL and DL without using the radio characteristics that maximise the throughputs. The total DL and UL throughputs are 433.10 Mbps and 326.72 Mbps, higher than the DL and UL required throughputs of 275.22 Mbps and 209.56 Mbps, respectively. The obtained results refer to the installation of a single RU node. In the case of limited deployment BSs, one RU node can fulfil the requirements of the UEs.

Concerning network latency contributions, it should be considered that the UEs located outside, in the peripherical zone, are not at the same distance from the RU node as those installed in the Control Centre, which is located in the central area of the Airbase. As such, the contributions associated with the ALs propagation latencies are different. The outdoor UEs are estimated to be around 4 km, at maximum, from the RU node, corresponding to an AL propagation latency of 0.0133 ms on the

transmitter and receiver sides, while the indoor UEs, which are around 2 km away, corresponding to an AL propagation latency of 0.0067 ms also on the transmitter and receiver sides.

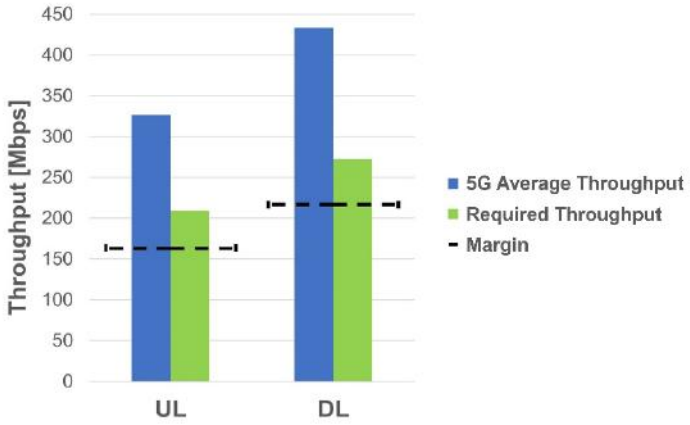

Figure 4.4 – Security and Control Systems – RU throughputs for the Airbase.

In addition to these latency contributions, it is necessary to analyse the influence of the installation of the MEC node to keep the delays of the packet transmission, queuing and processing as low as possible. The MEC node deployment option influences the total node latency, which results are presented in Table 4.3. These contributions are calculated using (3.20), (3.21) and (3.22) for the CU-Core, DU-CU and RU-DU options, respectively. The total node latency without installing the MEC node is also presented. By analysing the results, it is possible to verify that the total node latency exceeds the latency required by the service when the MEC node is not installed. As such, this option is excluded since estimating the optical link's length is impossible.

Table 4.3 – Security and Control Systems – Total node latency for each MEC node deployment option.

MEC Node Deployment Option	Total Node Latency [ms]
None	4.858
RU-DU	1.044
DU-CU	2.125
CU-Core	2.734

In these systems, the maximum optical link's length, computed using (3.26), considers the lowest contribution from the AL's propagation latency between the two UEs' possible environments (outdoor and indoor). Since the same RU node transfers the data packets from the indoor and outdoor UEs, distant UEs can establish communication if the service is ensured for the highest optical link length. This assumption can be made because the services' specifications are equal regardless of the UEs' location. The maximum optical link's length is used in (3.10) to calculate the maximum optical link's propagation latency. The results are shown in Table 4.4.

Tables 4.5 and 4.6 show the results obtained for the maximum E2E latency and the maximum E2E distance, that allows to determine the distance the MEC node can be deployed from the UEs to ensure the service requirements. Table 4.5 refers to indoor UEs, while Table 4.6 refers to outdoor UEs. The

differences in the E2E latency results between the two environments are due to the AL's propagation latency contributions.

Table 4.4 – Security and Control Systems – Maximum optical link's length and propagation latency for each MEC node option.

MEC Node Deployment Option	Maximum Optical Link Length [km]	Maximum Optical Link's Propagation Latency [ms]
None	-	-
RU-DU	176	0.822
DU-CU	112	0.523
CU-Core	75	0.351

Table 4.5 – Security and Control Systems – Maximum E2E latency and maximum E2E distance to indoor UEs for each MEC node option.

MEC Node Deployment Option	Maximum E2E Latency [ms]	Maximum E2E Distance [km]
None	-	-
RU-DU	1.839	180
DU-CU	2.661	116
CU-Core	3.098	79

Table 4.6 – Security and Control Systems – Maximum E2E latency and maximum E2E distance to outdoor UEs for each MEC node option.

MEC Node Deployment Option	Maximum E2E Latency [ms]	Maximum E2E Distance [km]
None	-	-
RU-DU	1.886	182
DU-CU	2.667	118
CU-Core	3.105	81

After analysing all the results, it is possible to verify that only the margin applied to the throughput of the RU node, illustrated in Figure 4.4, is exceeded in the UL and DL sites. Regarding the latency margin, the RU-DU, DU-CU, and CU-Core MEC node options can be considered, as the maximum E2E latency obtained is below the margin of 3.6 ms.

The frequency band used in the ALs connection influences the distance at which the RU node can be installed from the UEs. The highest percentage of UEs is concentrated inside the infrastructures. Therefore, the radius coverage is not prioritised because the building's area is restricted and smaller than the entire Airbase. However, a high UE density requires reliable connectivity while demanding low latency for real-time control and monitoring, leading to the necessity of a balance between coverage and throughput. The simulated system traffic is considered an intense network usage but with variations.

Based on these characteristics, the medium frequencies and millimetre wave frequency bands (3.6 GHz, 6.0 GHz and above 24.25 GHz) can be used for these specific localised applications. The frequencies of 3.6 GHz and 6.0 GHz can be deployed where coverage, reliability, and penetration through obstacles are required, supporting simultaneously numerous connected devices. However, it is necessary to consider the spectrum congestion and the limited bandwidth compared with the one provided by the millimetre wave bands. These latter are primarily used for short-coverage distance applications. They offer high bandwidth, enabling higher data rates, and due to the associated short range, they experience less interference, which is essential for critical services. However, a LoS connection is required, making

indoor deployment challenging, translated in the necessity of having a higher number of interior RU nodes.

As a result, assuming that the coverage of both types of cells (microcell and picocell) is maximised by using the three previous frequency bands, a hybrid network can be the best choice to guarantee the requirements of the services. Thus, the 3.6 GHz and 6.0 GHz frequencies can provide reliable and broader indoor coverage, making the microcells the best option. The picocells are adequate to use the millimetre wave bands, enhancing capacity and delivering low latency in specific areas, such as command centres or control rooms. In this way, the network structure is estimated to require more than one RU node if the number of indoor users increases. This requirement aims to provide better system redundancy, withstanding various vulnerabilities while maintaining continuous operations and protecting vital assets and information.

The RU node must ensure a longer coverage radius for outdoor UEs. However, the density of users is smaller, which means requesting large capacities to ensure the service is unnecessary. In this case, the most adequate frequency is 0.7 GHz, which provides wide-area coverage and is considered the best frequency to penetrate physical obstacles, crucial to ensure continuous communication between security devices, sensors and the Control Centre. Macrocells are the cells that achieve the most extended coverage radius, ensuring that the communication remains reliable.

The maximum E2E latency calculated with the RU-DU option reaches the lowest value compared to the other deployment options (DU-CU and CU-Core). The main objective is to reduce the latency's probability of exceeding the maximum allowed value, which means that the best option associated with the independent private network is the RU-DU inside the facilities, even though the maximum E2E latency results are close because the queuing latency added to the maximum E2E latency is only due to the Motion Detection Sensor packets (high packet size) since this is a high-priority service. The processing latency is also significantly low because only the RU and MEC nodes are required to process data.

Regarding the previously obtained results and the respective analysis, it is concluded that deploying an integrated private network is impossible. The UEs are installed inside the Airbase's premises, which means there is no need for extended coverage, being this a decision factor in selecting the type of independent private network. Protection is paramount for the infrastructure, leading to the necessity of having the highest degree of control and customisation. Thus, limited and exclusive access to the private network's resources must be provided, ensuring high-performance levels for its use cases. The fact that military facilities are versatile and have different levels of responsiveness makes it mandatory to have significant flexibility to customise the network architecture, structure, and services to meet its specific needs. These critical services also require redundancy and resilience, which must be managed by the entity responsible for the network structure. Therefore, the Portuguese Air Force has to ensure that the network has these specific performance needs by having direct control over the QoS parameters and taking responsibility for network maintenance, upgrades and support. Thus, the best choice is an independent private 5G LAN by the Portuguese Air Force.

4.2.2 Flight Simulator services

Regarding the Flight Simulator services, communication link requirements differ from Security and Control services. Flight Simulators are used for training purposes, and while real-time communication is still essential, the consequences of communication interruptions or errors are not as critical as in surveillance or detection. Higher data rates and low-latency communication are still desirable to provide pilots or trainees with a realistic and immersive experience. At the same time, robustness and reliability are crucial and achieved with lower-order modulations. Due to the extremely high data rates of the Virtual Reality service, to be able to provide the service using 5G, it is necessary to appeal to the radio characteristics that maximise the throughputs (maximum CQI and a maximum number of MIMO layers). However, it is not feasible since it would increase sensitivity to signal fading and propagation challenges. It also leads to higher computational requirements and processing delays.

According to Figure 4.5 a), 5G provides enough throughput in both UL and DL to ensure Flight Simulator services. Using the radio characteristics that maximise the 5G total DL and UL throughputs, the results are 1930.43 Mbps and 1456.29 Mbps, respectively. The required DL and UL throughputs are 1066.66 Mbps and 925.18 Mbps, respectively.

In Figure 4.5 b), it is possible to verify that if the radio characteristics are used close to the standard service utilisation (CQI of 12 and 4 MIMO layers), the total DL and UL throughputs are 723.39 Mbps and 545.72 Mbps, respectively. Therefore, 5G does not provide enough throughputs in the UL and DL. In both cases, the data rate requirements are at the high end of the potential interval; hence, the necessary UL and DL required throughputs that would exist in a practical situation would be lower and, in the last case, possibly ensured by 5G. For example, streaming high-definition video may need high data rates during peak usage, but these data rates can be lower at other times without affecting the user experience. The radio characteristics (MIMO layers and CQI) do not influence the latency contributions associated with the nodes and links, only the throughputs of the RU node.

It should be emphasised that the UEs are in the same department division, unlike the Security and Control Systems. Therefore, the AL propagation latency contribution of 0.0003 ms is applied to both the transmitter and receiver sites. Regarding the total node latency, presented in Table 4.7, it is possible to verify that when the MEC node is not installed, the total node latency exceeds the latency requirement associated with the Flight Simulator services. Thus, the network architecture without the MEC node is excluded from the analysis.

The maximum optical link’s propagation latency, presented in Table 4.8, is only calculated for the RU-DU, DU-CU and CU-Core deployment options. In this case, it is considered that the RU node is deployed near the department where the Flight Simulators are installed.

This decision was taken because, after calculating the throughputs of the RU node using the maximum radio characteristics, it was verified that it would not be possible to allocate all the Airbase systems (Security, Control and Flight Simulators) to the same RU node due to the Flight Simulator's high data rate requirements.

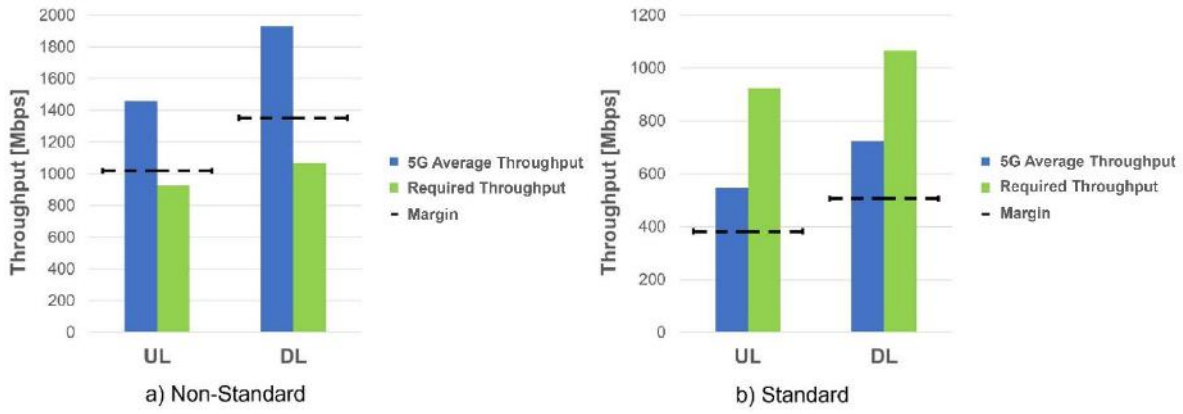

Figure 4.5 – Flight Simulator – RU throughputs using non-standard and standard radio characteristics.

Table 4.7 – Flight Simulator – Total node latencies for all MEC node deployment options.

MEC Node Deployment Option	Total Node Latency [ms]
None	4.959
RU-DU	0.879
DU-CU	1.909
CU-Core	2.839

Therefore, the calculation of the maximum E2E latency is practically influenced by the total node latency because the contribution of the AL propagation latencies are insignificant due to the proximity of the RU node to the UEs. The maximum optical link distance associated with each MEC node deployment option is also presented in Table 4.8.

Table 4.8 – Flight Simulator Systems – Maximum optical link's length and propagation latency for each MEC node option.

MEC Node Deployment Option	Maximum Optical Link Length [km]	Maximum Optical Link's Propagation Latency [ms]
None	-	-
RU-DU	186	0.869
DU-CU	125	0.584
CU-Core	70	0.327

The results obtained for the maximum E2E latency and the maximum E2E distance are shown in Table 4.9. Like the Security and Control Systems, the latency margin is 3.6 ms, so the RU-DU, DU-CU and CU-Core deployment options can be considered.

Compared to the Safety and Control services, the Flight Simulator services are restricted to a single department in the Airbase. Therefore, the interior space is relatively small, with a restrictive area and UEs close to one another. Based on the distance defined between the UEs and the RU node, it can be verified that the coverage radius associated with the femtocell is sufficient to ensure the service requirements. It is an adequate type of cell that guarantees a stable and robust signal connection in restrictive indoor spaces. It also operates on lower transmit power than microcells, reducing potential interference and ensuring that each Flight Simulator have a robust network connection to meet the requirements.

Table 4.9 – Flight Simulator Systems – Maximum E2E latency and maximum E2E distance for each MEC node option.

MEC Node Deployment Option	Maximum E2E Latency [ms]	Maximum E2E Distance [km]
None	-	-
RU-DU	1.749	186
DU-CU	2.494	125
CU-Core	3.167	70

As such, the femtocells using millimetre wave frequency bands can ensure high data rates, low latency, and secure communication capabilities. The challenges associated with the millimetre wave technology can be mitigated by strategically deploying the RU node around the Flight Simulator Department. This deployment provides coverage exactly where needed, minimising interference. This cell type can also be easily scaled up to accommodate changes in the number of services used. This choice allows offloading traffic from the other RU nodes, ensuring the services' requirements.

Regarding the best MEC node deployment option, installing the RU-DU option inside the Airbase N.º6 premises is considered the most adequate choice. This deployment ensures that latency-sensitive data processing, including real-time user interactions, occurs close to the edge, enabling immediate adjustments in the simulation tests. From the analysis of Table 4.9, it is possible to conclude that this deployment has the lowest E2E latency, which leads to an immediate and realistic user experience.

Therefore, the choice of the most suitable type of private network is influenced by the results obtained in Figure 4.5 a) and Figure 4.5 b) since the latency margin is not exceeded. Figure 4.5 a) shows that the throughput margin is not exceeded when the radio characteristics that maximise the throughputs of the RU node are used. Thus, network slicing (RAN and Core sharing) is the best deployment for an integrated private network. It allows dedicated resources to be allocated, ensuring the services receive the necessary bandwidth, latency and QoS levels. The isolation prevents other services from affecting the performance of the simulation. Therefore, during peak usage, a Service Level Agreement (SLA) can be defined so that the Flight Simulator slice can continue to ensure smooth and consistent performance.

Figure 4.5 b) shows that the margin applied to the RU node throughputs is exceeded on the UL and DL sites, requiring an independent private network deployment. Because the service is non-critical, some latency or occasional performance variations can be tolerated without significant negative consequences. Therefore, an MNO may deploy and manage the private network infrastructure, where resources are shared among multiple users, as multitenancy optimises resource utilisation. The customisation options can be more standardised because the service's priority is lower than the Security and Control services. Therefore, an MNO can provide predefined network slices based on the Portuguese Air Force's requirements, making maintenance and support from outside. Network security and isolation are also essential, although a high level of measures is unnecessary, making the share of the infrastructure network possible without compromising the respective functionality.

When comparing these two approaches, it should be considered that the non-standard radio characteristics selected are susceptible to interference and noise, requiring a complex hardware deployment, limited benefits in non-optimal conditions and incompatibility with most devices. Thus, if

these factors significantly influence the performance of the service, the Portuguese Air Force's use of an independent 5G LAN must be considered when adopting the non-standard radio characteristics.

In conclusion, choosing the type of private network to be installed at the Airbase must consider the systems and requirements of the respective services. Based on the analyses made and assessing the options for the type of installation, the Portuguese Air Force should adopt an independent 5G LAN covering the systems previously analysed. It is an adequate option due to its capacity to deliver secure, dependable, low-latency, and highly adaptable communication solutions customised to the particular needs of military and defence activities. Although installing an integrated private network is possible in the case of non-critical Flight Simulator services with non-standard radio characteristics, there is always the need to prioritise the mission associated with an Airbase and the respective responsibilities. In this case, only an independent private network allows for complete control over compliance and the ability to enforce security and governance measures effectively.

4.3 WAM System Scenario

4.3.1 Air Traffic Control service

The WAM System employs GSs with sensors and receivers strategically placed across a wide area. The GSs have an antenna mast of 12 m and an average altitude of approximately 240 m above the mean sea level. The flight level FL300 (9 144 m) is selected to test if the maximum flight altitude used in [61] allows to establish communication between the UEs and the GSs. This flight level, used as the distance between the transmitting UEs and the RU node, was used in [61] as a test flight level to analyse and study the accuracy of the WAM system.

The LoS radio horizon distance is computed using (3.39). The GS's average altitude is used as the effective distance of the GS's antenna to the Earth's centre, and the flight level FL300 is used as the effective distance of the aircraft's antenna to the Earth's centre, both above the MSL. Based on the values assigned to the respective variables, a radio horizon distance of 308 km is obtained. This value corresponds to the maximum radio link length in LoS with optimal conditions. It is computed to check if the distance between the transmitting UEs and the RU node is viable for establishing communication. The approach taken in this model neglects the distance between the GSs and the RU node because it is insignificant compared to the flight level selected.

Despite the aircraft's movement, the scenario analysis is done at the instant when 3 GSs capture information referent to a target. In this case, the RU node that transmits and receives the Air Traffic Control data packets is the same, collecting the data from the 3 GSs and sending it to the Control Centre. A CQI of 9 is used in the simulation. It is important to note that the primary focus of a WAM System is not achieving high QoS but delivering precise and timely location information to track objects. Thus, very high data rates are not required.

Figure 4.6 shows that 5G provides enough UL and DL throughputs to guarantee all users' connectivity. The DL and UL average throughputs are 475.01 Mbps and 358.34 Mbps, above the required 355.16 Mbps and 273.76 Mbps, respectively.

Regarding the AL propagation latencies contributions, the results are influenced by the altitude of the aircraft and the straight-line distance between the Control Centre (EMFA) and the Airbase used as an example (Airbase Nº.1), as shown in Figure 4.7. The AL propagation latency contributions on the transmitter and the receiver sides are 0.0305 ms and 0.0367 ms, respectively.

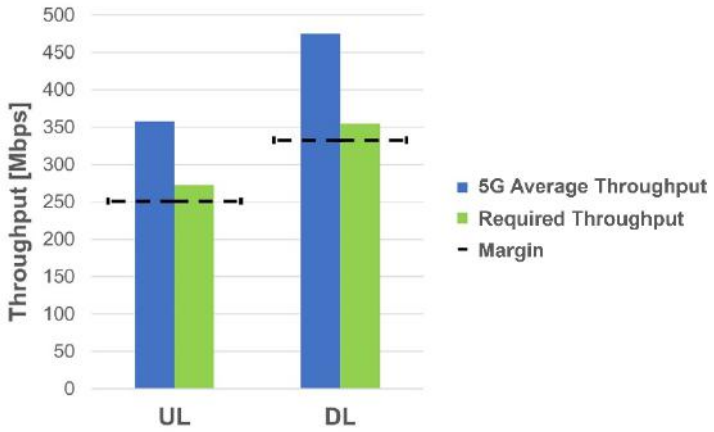

Figure 4.6 – WAM System – RU throughputs for the Aircraft-GS link communication.

After analysing the results in Table 4.10, it is possible to verify that when opting for a network architecture without an MEC node deployment, the total node latency is much higher than the latency required by the service. Therefore, this network structure is excluded since estimating the length of the optical links is impossible. The remaining options are below the requested value.

Table 4.10 – Air Traffic Control service – Total node latencies for all MEC node deployment options.

MEC Node Deployment Option	Total Node Latency [ms]
None	113.058
RU-DU	5.128
DU-CU	5.988
CU-Core	6.858

The maximum optical link length, presented in Table 4.11, is mainly influenced by the total node latency contribution, which is influenced by the MEC node deployment option. The total node latency is higher than both AL propagation latency contributions in this case. The respective maximum optical link's propagation latency is calculated based on the length of the links, and it is also presented in Table 4.11.

From the analysis of Table 4.12 and the obtained UL and DL required throughputs presented in Figure 4.6, it is possible to verify that the throughput margin is exceeded on the UL and DL side. The E2E latency margin of 7.6 ms is not exceeded for the RU-DU, DU-CU and CU-Core MEC node deployment options. Therefore, deploying an integrated private network is impossible. The maximum E2E distance is also presented in Table 4.12.

Figure 4.7 – Map positions of the WAM System's GSs, Control Centre (EMFA) and Airbase Nº.1 with a representation of a straight-line connection (11 km) between the Control Centre and the RU node.

Table 4.11 – Air Traffic Control service – Maximum optical link's length and propagation latency for each MEC node option.

MEC Node Deployment Option	Maximum Optical Link Length [km]	Maximum Optical Link's Propagation Latency [ms]
None	-	-
RU-DU	168	0.785
DU-CU	116	0.542
CU-Core	64	0.299

Table 4.12 – Air Traffic Control service – Maximum E2E latency and maximum E2E distance for each MEC node option.

MEC Node Deployment Option	Maximum E2E Latency [ms]	Maximum E2E Distance [km]
None	-	-
RU-DU	5.986	188
DU-CU	6.602	136
CU-Core	7.229	84

Regarding the distance between the UEs and the RU node, the macrocell is the only cell type that ensures the required coverage radius, offering signal propagation that guarantees the connection of many users to a single RU node. The most suitable frequency band is the 0.7 GHz band because it provides a longer coverage radius by allowing the tracking of a wide geographical area. It also ensures viable communication since it generates a robust signal that is adequate and required for air operations safety. The choice of the macrocell with a frequency of 0.7 GHz is supported by its coverage, reliability, interference-resistant and throughput characteristics.

Since the Air Traffic Control service is not mission-critical, enabling effective resource utilisation through dynamic resource allocation is possible depending on the traffic volume. Moreover, the infrastructure can be shared with an MNO to reduce the installation costs because the GSs are dispersed over a large geographical area. In the case of interference management, WAM systems frequently operate in

congested airspace, having interference from other services or systems that can affect their performance. The latency, reliability, and throughput requirements from various aircraft types may vary, which leads to the need to create dedicated slices with personalised QoS profiles to ensure that each data type receives the proper level of service.

Regarding the MEC node deployment, the RU-DU is the best option. However, the CU-Core is the most adequate due to the geographical distribution. The latter ensures that the maximum E2E latency keeps below the required value, reducing the MEC node's complexity and processing capacity. The maximum E2E latency associated with this deployment results mainly from the processing latency of a fixed number of nodes, although it can oscillate due to traffic aggregation. Therefore, it is necessary to consider this factor, and in this case, the RU-DU option can achieve the lowest E2E latency. However, the CU-Core option balances processing and system complexity because the network structure is applied to a large geographical area, complicating scalability if the number of RU nodes needs to be increased.

In conclusion, the type of independent private network should ensure all of these specific requirements, operational needs and technical constraints. An independent 5G LAN network by an MNO is indicated because it provides customised, efficient, and cost-effective network performance. It also provides regulated and dedicated communication channels, lowering the possibility of network interference or congestion that could compromise reliability, which reduces the risk of unauthorized access. Like the Flight Simulator services, an SLA can also be defined so that the slice can continue to ensure smooth and consistent performance of the Air Traffic Control service.

4.3.2 Weather Monitoring services

In the WAM System’s ground communications, collecting, analysing, and disseminating weather-related data is essential to support aviation operations. The analysis is referent to the Video Surveillance and Sensor services installed on GSs closer to the RU node. Unlike the Air Traffic Control service, the distance between the RU node and the GSs is not despised. The RU node that receives the data packets from the three GSs is the same one that transmits them to the Control Centre. Because this node allocates the three services associated with the WAM Systems, the CQI of 9 used for the Air Traffic Control service is also used for the Weather Monitoring ones.

Figure 4.8 shows that 5G provides enough UL and DL throughputs to guarantee all users’ connectivity. The DL and UL average throughputs are 508.14 Mbps and 383.34 Mbps, above the required 353.41 Mbps and 285.51 Mbps, respectively.

Concerning the network latency contributions, the transmitter site's AL propagation latency differs from the receiver site. The data is transmitted from the sensors and cameras to the RU node and from the RU node to the Control Centre. Therefore, the transmitter site's AL propagation latency (0.0006 ms) is lower than the respective Air Traffic Control service. The AL propagation latency on the receiver site is 0.0367 ms.

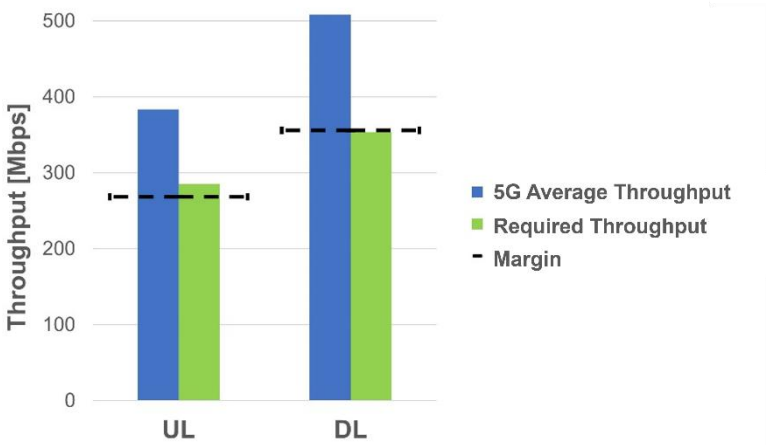

Figure 4.8 – WAM System – RU throughputs for the ground communications.

The total node latencies influenced by each MEC node deployment option are presented in Table 4.13. From the result analysis, it is verified that the non-deployment MEC node and the CU-Core options exceed the service-required latency. Therefore, these two types of architecture are excluded since estimating the length of the optical links is impossible.

Table 4.13 – Weather Monitoring services – Total node latencies for all MEC node deployment options.

MEC Node Deployment Option	Total Node Latency [ms]
None	30.263
RU-DU	3.093
DU-CU	7.963
CU-Core	10.283

Therefore, the contributions of the RU-DU and DU-CU options for calculating the maximum optical link's propagation latency are presented in Table 4.14.

Table 4.14 – Weather Monitoring services – Maximum optical link's length and propagation latency for each MEC node option.

MEC Node Deployment Option	Maximum Optical Link Length [km]	Maximum Optical Link's Propagation Latency [ms]
None	-	-
RU-DU	411	1.921
DU-CU	121	0.565
CU-Core	-	-

The maximum E2E latency and maximum E2E distance obtained from estimating the length of the optical links are shown in Table 4.15. As the service is not critical, the latency margin is 9.5 ms, meaning that the RU-DU and DU-CU MEC node deployment options will ensure the service even if the maximum length of the optical links is chosen. The results used to calculate the distance at which the MEC node can be installed are also shown in Table 4.15. In the case of the RU-DU option, the maximum E2E distance value is high because the total node latency is significantly lower than the latency required by the services (10 ms). This gap is reflected in the computation of the maximum optical link length.

Table 4.15 – Weather Monitoring services – Maximum E2E latency and maximum E2E distance for each MEC node option.

MEC Node Deployment Option	Maximum E2E Latency [ms]	Maximum E2E Distance [km]
None	-	-
RU-DU	5.051	422
DU-CU	8.565	132
CU-Core	-	-

The frequency band used to establish the AL's communication influences the maximum distance at which the UEs can be from the RU node. In order to ensure the distance previously selected for these services, the use of microcells is considered.

The adequate frequency band also depends on the geographical location. If the RU node is deployed in a rural area, it is not necessary to prioritise high data rates, so the 0.7 GHz frequency band is a suitable choice. If deployed in an urban or suburban area, it is necessary to balance capacity and coverage, leading to the selection of the 3.6 GHz and 6.0 GHz frequencies. Finally, if the location is in a dense urban area, high capacity is required, especially for the video surveillance service, with the millimetre band as the most suitable frequency.

As a non-critical service, the video and images captured by the surveillance cameras do not have to be high quality. However, it is necessary to guarantee the minimum requirements that allow users in the Control Centre to correctly analyse the information coming from the video surveillance cameras and sensors. As services are provided outdoors, ensuring the penetration of possible obstacles is necessary to guarantee the required latency. However, it is also necessary to consider that the RU node receives standard video services from other applications (i.e., video conferencing). Therefore, it requires enough bandwidth to provide both types.

From the analysis of the UL and DL required throughputs in Figure 4.8, it is possible to conclude that the required throughput on the UL side is above the defined margin. However, the maximum E2E latency is not exceeded. As a result, an independent private network should be deployed. These services do not require allocating dedicated resources (bandwidth, latency, capacity) tailored to the respective UEs. However, allocating capacity based on the desired QoS without interference from other applications and UEs continues to be necessary. The demands of Video Surveillance and Sensor services change over the day, so resource allocation should be made based on the necessity applied by the Control Centre. From these characteristics, an independent 5G LAN network by an MNO is the best independent private network because it can allocate virtual networks for different services while maintaining QoS and isolation.

It should be noted that in a real scenario, the RU node should be shared by the services that comprise the WAM System. As such, the network that allocates the Air Traffic Control service should also allocate the Weather Monitoring services, which means that the CU-Core is not an option. Thus, the RU-DU deployment is considered the best choice regarding the constraints applied because Air Traffic Control is prioritised over data collection via surveillance cameras and sensors.

In conclusion, deploying an independent 5G LAN by an MNO within the Portuguese Air Force WAM system represents a collaborative strategy that complements the strengths of both sides. While

preserving control, compliance, interoperability, and data integrity standards, it offers an unmatched level of security, dependability, low latency, and flexibility. In order to maintain the security and safety of the airspace, this coordinated effort guarantees that weather and airspace data remains accurate, preserving the integrity of critical information.

4.4 991 Squadron Scenario

4.4.1 Remote-Controlled UAV Systems – inside premises

The approach applied to the 991 Squadron scenario is similar to the WAM System. In this case, the UAV is flying at 300 m. It is estimated that the UAV can detect 18 GSs, with the furthest one up to 18.5 km [62]. This analysis considers the moments of testing the UAV and checking specific parameters, which take place within the Airbase's perimeter where the Squadron is inserted. The RU node that transmits and receives the service's data packets is the same, and the distance between the transmitting UEs and the RU node corresponds to the UAV flight level.

Regarding the radio characteristics, it is crucial to match the communication capabilities of the UAV with the specific requirements of the mission. High data rates can be necessary for real-time decision-making and mission success, but they also come with considerations such as communication range, available bandwidth, and signal strength. Therefore, an average CQI of 12 is used. From the analysis of Figure 4.9, it is possible to conclude that 5G provides enough UL and DL throughput to guarantee all users' connectivity inside the Airbase's perimeter. The DL and UL average throughputs are 676.21 Mbps and 510.13 Mbps, above the required 344.86 Mbps and 123.81 Mbps, respectively.

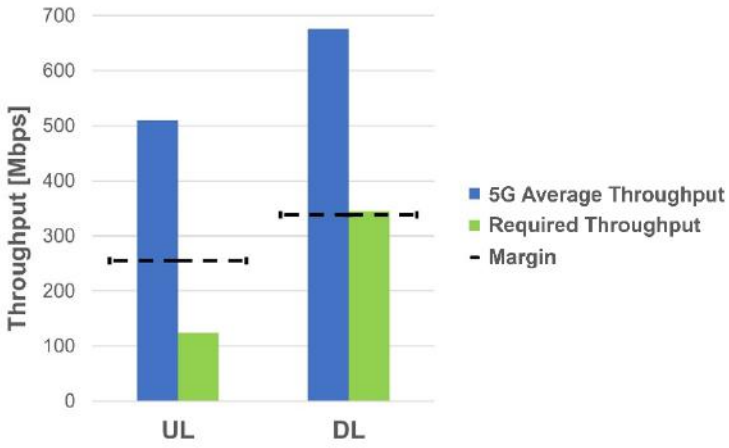

Figure 4.9 – 991 Squadron – RU throughputs inside the premises.

In this scenario, the transmitting and receiving UEs are assumed to be at the same distance from the RU node. Therefore, the ALs propagation latencies contributions are equal on both sides, with a value of 0.0013 ms. The total node latency is presented in Table 4.16 for all the MEC node deployment options. By analysing the results, it is possible to verify that the total node latency exceeds the latency required by the system services when the MEC node is not installed. The remaining options have a total node latency lower than the latency required by the Remote-Controlled UAV services.

As in the previous scenarios, the maximum length that the optical links can have is calculated based on the results obtained for the total latency of the nodes and the propagation latency associated with the ALs. The results are presented in Table 4.17. These services have extremely low latency, and the respective contributions (total node latency and AL propagation latencies) are also minimal. Therefore, the estimated values for the optical links' length are lower than those obtained for the other scenarios.

Table 4.16 – Remote-Controlled UAV services inside premises – Total node latencies for all MEC node deployment options.

MEC Node Deployment Option	Total Node Latency [ms]
None	1.317
RU-DU	0.207
DU-CU	0.237
CU-Core	0.267

The results obtained for the maximum E2E latency and the maximum E2E distance are shown in Table 4.18. Regarding the MEC node deployment options, the RU-DU, DU-CU and CU-Core are below the margin of 0.45 ms defined to the required latency. The analysis of Figure 4.9 makes it possible to verify that only the required throughput on the UL side is significantly below the margin. In contrast, the required throughput on the DL side is slightly above.

Table 4.17 – Remote-Controlled UAV services inside premises – Maximum optical link's length and propagation latency for each MEC node option.

MEC Node Deployment Option	Maximum Optical Link Length [km]	Maximum Optical Link's Propagation Latency [ms]
None	-	-
RU-DU	17	0.079
DU-CU	15	0.070
CU-Core	14	0.065

In this scenario, operations are carried out close to the Control Centre, reducing the required coverage radius. In addition to this factor, the data rates are lower than the Security and Control services since the analysis concerns only 3 UAVs. The distance between the UEs and the RU node leads to choosing microcells and picocells to create a highly customised and efficient network infrastructure for a specific operational area. The microcells offer precise control over coverage areas, minimising interference from other devices. This cell type is selected considering the UAVs are in the Airbase area. i.e. operational and flying within the premises no more than 2 km from the Control Centre.

Table 4.18 – Remote-Controlled UAV services inside premises – Maximum E2E latency and E2E distance for each MEC node option.

MEC Node Deployment Option	Maximum E2E Latency [ms]	Maximum E2E Distance [km]
None	-	-
RU-DU	0.289	18
DU-CU	0.310	16
CU-Core	0.335	15

Based on this description, the 3.6 GHz is the most suitable frequency, as it establishes a balance between coverage and capacity, guaranteeing reliable control of the UAV. It has a moderate obstacle penetration if Non-Line of Sight (NLoS) zones exist. Thus, it is sufficient for all outdoor operations in the

area corresponding to the BS's facilities, even though it has a limited range compared with the 0.7 GHz frequency.

As for maintenance, inspection or simulation tests of UAV systems, which are carried out inside the infrastructure, picocells are a suitable option as they provide highly localised coverage, making them ideal for close-range UAV operations. When the UAV operations are restricted to a hangar, using millimetre wave frequencies can be a practical choice, as the necessary infrastructure exists to support the communication needs in the hangar environment. These bands can also provide low-latency communication, ensuring the control signals and video streams have a minimal delay.

In this scenario, the best option for installing the MEC node is inside the facilities between the RU and DU nodes to reduce the latency's probability of exceeding the maximum allowed value. It is also the option that achieves the lowest latency for the services.

Regarding the previous analysis, it is concluded that deploying an integrated private network is impossible. In this scenario, it is necessary to have complete control over the network to prioritise the needed resources. Thus, isolation from traffic is requested to ensure consistent performance. In order to achieve ultra-low latency communications, it is essential to deploy the network infrastructure close to the Control Centre to allow real-time tracking of the UEs. Reliability is another crucial factor that affects critical operations when not guaranteed, leading to the necessity of having an optimised network explicitly designed for the Remote Control service. There are also situations where the UAV demands specific requirements from changes in the environment, like variations in the wind, which demands the allocated resources to be applied explicitly by the network. As a result, after analysing all the service characteristics, it can be concluded that the best option for a private independent network is the 5G LAN by the Portuguese Air Force.

4.4.2 Remote-Controlled UAV Systems – outside premises

In this case scenario, the RU node that transmits and receives the data packets differs, and the distance between the transmitting UE and the RU node corresponds to the farthest GS the UAV can detect in LoS. Thus, there is an RU node to which the Control Centre sends the Control Manipulation data packets, which is different from the one that the UAV sends the Telemetry and Video Streaming data packets. The Control Manipulations are sent in the UL of the Control Centre site and received in the DL of the UAV site. Both the Video Streaming and the Telemetry data packets are sent in the UL of the UAV site and received in the DL of the Control Centre site.

5G provides enough DL and UL throughputs outside the facilities to guarantee connectivity. Figure 4.10 shows that the DL and UL average throughputs are 676.21 Mbps and 510.13 Mbps, respectively. On the Control Centre site, the required DL and UL throughputs are 338.38 Mbps and 66.18 Mbps, respectively, and on the UAV site, the required DL and UL throughputs are 128.47 Mbps and 119.47 Mbps, respectively. Thus, both sites have throughputs below the average throughput of the network.

Compared to the scenario analysed inside the premises of the Airbase, the distance between the transmitting UEs and the RU node is significantly larger than the distance between the receiving UEs

and the other RU node. Thus, the contribution of the AL propagation latency in transmission (0.0617 ms) is higher than the AL propagation latency in reception (0.0013 ms).

The fact that the services to be analysed are the same and have the same radio characteristics means that the total node latency, influenced by the MEC node deployment option, is the same for the inside and outside the premises. This latency contribution only depends on the number of nodes in the network structure. The results are presented in Table 4.16.

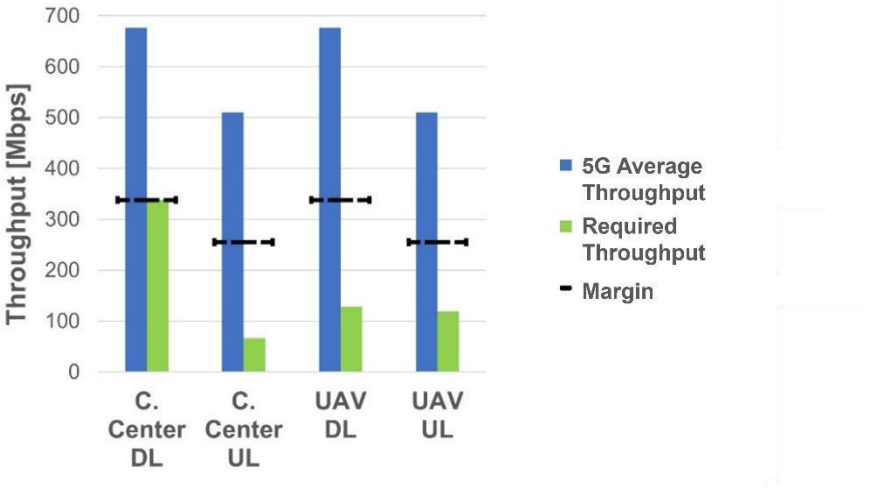

Figure 4.10 – 991 Squadron – RU throughputs outside the premises.

However, the maximum values of the optical link length differ because the contribution of the AL propagation latency on the transmitter side differs from the AL propagation latency when the UAV is on the Airbase premises. As in the analysis of the previous scenario, the network architecture without the MEC node cannot be analysed since the total node latency is higher than the extremely low latency required by the service. It is, therefore, only possible to estimate the length of the optical links for network structures that have the MEC node installed between the RU-DU, DU-CU and CU-Core nodes. The results are presented in Table 4.19.

From the analysis of Table 4.20, the RU-DU, DU-CU and CU-Core options do not exceed the latency margin of 0.45 ms. On the other hand, it is possible to verify, from the analysis of Figure 4.10, that the required DL throughput in the Control Centre site slightly exceeds the margin defined for the DL RU node throughput.

Table 4.19 – Remote-Controlled UAV services outside premises – Maximum optical link's length and propagation latency for each MEC node option.

MEC Node Deployment Option	Maximum Optical Link Length [km]	Maximum Optical Link's Propagation Latency [ms]
None	-	-
RU-DU	14	0.065
DU-CU	12	0.056
CU-Core	11	0.051

Table 4.20 – Remote-Controlled UAV services outside premises – Maximum E2E latency and maximum E2E distance for each MEC node option.

MEC Node Deployment Option	Maximum E2E Latency [ms]	Maximum E2E Distance [km]
None	-	-
RU-DU	0.335	33
DU-CU	0.356	31
CU-Core	0.371	30

When the distance between the UAVs and the RU node is more than 2 km, microcells no longer provide the required coverage to ensure communication. The most suitable option is, therefore, macrocells. UAVs are estimated to detect the furthest RU node up to 18.5 km. By analysing Table 4.20, it is possible to verify that all the MEC node deployment options allow for establishing communication at that distance. As the maximum coverage distance of the macrocell is 30 km, it is possible to ensure communication between the UAVs and the RU node.

In this scenario, the UAVs are dispersed across a vast region. As a critical scenario, it requires a strategic deployment of the RU nodes and the implementation of network management and handover mechanisms to facilitate seamless transitions between the RU nodes as the UAVs move within the coverage area. Regarding the frequency, the 0.7 GHz offers excellent outdoor coverage, is less affected by environmental conditions, and maintains connectivity when UAVs operate near structures.

The best MEC node deployment option is between each RU-DU node that collects data from the UAV. When the communication is established, it corresponds to the RU node closest to the UAV. Even though this is a simulated possibility, it is the option that achieves the lowest latency, which is a critical condition for the proper functioning of the services. However, regarding scalability, it is necessary to consider some constraints when opting for this architecture. The RU-DU option increases the complexity of the network architecture, affecting the capacity to accommodate increased traffic and processing demands efficiently. In this case, if the MEC node experiences issues, the entire communication path between the RU and DU nodes is affected, compromising the entire network structure. Therefore, the CU-Core deployment option should also be considered because it ensures the latency requirements and reduces the complexity of the network architecture.

In conclusion, an independent private network deployment is necessary. Concerning all the service requirements in Section 4.4.1, it is crucial to demand them outside the reserved military area. Compromised or disrupted communications are not tolerable, even when the UAV is several kilometres away. Thus, ensuring the service's dedicated resources, security, and isolation is necessary. The Remote Control service must work in a large coverage area to guarantee that the UAV's control signals are reachable in the Control Centre. In this way, consistent and uninterrupted connectivity is crucial for real-time control and QoS. The network management and control mechanisms continue to be prioritised. They must be optimised to establish communication considering environmental adversities, such as increased volume traffic and interference, which depends on the region the UAV is flying over. Therefore, considering the costs and management of deploying a private network that can be extended for a long coverage area but with reduced investment in the ground infrastructure is required. Thus, a private 5G LAN by an MNO is the best choice. It allows integration with existing infrastructure, scalability,

authentication mechanisms and security through encryption. In this case, regulatory compliance with spectrum management is associated with a dedicated network slice and a wide distribution of RU nodes.

This scenario provides services with extremely low latency. It is, therefore, necessary to analyse both situations. Installing a 5G private LAN entirely controlled by the Portuguese Air Force within the Airbase's perimeter is possible because system maintenance is restricted to a specific area. However, when the UAV is moving, the distance must be considered.

The fact that the UAV is a mobile UE makes it necessary to guarantee its requirements in any geographical area. As such, the private 5G LAN by the Portuguese Air Force is not a good strategy when the UAV is outside the Airbase's perimeter. It is, therefore, necessary to resort to an MNO with the ability to incorporate redundancy, failover and handover mechanisms into their networks to ensure high reliability. This capacity is crucial for UAV operations, where uninterrupted connectivity is essential to prevent mission disruption. MNOs also continuously invest in network innovation and improvement, meaning the Portuguese Air Force can benefit from the latest technological advancements and network enhancements without needing to develop them internally.

4.5 Systems Redundancy

The service's systems redundancy is intended to enhance reliability, fault tolerance, and resilience by providing backup options in case of component failure, errors, or disruptions. The following analysis focuses on two perspectives. One refers to the redundancy ensured by the throughputs provided by the RU nodes, and the other refers to the redundancy ensured by the network structure. The RU node's redundancy is more localised over a smaller coverage radius. In contrast, the redundancy provided by the network structure covers a larger geographical area. The analysis covers the systems common to all the Portuguese Air Force facilities, i.e., the Security and Control Systems. It also covers the WAM System due to the distribution of GSs over a large geographical area, which makes the analysis specific and with a different approach.

Concerning the Airbase scenario, the Airbase N.º6 is used as the object of study. Figure 4.11 shows four Portuguese Air Force facilities within a radius of 30 km centred at the Airbase, corresponding to the maximum coverage distance the RU node reaches in this scenario. However, the fact that the required throughput exceeds the defined margin means that it is impossible to consider the same RU node to ensure the redundancy of the same services within a coverage radius of up to 30 km, i.e., the same RU node cannot provide to more than one facility unit the same services using the 5G network. As a result, the remaining facilities must install more than one backup RU node ready to switch on control if the primary RU node fails. The backup nodes have the same throughputs and functionalities, ensuring a seamless transition. The RU node should have the exact specifications as the RU node from the Airbase scenario to ensure the exact services requirements.

The redundancy ensured by the network structure is related to the maximum E2E distance. Once the RU-DU option has been selected, the maximum distance the MEC node can be deployed from the UEs is influenced by the respective maximum E2E distance. As shown in Figure 4.12, if the RU nodes are

characterised with the exact specifications as the RU node deployed at the Airbase scenario, the facilities within the computed radius have their services ensured because the distance from each facility to the circumference, corresponding to the possible locations to deploy the MEC node, is always less than 91 km. In this case, if all RU nodes could be allocated to the same MEC node, each RU node should be part of an architecture with a specific optical link length, depending on the distance from the MEC node, to fulfil the exact Security and Control Systems requirements. Considering the simulation's parameters, the respective services are also ensured if an MEC node is at a maximum of 91 km from each facility.

Figure 4.11 – Portuguese Air Force facilities covered by the 30 km radius of the RU node at Airbase N.º6.

Regarding the WAM system, it is impossible to ensure redundancy for more than 3 GSs at a time due to the maximum coverage radius allowed for the RU node. If the GSs are located close to each other, as shown in Figure 4.7, installing more than one RU node is necessary to ensure redundant communications within the 5G network since the margin is exceeded if just one RU node is used. In cases where at least two GSs are more than 30 km apart, it is necessary to install a single RU node for each GS and consider installing a backup RU node in case of failure. Therefore, increasing the deployment of RU nodes to twice the required number is necessary. Regarding the system's redundancy, it is considered that the WAM system is characterised as the Air Navigation Portugal (NAV Portugal) implemented system, with results suggesting that the system has a reasonable degree of redundancy, displaying negligible reductions in coverage of as low as 2% when two out of twelve GSs are removed [61].

Concerning the maximum E2E distance, it is necessary to analyse the two types of services since the distances from the UEs to the RU node are different. About the Air Traffic Control service, the maximum distance the MEC node can be installed from the analysed UEs (aircraft) is 42 km, computed using the selected CU-Core option presented in Tabel 4.12. It is the most suitable option for the service type based on the environment and requirements. In this way, all MEC nodes installed at a maximum

distance of 42 km from the UEs can fulfil the requirements of the Air Traffic Control service. This statement can be applied to the entire geographical area covered by the GSs.

In the case of the Weather Monitoring services, the maximum distance at which the MEC node can be installed from the UEs is computed using the maximum E2E distance obtained by the RU-DU option, presented in Table 4.15, since it allows the lowest E2E latency to be obtained, even though it corresponds to a significant maximum E2E distance of 211 km. Based on this distance, it would be possible to deploy an MEC node at the distance required by a significant percentage of GSs to ensure the respective service latency. In this way, the architecture of the WAM System network could be expanded so that a single MEC node could allocate all the RU nodes. However, the redundancy of the service would be compromised since a failure in the MEC node would affect the communication of the entire network. Therefore, installing more than one MEC node in strategic sites is required to guarantee the date collection of all the GSs.

Based on the previous analysis and reinforcing that the redundancy of the systems is crucial to critical and non-critical services, some constraints, like cost, complexity, and maintenance, must be considered. Redundancy implementation can be expensive because it usually involves duplicating resources and infrastructure parts. For some systems, this extra cost might not be justifiable. Regarding complexity, it can be more challenging to design, implement, and maintain a system with redundancy. Lastly, ensuring that all redundant components are in working order and synchronised is an ongoing task, being labour-intensive and requiring constant maintenance with additional resources.

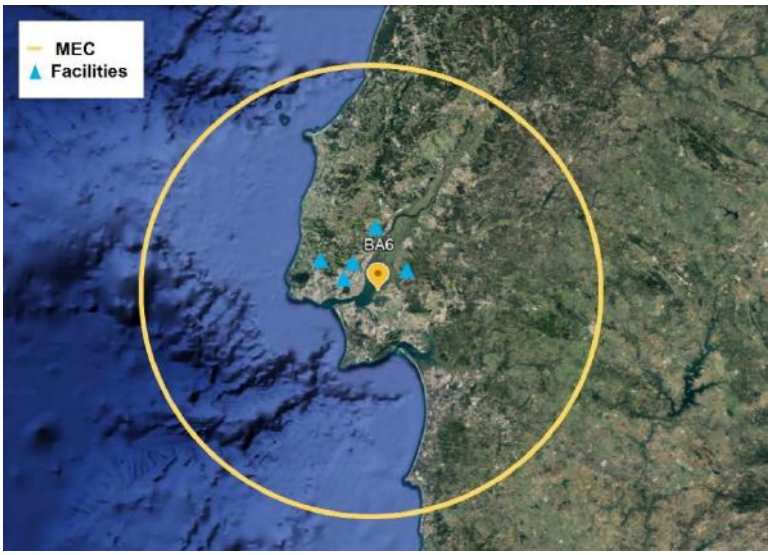

Figure 4.12 - Possible MEC node deployment locations that ensure the services requirements of Airbase N.º6.

In conclusion, in the case of Security and Control Systems, it is necessary to ensure the redundancy of all services as they drastically influence and condition the operability of the Portuguese Air Force facilities in the event of a failure. As such, it is impossible not to resort to redundancy in these services for indoor and outdoor environments and inter facilities. In the case of the WAM System, and despite being considered a non-critical service, redundancy is required due to the extensive geographic distribution.

Chapter 5

Conclusion

The main results from the work are presented in this chapter, which completes the thesis. It starts by formulating the addressed problem, and then the conclusions from the several chapters are presented. The developed model is then summarised, and recommendations for further research are given. The chapter concludes with suggestions for improving upcoming uses of 5G private networks in the military context.

The main objective of this thesis is to analyse the feasibility and potential of installing 5G private networks at Portuguese Air Force facilities. The approach is designed to understand the advantages and disadvantages of the different operating scenarios and the considerations about the respective types of private networks. Therefore, a model is proposed and implemented in a simulator to compute the system's capacity, throughputs, latency, and coverage and estimate the accuracy associated with different MEC node deployment options and radio characteristics. Results are presented, allowing the development of a qualitative and quantitative analysis of each scenario. The five chapters of this thesis are summarised below.

Chapter 1 provides the motivation and objectives for the work, as well as its structure and organisation. It starts with a brief overview of the current status of mobile communication systems, emphasising the need to use the 5G network and explaining the main benefits and improvements that can be achieved with it. The Portuguese Air Force paradigm is then presented by analysing two previously updated systems, emphasising the increase in performance with the implementation of 5G private networks. After the previously described overview, the thesis's motivation and contents are presented.

Chapter 2 presents the fundamental concepts needed to understand the thesis work. The contents are structured hierarchically, starting by differentiating the NSA and SA architectures of 5G. Then, the radio interface is studied by briefly explaining the TDD and FDD modes, the 5G numerologies and frequency bands used in Portugal. This initial contextualisation provides a detailed overview of the general characteristics of the 5G network. Next, the SDN and NFV concepts are described. The association of these concepts enables the virtualisation of network functions previously tied to hardware to run efficiently on cloud infrastructures, leading to a process that simultaneously reduces the physical network resources and guarantees that the available ones are used more efficiently. The prior study leads to an understanding of the network slicing concept, which is also discussed. This latter divides the physical network into many independent virtual slices that supply various resources to different traffic types, modifying the network to satisfy the heterogeneous services NR is expected to provide. The O-RAN architecture is also studied, being developed and improved to further the growth of 3GPP RAN architecture in non-public networks. It is based on the C-RAN concepts and uses increasingly software-defined wireless communications and network functionalities. Afterwards, the latency contributions of the nodes and links and the respective definitions associated with the O-RAN architecture are presented, with the introduction of the MEC node as a highlight of the impact on the total latency network. Next, the 5G systems services and applications are characterised, followed by the private networks' classification. 5G private networks can be deployed as an SA or public network integrated mode. These concepts are fundamental when analysing results and in the process of selecting the most suitable type of private network. State of the art is presented at the end of the chapter, summarising the most relevant information related to the thesis.

Chapter 3 concerns the proposal, description, implementation, and assessment of the model for analysing the parameters selected to determine the most adequate 5G private network. The theoretical model is briefly described at the beginning of the chapter, along with an outline of its objectives and fundamental assumptions. Subsequently, the developed model's implementation is explained in depth,

complete with flowcharts that illustrate the methods used in the simulator. The chapter concludes with a comprehensive analysis of the results through comparison with data from other systems and the literature.

The model is intended to adapt to the network's characteristics and the user's profile, with service differentiation concerning the performance parameters assigned to the network demands. Thus, the specifications associated with the different parameters are presented with the respective options, if applicable. The examined services listed in Annex C are part of the 5G applications, where the standards for E2E latency are more stringent. These service requirements can only be implemented by examining different strategies to reduce the latency between the network's two endpoints. Then, the model construction is described, explaining the programme's process to calculate the respective variables associated with the latency contributions, the radio link capacities and the 5G node throughputs.

The model implementation used in this thesis is divided into two parts. The model starts by reading the network, service and user specifications as input parameters, and it stores the crucial variables to perform further calculations. These calculations are strongly influenced by the service mix applied to the transmitter and receiver sides of the RU, DU and CU nodes and the MEC node deployment option. In this model, the sum of the data rates of the services does not exceed the respective node's throughputs. In the second part of the model, the required E2E latency and the UL and DL RU node throughputs are used to calculate the margin values applied to each system, depending on the type of services (critical or non-critical). The main objective is to obtain the output correspondent to an integrated private network whenever possible. Thus, the conditions applied to determine the type of private network differ based on the type of service classification.

The required outputs from applying the first flowchart of the model are the maximum E2E latency and the RU node throughputs. These results are introduced in the inputs of the second flowchart used to calculate the values of the margins defined to determine the network integration mode. It is then possible to estimate the length of the links between nodes and their associated throughputs depending on the type of service analysed.

Chapter 4 gives an overview of the analysis of the scenario's performance, the proposed solutions and their implementation. The chapter starts by discussing the Airbase, WAM System and 991 Squadron simulation environments. For each scenario's systems, a presentation of possible strategies based on frequency band, type of private network and the best location for installing the RU node is given to ensure the service requirements. The independent RU, DU and CU node architecture and the Splitting Option 7.2 are reference choices to all scenarios simulation. The MEC node deployment options are also tested to understand each network latency reduction strategy better. Moreover, since a more significant traffic density is expected in the areas with higher mobile data usage, the RU node traffic, the aggregation factor and the CQI value are the main differences between scenarios.

After analysing all scenario results, it can be seen that the 5G network can ensure the throughputs required by almost all systems, except the Flight Simulator Systems with non-standard radio characteristics. However, it should be noted that the throughputs of the 5G RU node depends on factors that can vary according to the desired purpose, the installation location and the frequency band used.

Therefore, in each scenario's simulation parameters, the CQI values were chosen based on the respective services' characteristics, functionalities and environment properties. The fact that there are critical and non-critical services in the same scenario means that the margins applied to the throughputs of the RU node are different. As this is a decisive factor in choosing the type of private network, it was found that for the same scenario, there could be two recommendations for the type of private network to be installed. As such, it was realised that the network type decision should also consider the monetary factor, the area occupied by the network components and the respective maintenance in addition to the conditions presented in each service analysis. These aspects significantly impact long-term use, and since the services are always inserted in a military environment, security and restriction of data sharing must be prioritised. Thus, choosing a single private network is the best deployment strategy in this case. While this is a generalised point of view, the following conclusions are developed based on analysing the systems associated with each scenario.

For the Security and Control services, the choice of the CQI value significantly impacted the throughputs provided by the 5G RU node. For these services, it was necessary to balance the CQI value with the purpose of the applications. The value 8 was chosen because this system prioritises consistent and viable performance over maximised throughputs. A high CQI can be responsive to variations in QoS, leading to inconsistent performance. Using less efficient, more secure and less predictable communication methods associated with a lower CQI value is preferable. The maximum CQI is 15. The RU node throughputs calculated are referent to a single node. As such, it was verified that it would be possible to allocate all the Security and Control services in addition to the services assigned to the general communications, which were also considered.

However, the margin applied to the throughputs of the RU node is exceeded at the UL and DL sites. After this verification, it was automatically concluded that installing an integrated private network would be impossible. Despite this, it was still necessary to analyse the latency according to the chosen network structure. Depending on the environment in which the UEs were installed, it was found that the variations in the results obtained for the maximum E2E latency were insignificant, with the latency contributions associated with the ALs being responsible for the difference. Although the results did not vary substantially according to the MEC node deployment option for indoor and outdoor UEs, it was concluded that the best choice would be the RU-DU inside the premises of the Airbase to prevent latency increase in some high-traffic circumstances. Concerning coverage, it can be concluded that a hybrid network is the best choice to guarantee the requirements of the services.

The Flight Simulator Systems often simulate complex scenarios, such as emergency procedures, extreme weather conditions and air traffic interactions, requiring transmitting and receiving a vast range of data in real-time. Therefore, a higher CQI value is required to provide these applications with high-definition graphics and QoE without artefacts and interruptions. Two different groups of radio characteristics were studied. Although the non-standard radio characteristics allow the 5G RU node to have sufficient throughput to allocate the data rates of the Flight Simulator services, it was found that this option would result in more disadvantages than advantages, mainly in terms of latency contributions and compatibility. Therefore, a CQI value of 12 and 4 MIMO layers were chosen. However, this option

did not give the RU node the throughputs to allocate the respective services. As such, the defined margin was also exceeded, and it was concluded that deploying an independent private network would be necessary. Regarding coverage, the fact that the RU node is installed about 200 m from the UEs makes the frequency band used different from the other systems analysed. The deployment option for the MEC node is chosen based on the same reasons as the Security and Control services.

Regarding the WAM System scenario, the services were analysed separately because of the different ALs propagation latency contributions. Therefore, different results were obtained for the maximum E2E latency and the maximum E2E distance between the two systems. Regarding the radio characteristics, a CQI of 9 was used for both systems because it ensures excellent channel conditions with minimal interferences and distortion, essential for maintaining the integrity of the communication links in air traffic management and weather monitoring.

Concerning the Air Traffic Control service, the margin applied to the throughputs of the RU node was exceeded. Therefore, the installation of an independent private network was required. However, for the Weather Monitoring services, an integrated private network could be chosen in a practical application because it can be considered that a negligible amount of data rate on the UL site exceeded the margin. Based on this study, it is concluded that it is impossible to allocate the services of the two systems to a single RU node and that there is the possibility of installing two types of private networks, depending on the system profile.

Since both systems are non-critical, they are not assigned as high priority, so the queuing latency must be considered, especially for the Air Traffic Control service. It means that a slight change in traffic is traduced into a significant increase in the maximum E2E latency. It was concluded that using different MEC node deployment options for both systems was not advantageous. Therefore, the RU-DU option was selected to reduce the network architecture's complexity and achieve the E2E latency with the lowest value. Regarding the frequency and type of cell, it was concluded that the type of cell was chosen according to the distance from the UEs to the RU node, like the frequency band. Thus, the decision was made individually.

The scenario analysis of the 991 Squadron, instead of being separated according to the type of services, was separated according to the environment and place where the UAVs carry out their mission, i.e., inside the area reserved for the Airbase or far from it. Regardless of the type of environment, it was decided to use the same CQI value because these services require extremely low latency, uninterrupted control, reliability, and connectivity. As such, it was decided to use a value that would ensure these properties and, at the same time, not interfere with the other surrounding systems.

Regarding the throughput provided by the RU node, it was found that the margin was exceeded by a minimal range inside the premises. As such, the programme's output showed that installing an independent private network was necessary. In this case, and unlike the WAM System, it was concluded that this would be the best option due to the characteristics associated with the Remote Control UAV services requirements.

Regarding the services analysed outside the premises, it was verified that in the case of the RU node that receives the data packets from the UAV, the margin is not exceeded on both the UL and DL sites. However, the throughput margin of the RU node that sends the data packets to the Control Centre is exceeded in the DL site, also by a minimal interval. Therefore, it was concluded that given the distribution of UAVs and the network structure, such as the WAM System, it was necessary to use a network with a large geographical distribution structure. In this way, it is more cost-effective and less expensive if the network structure is already built. Regarding the type of cells and the frequency to be used, the two scenarios were analysed independently, as different coverages were required.

Although the installation of an independent private network is necessary for inside and outside the premises, ensuring the required E2E latency is also required. As these services are highly critical, and there may be traffic variations inside and outside the Airbase, installing the MEC node to obtain the lowest E2E latency is necessary. As such, the RU-DU option was chosen for both cases.

In terms of future work, the implemented model should be optimised to consider the attenuation applied to the ALs in the transmission and reception of data packets to obtain a more accurate latency value for the radio links. The model should also be studied and tested in more remote areas since the priority and user traffic would differ. The collocated node architectures should also be a study case regarding latency contributions and throughputs since this thesis did not analyse them. The coverage provided by the selected cells should also be studied because it was just estimated based on the cells and environment characteristics. It is also proposed the study of hybrid private networks to optimise the use of services according to their degree of criticality since this model considered just one type of private network for each scenario.

Annex A

User’s Manual

This Annex presents the simulator instructions and configuration.

A.1 Simulator Instructions and Configuration

To run the model simulator it is necessary to configure the Network_specification.xlsx, the User_specification.xlsx and the Service_specification.xlsx files that define the input parameters. Then, run the script “main.m” in the Programme folder. The input parameters allow the programme user to change the network's characteristics.

Table A.1 – Network specifications – input parameters configuration (adapted from [14]).

NA (Network Architecture)	1	5G architecture with independent RU, DU and CU.
MEC (MEC Node Deployment Option)	0	No MEC.
	1	MEC node between the CU and Core nodes.
	2	MEC node between the DU and CU nodes.
	3	MEC node between the RU and DU nodes.
NL (Network Link)	0	DL.
	1	UL.
	2	DL and UL.
FH1	7.2	Splitting Option 7.2 on the transmitter side.
FH2	7.2	Splitting Option 7.2 on the receiver side.
MH1	2	Splitting Option 2 in the MH link on the transmitter side.
MH2	2	Splitting Option 2 in the MH link on the receiver side.
BH1	25	BH link capacity (Gbps) on the transmitter side.
BH2	25	BH link capacity (Gbps) on the receiver side.
TL1	100	TL capacity (Gbps) on the transmitter side.
TL2	100	TL capacity (Gbps) on the receiver side.
NP1	1	Numerology number used on the transmitter side.
NP2	1	Numerology number used on the receiver side.
SF1	1	Scaling factor on the transmitter side.
SF2	1	Scaling factor on the receiver side.
FS	0.57	Frame structure (downlink usage ratio).
AF1	0.7	Average factor on the transmitter side.

Table A.2 – (contd.) - Network specifications – input parameters configuration (adapted from [14]).

AF2	0.7	Average factor on the receiver side.
MM1	Number of MIMO layers on the transmitter side.	
MM2	Number of MIMO layers on the receiver side.	
BW1	System bandwidths on the transmitter side.	
BW2	System bandwidths on the receiver side.	
CQI1	Average channel quality indicators on the transmitter side (between 1 and 15).	
CQ2	Average channel quality indicators on the transmitter side (between 1 and 15).	

Table A.3 – User specification – input parameters configuration (adapted from [14]).

DT1/DT2	Distances between the UEs and the radio node in the transmitter and receiver sides.
US	Service to be simulated (between 1 and 17).
NRUU_Tx	Numbers of users connected to the RU node on the transmitter side.
NRUU_Rx	Numbers of users connected to the RU node on the receiver side.
NDUU_T	Numbers of users connected to the DU node on the transmitter side.
NDUU_Rx	Numbers of users connected to the DU node on the receiver side.
NCUU_Tx	Numbers of users connected to the CU node on the transmitter side.
NCUU_Rx	Numbers of users connected to the CU node on the receiver side.
List of RU_Tx	List of percentages of users connected to the RU node on the transmitter side.
List of RU_Rx	List of percentages of users connected to the RU node on the receiver side.
List of DU_Tx	List of percentages of users connected to the DU node on the transmitter side.
List of DU_Rx	List of percentages of users connected to the DU node on the receiver side.
List of CU_Tx	List of percentages of users connected to the CU node on the transmitter and receiver side.
List of CU_Rx	List of percentages of users connected to the CU node on the receiver side.

Table A. 4 – Service specification – inputs parameters configuration (adapted from [14]).

List of Services	List of services with the required data rates and the allowed E2E latencies.

Annex B

Latency Adaptation Parameters

This Annex presents a table with each service's latency adaptation parameter.

Table B.1 – Latency adaptation parameters.

Service	**Service Number**	ρ_{lat}
Internal Control Manipulations	1	0.2
Video Streaming	2	1
Sensor Motion Detection	3	0.6
Remote Control	4	0.04
Virtual Reality	5	0.2
Remote Control Video Sensors	6	0.6
Network-Based Sensor Sharing	7	0.02
External Control Manipulations	8	0.001
High-Quality Video Streaming	9	0.001
Telemetry Link	10	0.001
Voice	11	1
Video Conference	12	1
Web Browsing	13	1
Email	14	1
Social Networking	15	1
File Transfer	16	1
Airspace Control	17	0.02

Annex C

Service Requirements

This Annex presents the requirements 5G systems must fulfil to provide the services.

Table C.1 – Service requirements.

Service System	Service	Latency [ms]	Data Rate [Mbps]	Packet Size [Bytes]	Priority	References
Security and Control	Internal Control Manipulations	4	0.512	20	2	[14]
	Video Streaming	10	2	188	2	[34]
	Sensor Motion Detection	6	0.25	500	2	[63]
Flight Simulators	Remote Control	4	0.512	20	5	[64]
	Virtual Reality	5	400	650	5	[64]
Weather Monitoring	Remote Control Video Sensors	10	2.25	20	3	[34]
Air Traffic Control	Network-Based Sensor Sharing	8	4	500	3	[14, 61]
Remote-Controlled UAV	External Control Manipulations	0.5	1	10	1	[62, 65]
	High-Quality Video Streaming	1.5	10	1000	1	[62, 65]
	Telemetry Link	1	0.1	20	1	[62, 65]
-	Voice	100	0.032	218	3	[14, 34]
-	Video Conference	150	2	800	5	[14, 34]
-	Web Browsing	300	0.5	512	9	[14, 34]
-	Email	300	0.512	128	12	[14, 34]
-	Social Networking	300	2	1000	8	[14, 34]
-	File Transfer	300	1	4096	10	[14, 34]
-	Local Airspace Control	100	2	400	3	[66]

Annex D

CQI Index

This Annex presents the modulation order, R_{code_max} and the spectral efficiency in order of the CQI.

Table D.1 – CQI index for throughputs (extracted from [14, 34]).

CQI Index	Modulation Order	R_{code_max}	Spectral Efficiency
0	-	-	-
1	2	0.076	0.152
2	2	0.188	0.377
3	2	0.438	0.877
4	4	0.369	1.477
5	4	0.479	1.914
6	4	0.602	2.406
7	6	0.455	2.731
8	6	0.554	3.322
9	6	0.650	3.902
10	6	0.754	4.523
11	6	0.853	5.115
12	8	0.694	5.555
13	8	0.778	6.227
14	8	0.864	6.914
15	8	0.926	7.406

Annex E

5G Link Capacity

This Annex presents the link capacity depending on the splitting option.

Table E.1 – 5G links capacities (adapted from [14]).

Splitting Option	Link throughput	Reference Values
Option 7.2 (30 kHz of SCS as reference)	DL: 5.3 Gbps	N_{SC}: 3276 (N_{PRB}*12 subcarriers) N_{SY} :14 N_Q: 8 $D_{MAC_{info}}$: 121
	UL: 29.4 Gbps	N_{SC}: 3276 (N_{PRB}*12 subcarriers) N_{SY} :14 N_Q: 32 $D_{MAC_{info}}$: 80
Option 2 (250 Mbps of throughput as reference)	DL: 6.7 Gbps	R_p: 250 B: 100 B_c: 20 N_L: 8 $N_{L,c}$: 2 M: 256 M_c: 64
	UL: 5.0 Gbps	R_p: 83 B: 100 B_c: 20 N_L: 8 $N_{L,c}$: 1 M: 64 M_c: 16

Annex F

Scenarios Configuration

This Annex presents the radio characteristics and the respective simulated traffic of each scenario.

Table F.1 – Average number of users per node - Security and Control Systems.

RU	DU	CU
400	1200	6000

Table F.2 – Security and Control Systems receiver and transmitter service mix.

Service	1	2	3	4	5	6	7	8	9	10	11	12	13	14	15	16	17
RU mix [%]	13	12.5	12.5	0	0	0	0	0	0	0	28	4	12	7	5.5	3	2.5
DU mix [%]	11	10.5	10.5	0.25	0.25	0.5	5	0	0	0	32	3	13	3	7	2	2
CU mix [%]	8	7.5	7.5	0.1	0.1	0.25	2.5	0.15	0.15	0.15	34	3	15	7	8	4	2.6

Table F.3 – Average number of users per node – Flight Simulator Systems.

RU	DU	CU
400	1200	6000

Table F. 4 – Flight Simulator Systems receiver and transmitter service mix.

Service	1	2	3	4	5	6	7	8	9	10	11	12	13	14	15	16	17
RU mix [%]	0	0	0	0.5	0.5	0	0	0	0	0	40	9.5	16	11	13	7	2.5
DU mix [%]	10	7.5	7.5	0.5	0.5	0.5	7	0	0	0	32	3	13	7	6	3.5	2
CU mix [%]	8	7.5	7.5	0.1	0.1	0.25	2.5	0.15	0.15	0.15	34	3	15	7	8	4	2.6

Table F.5 – Average number of users per node – WAM System.

RU	DU	CU
200	800	4000

Table F.6 – WAM System receiver and transmitter service mix.

Service	1	2	3	4	5	6	7	8	9	10	11	12	13	14	15	16	17
RU mix [%]	0	0	0	0	0	3	30	0	0	0	26	6	16	4	13	2	0
DU mix [%]	6	8	8	0.5	0.5	1	12.5	0	0	0	28	5	11	4.5	12	1	2
CU mix [%]	5	8	8	0.05	0.05	0.1	11	0.3	0.3	0.3	33	4	11	4	11	2	1.9

Table F.7 – Average number of users per node – UAV System – inside.

RU	DU	CU
400	1200	6000

Table F.8 – UAV System receiver and transmitter service mix – inside.

Service	1	2	3	4	5	6	7	8	9	10	11	12	13	14	15	16	17
RU mix [%]	0	0	0	0	0	0	0	0.75	1.5	2.25	38	9	20	7	16	3	2.5
DU mix [%]	10	9.5	9.5	0	0	0	0	0.5	0.5	0.5	32	4	13	4	11	3	2.5
CU mix [%]	9	8	8	0.05	0.05	0.25	2.5	0.3	0.3	0.3	36	3.25	14	3	11	2	2

Table F.9 – Average number of users per node – UAV System – outside.

Trans. RU	Rec. RU	DU	CU
300	400	1200	6000

Table F.10 – UAV System receiver and transmitter service mix – outside.

Service	1	2	3	4	5	6	7	8	9	10	11	12	13	14	15	16	17
Trans. RU mix [%]	0	0	0	0	0	0	0	0.4	0.6	1	39	8	21	8	16	3	3
Rec. RU mix [%]	0	0	0	0	0	1	10	0.75	1.5	2.25	42	5	17	4	14	2.5	0
DU mix [%]	10	9.5	9.5	0	0	0	0	0.5	0.5	0.5	32	4	13	4	11	3	2.5
CU mix [%]	9	8	8	0.05	0.05	0.25	2.5	0.3	0.3	0.3	36	3.25	14	3	11	2	2

Table F.11 – Radio characteristics systems.

Systems	MIMO layers	Numerology	Bandwidth [MHz]	CQI	Scaling factor	DL Frame Structure	Average factor
Security and Control	4	1	100	8	1	0.57	0.7
Flight Simulators	4	1	100	12	1	0.57	0.7
Weather Monitoring	4	1	100	9	1	0.57	0.7
Air Traffic Control	4	1	100	9	1	0.57	0.7
Remote-Controlled UAV	4	1	100	12	1	0.57	0.7

Table F.12 – UE distances from the RU node for the simulated systems.

Systems	Transmitter UE distance [m]	Receiver UE distance [m]
Security and Control - indoor	2000	2000
Security and Control - outdoor	4000	4000
Flight Simulators	200	200
Air Traffic Control	9144	11000
Weather Monitoring	200	11000
UAVs – inside	400	400
UAVs – outside	18500	400

References

[1] H. Holma, A. Toskala and T. Nakamura, *5G Technology: 3GPP New Radio*, John Wiley & Sons, New York, USA, 2020, https://books.google.pt/books?id=hkHADwAAQBAJ&lpg=PR17&ots=AGA0NJ2ywN&dq=5G%20Technology%3A%203GPP%20New%20Radio&lr&hl=pt-PT&pg=PR17#v=onepage&q=5G%20Technology:%203GPP%20New%20Radio&f=false, Nov. 2022.

[2] T. Nakamura, "5G Evolution and 6G", in *Proc. of 2020 IEEE Symposium on VLSI Technology*, Honolulu, HI, USA, June 2020, https://ieeexplore.ieee.org/abstract/document/9265094, .

[3] S. Eswaran and P. Honnavalli, "Private 5G networks: a survey on enabling technologies, deployment models, use cases and research directions", *Telecommunication Systems*, Nov 2022, https://link.springer.com/article/10.1007/s11235-022-00978-z, Dec 2022.

[4] J. Padros-Garzon, P. Ameigeiras, J. Ordonez-Lucena, P. Munoz, O. Adamuz-Hinojosa and D. Camps-Mur, "5G Non-Public Networks: Standardization, Architectures and Challenges", *IEEE Access*, Vol. 9, Nov 2021, pp. 153893-153908, https://ieeexplore.ieee.org/document/9611236/, Nov. 2022.

[5] FAP – Força Aérea Portuguesa- Missão, https://www.emfa.pt/p-181-missao_visao, Oct 2023.

[6] B. Ferreira, *Otimização da Cobertura dos Serviços de Comunicação*,M.Sc. Thesis, Instituto Superior Técnico, Lisbon, Portugal, 2021.

[7] A. Agamyrzyansc, *Análise dos limites de capacidade e cobertura em redes ad-hoc de UAVs*, M.Sc. Thesis, Instituto Superior Técnico, Lisbon, Portugal, 2018.

[8] Samsung, *5G Standalone Architecture*, Internal Report, Samsung Electronics Co., Ltd, Suwon-si Gyeonggi-do, Korea, 2021 (https://images.samsung.com/is/content/samsung/assets/global/business/networks/insights/white-papers/0107_5g-standalone-architecture/5G_SA_Architecture_Technical_White_Paper_Public.pdf), Dec 2022.

[9] WLINK – WLINK Technology Co., Limited, https://www.wlink-tech.com/art/5g-nsa-and-sa-difference, Dec 2022.

[10] S. Husain, A. Kunz and J. Song, "3GPP 5G Core Network: An Overview and Future Directions", *Journal of Information and Communication Convergence Engineering*, vol. 20, no. 1, Mar. 2022, pp. 8-15, https://doi.org/10.6109/JICCE.2022.20.1.8, Oct 2022.

[11] M. Enescu, *5G New Radio: A Beam-based Air Interface*, John Wiley & Sons, New York, USA, 2020, https://books.google.pt/books?id=-THSDwAAQBAJ&lpg=PR13&ots=TJ1VF8SK_H&dq=5G%20New%20Radio%3A%20A%20Beam-based%20Air%20Interface&lr&hl=pt-

PT&pg=PR13#v=onepage&q=5G%20New%20Radio:%20A%20Beam-based%20Air%20Interface&f=false, Nov. 2022.

[12] G. Zebari, D. Zebari and A. Al-zebari, “FUNDAMENTALS OF 5G CELLULAR NETWORKS: A REVIEW”, *Journal of Information Technology and Informatics*, vol. 1, no. 01, Apr. 2021, pp. 1-5, https://qabasjournals.com/index.php/jiti/article/view/22, Dec 2022.

[13] ETSI, *System architecture for the 5G System (5GS) (3GPP TS 23.501 version 17.4.0 Release 17)*, RTS/TSGS-0223501vh40, Internal Report, France, (https://www.etsi.org/deliver/etsi_ts/123500_123599/123501/17.04.00_60/ts_123501v170400p.pdf), May 2022.

[14] A. Carvalho, L. Correia and A. Grilo, “Analysis of Strategies for Minimising End-to-End Latency in 4G and 5G Networks”, in *Proc. of 2022 International Conference on Broadband Communications for Next Generation Networks and Multimedia Applications (CoBCom)*, Graz, Austria, July 2022, https://ieeexplore.ieee.org/abstract/document/9880722, Nov 2022.

[15] L. Correia, *Mobility and Traffic*, Course Notes, Instituto Superior Técnico, Lisbon, Portugal, 2022.

[16] ANACOM - ANACOM creates conditions for consistent and competitive development of 5G in Portugal, https://www.anacom.pt/render.jsp?contentId=1493002, Dec 2022.

[17] GSMA, 6 GHz in the 5G Era Global Insights on 5925-7125 MHz, Internal Report, GSMA, 2022 (https://www.gsma.com/spectrum/wp-content/uploads/2022/07/6-GHz-in-the-5G-Era.pdf).

[18] A. Tikhomirov, E. Omelyanchuk and A. Semenova, “Recommended 5G frequency bands evaluation” in IEEE Network, in *Proc. of 2018 Systems of Signals Generating and Processing in the Field of on Board Communications*, Moscow, Russia, Mar 2018, https://ieeexplore.ieee.org/abstract/document/8350639, Oct 2023.

[19] S. Sun, T. S. Rappaport, M. Shafi, P. Tang, J. Zhang and P. J. Smith, “Propagation Models and Performance Evaluation for 5G Millimeter-Wave Bands”, *IEEE Transactions on Vehicular Technology*, Vol. 67, , June 2018, pp. 8422 – 8439, https://ieeexplore.ieee.org/abstract/document/8386686, Oct 2023.

[20] N. Zhao, M. Jing and Z. Yan, “Power Division for Green Cellular Network”, *IEEE Network*, Sep. 2022, pp. 1-7, https://ieeexplore.ieee.org/document/9877932/, Nov 2022.

[21] M. Trung, “Multiplexing Techniques for Applications Based-on 5G Systems”, in Somayeh Mohammady (ed.), *Multiplexing - Recent Advances and Novel Applications*, IntechOpen, Dublin, Ireland, 2022, https://www.intechopen.com/chapters/79928, Dec 2022.

[22] J. Flores de Valgas, J. Monserrat, H. Arslan and M. Condoluci, “Flexible Numerology in 5G NR: Interference Quantification and Proper Selection Depending on the Scenario”, *Mobile Information Systems*, Vol. 2021, Mar 2021, pp. 1-9, https://www.hindawi.com/journals/misy/2021/6651326/, Nov 2022.

[23] N. Correia, F. Al-Tam and J. Rodriguez, “Optimisation of Mixed Numerology Profiles for 5G Wireless Communication Scenarios”, *Sensors*, Vol. 21, No. 4, Fev 2021, p. 1494, https://www.mdpi.com/1424-8220/21/4/1494, Dec 2022.

[24] A. Nauman, T. Nguyen, Y. Qadri, Z. Nain, K. Cengiz and S. Kim, “Artificial Intelligence in Beyond 5G and 6G Reliable Communications”, *IEEE Internet of Things Magazine*, Vol. 5, No. 1, Mar 2022, pp. 73-78, https://scholar.google.com/scholar?hl=pt-PT&as_sdt=0%2C5&q=Artificial+Intelligence+in+Beyond+5G+and+6G+Reliable+Communications&btnG=, Dec 2022.

[25] L. Ji, S. He, W. Wu, C. Gu, J. Bie and Z. Shi, “Dynamic Network slicing Orchestration for Remote Adaptation and Configuration in Industrial IoT”, *IEEE Transactions on Industrial Informatics*, Vol. 18, No. 6, June 2022, pp. 4297-4307, https://ieeexplore.ieee.org/abstract/document/9629333, Dec 2022.

[26] E. Ahvar, S. Ahvar, S. Raza, J. Vilchez and G. Lee, “Next Generation of SDN in Cloud-Fog for 5G and Beyond-Enabled Applications: Opportunities and Challenges”, *Network*, Vol. 1, No. 1, June 2021, pp. 28-49, https://www.mdpi.com/2673-8732/1/1/4, Dec 2022.

[27] A. Arulappan, G. Raja, K. Passi and A. Mahanti, “Optimisation of 5G/6G Telecommunication Infrastructure through an NFV-Based Element Management System”, *Symmetry*, Vol. 14, No. 5, May 2022, pp. 978, https://www.mdpi.com/2073-8994/14/5/978, Dec 2022.

[28] D. Ficzere, “Complex network theory to model 5G Network slicing”, in *Proc. of NOMS 2022-2022 IEEE/IFIP Network Operations and Management Symposium*, Budapest, Hungary, Apr 2022, https://ieeexplore.ieee.org/abstract/document/9789715, Dec 2022.

[29] M. Malik, A. Kothari and R. A. Pandhare, “Network slicing In 5g: Possible Military Exclusive Slice”, in *Proc. of 2022 1st International Conference on the Paradigm Shifts in Communication, Embedded Systems, Machine Learning and Signal Processing (PCEMS),* Nagpur, India, May 2022, https://ieeexplore.ieee.org/abstract/document/9807927, Dec 2022.

[30] A. Kanwal, M. Khalid, I. Ejaz, Tasbeeha and S. Rathore, “Advantages of Co-Deployment of C-RAN and MEC in 5G”, in *Proc. of 2021 International Bhurban Conference on Applied Sciences and Technologies (IBCAST)*, Islamabad, Pakistan, Jan 2021, https://ieeexplore.ieee.org/abstract/document/9393261, Nov 2022.

[31] N. Verma and P. Mishra, “Traffic Scheduler for BBU Resource Allocation in 5G CRAN”, in *Proc. of 2022 8th International Conference on Advanced Computing and Communication Systems (ICACCS)*, Coimbatore, India, Mar 2022, https://ieeexplore.ieee.org/abstract/document/9785313, Nov 2022.

[32] M. Jibril, N. Hassen and M. Tadesse, “Load Balancing in 5G C-RAN using Swarm Intelligence (SI) Algorithms”, *International Journal of Communications*, Vol. 6, Oct 2021, pp. 13-17, https://www.iaras.org/iaras/home/caijoc/load-balancing-in-5g-c-ran-using-swarm-intelligence-si-algorithms, Dec 2022.

[33] A. Havolli, A. Maraj and L. Fetahu, “Cloud Radio Access Network for Next Generation Mobile Networks; practical implementation benefits”, in *Proc. of 2022 45th Jubilee International Convention on Information, Communication and Electronic Technology (MIPRO)*, Opatija, Croatia, May 2022, https://ieeexplore.ieee.org/abstract/document/9803365, Dec 2022.

[34] S. Domingues, *Analysis of the Performance of Multi-Access Edge Computing Network slicing in 5G*, M.Sc. Thesis, Instituto Superior Técnico, Lisbon, Portugal, 2019, https://grow.tecnico.ulisboa.pt/~grow.daemon/wp-content/uploads/2020/01/Thesis_S%C3%A9rgioD.pdf, Oct 2023.

[35] B. Ali, M. Gregory and S. Li, “Multi-Access Edge Computing Architecture, Data Security and Privacy: A Review”, *IEEE Access*, Vol. 9, Jan 2021, pp. 18706-18721, https://ieeexplore.ieee.org/abstract/document/9330515, Nov 2022.

[36] L. Nadeem, M. Azam, Y. Amin, M. Al-Ghamdi, K. Chai, Khan, M. F. Nadeem, Khan and M. Adnan, “Integration of D2D, Network slicing, and MEC in 5G Cellular Networks: Survey and Challenges”, *IEEE Access*, Vol. 9, Mar 2021, pp. 37590-37612, https://ieeexplore.ieee.org/abstract/document/9366869, Dec 2022.

[37] K. Cao, Y. Liu, G. Meng and Q. Sun, “An Overview on Edge Computing Research”, *IEEE Access*, Vol. 8, May 2020, pp. 85714-85728, https://ieeexplore.ieee.org/abstract/document/9083958, Nov 2022.

[38] E. Dahlman, S. Parkvall and J. Skold, *5G NR: The next generation wireless access technology*, Academy Press, Massachusetts, EUA, 2020, https://books.google.pt/books?hl=pt-PT&lr=&id=-bfjDwAAQBAJ&oi=fnd&pg=PP1&dq=5G+NR:+The+next+generation+wireless+access+technology&ots=5Lksx0KWaq&sig=PG6eTrTbCm0ANvMb39__5UiKow4&redir_esc=y#v=onepage&q=5G%20NR%3A%20The%20next%20generation%20wireless%20access%20technology&f=false, Nov 2018.

[39] H. Attar, H. Issa, J. Ababneh, M. Abbasi, A. Solyman, M. Khosravi, R. Sais Agieb and A. Kumar, “5G System Overview for Ongoing Smart Applications: Structure, Requirements, and Specifications”, *Computational Intelligence and Neuroscience*, Vol. 2022, Oct 2022, pp. 1-11, https://www.hindawi.com/journals/cin/2022/2476841/, Dec 2022.

[40] S. Marinheiro, *Analysis of the Implementation of Network Slicing in 5G Radio Networks*, M.Sc. Thesis, Instituto Superior Técnico, Lisbon, Portugal, 2021, https://grow.tecnico.ulisboa.pt/wp-content/uploads/2021/02/Thesis_SergioMarinheiro.pdf, Oct 2022.

[41] J. Navarro-Ortiz, P. Romero-Diaz, S. Sendra, P. Ameigeiras, J. Ramos-Munoz and J. Lopez-Soler, “A Survey on 5G Usage Scenarios and Traffic Models”, *IEEE Communications Surveys & Tutorials*, Vol. 22, No. 2, Feb 2020, pp. 905-929, https://ieeexplore.ieee.org/abstract/document/8985528, Dec 2022.

[42] L. Banda, M. Mzyece and F. Mekuria, “5G Business Models for Mobile Network Operators—A Survey”, *IEEE Access*, Vol. 10, Sep 2022, pp. 94851-94886, https://ieeexplore.ieee.org/abstract/document/9881490, Dec 2022.

[43] R. Prakash, *Transforming enterprise and industry with 5G private networks*, Qualcomm Technologies, 2022 (https://www.qualcomm.com/news/onq/2020/10/transforming-enterprise-and-industry-5g-private-networks).

[44] M. Wen, Q. Li, K. Kim, D. Lopez-Perez, O. Dobre, V. Poor, P. Popovski and T. Tsiftsis, "Private 5G Networks: Concepts, Architectures, and Research Landscape", *IEEE Journal of Selected Topics in Signal Processing*, Vol. 16, No. 1, Jan 2022, pp. 7-25, https://ieeexplore.ieee.org/abstract/document/9661406, Nov 2022.

[45] M. Filho, *Analysis of the Implementation of Private Networks in 5G*, M.Sc. Thesis, Instituto Superior Técnico, Lisbon, Portugal, 2022.

[46] A. Larmo, . P. V. Butovitsch, . P. C. Millos and P. Berg, "Critical Capabilities for Private 5G Networks", *Ericsson*, Dec 2019, https://www.ericsson.com/4ac664/assets/local/reports-papers/white-papers/criticalcapabilities5g.pdf, Oct 2023.

[47] GSMA, 5G industry campus network deployment guideline, Internal Report, GSMA, 2020 (https://www.google.com/url?sa=t&rct=j&q=&esrc=s&source=web&cd=&ved=2ahUKEwj99vekmOSBAxXeQaQEHdLqCW0QFnoECBQQAQ&url=https%3A%2F%2Fwww.gsma.com%2Fnewsroom%2Fwp-content%2Fuploads%2FNG.123-v1.0-3.pdf&usg=AOvVaw0tfnExCTQ3qYh0VmsDnj6_&opi=89978449).

[48] J. Liao and X. Ou, "5G Military Application Scenarios and Private Network Architectures", in *Proc. of 2020 IEEE International Conference on Advances in Electrical Engineering and Computer Applications(AEECA)*, Dalian, China, Aug 2020, https://ieeexplore.ieee.org/abstract/document/9213507, Dec 2022

[49] ITU-R – Radiocommunication Sector of ITU, *Report on IMT Vision – Framework and overall objectives of the future development of IMT for 2020 and beyond*, ITU-R M.2083-0, ITU-R, 2015, https://www.google.com/url?sa=t&rct=j&q=&esrc=s&source=web&cd=&ved=2ahUKEwjchqKSmeSBAxWbUKQEHcaoCw0QFnoECBkQAQ&url=https%3A%2F%2Fwww.itu.int%2Fdms_pubrec%2Fitu-r%2Frec%2Fm%2FR-REC-M.2083-0-201509-I!!PDF-E.pdf&usg=AOvVaw3OozdjQqLp0gGFtPrJApng&opi=89978449, Oct 2023.

[50] M. Malik, "5G For Military Communication: Automation of Kill Cycle", in *Proc. of 2021 International Conference on Technological Advancements and Innovations (ICTAI)*, Tashkent, Uzbekistan, Nov. 2021, https://ieeexplore.ieee.org/abstract/document/9673415, Nov 2022.

[51] P. Gronsund, A. Gonzalez, K. Mahmood, K. Nomeland, J. Pitter, A. Dimitriadis, T.-K. Berg and S. Gelardi, "5G Service and Slice Implementation for a Military Use Case". in *Proc. 2020 IEEE International Conference on Communications Workshops (ICC Workshops)*, Dublin, Ireland, June 2020, https://ieeexplore.ieee.org/abstract/document/9145236, Oct 2023.

[52] L. Bastos, G. Capela, A. Koprulu and G. Elzinga, "Potential of 5G technologies for military application", in *Proc. of 2021 International Conference on Military Communication and Information Systems (ICMCIS)*, The Hague, Netherlands, May 2021, https://ieeexplore.ieee.org/abstract/document/9486402, Nov 2022.

[53] ITU-T – Telecommunication Standardization Sector of ITU, *Report on 5G wireless fronthaul requirements in a passive optical network context*, Supplement 66, ITU-T, 2019.

[54] A. Burk and D Lemberg, *Overview and Predictive Analysis for Latency Optimized Telecommunication Networks*, PowerPoint Presentation, Vodafone, Rüsselsheimm Germany, 2018, https://www.hs-rm.de/fileadmin/persons/khofmann/Gastvortraege/Vortragsfolien/20181026-Burk-Lemberg-vodafone-5G.pdf, Oct 2023.

[55] J. Rischke, P. Sossalla, S. Itting, F. H. P. Fitzek and M. Reisslein, "5G Campus Networks: A First Measurement Study", *IEEE Access*, Vol. 9, Aug 2021, pp. 121786 – 121803, https://ieeexplore.ieee.org/abstract/document/9524600, Oct 2023.

[56] A. Virdis, G. Nardini, G. Stea and D. Sabella, "End-to-End Performance Evaluation of MEC Deployments in 5G Scenarios", *Journal of Sensor and Actuator Networks*, Vol. 9, No.4, Dec 2020, pp. 57, https://www.mdpi.com/2224-2708/9/4/57, Oct 2023.

[57] ITU-T – Telecommunication Standardization Sector of ITU, *Report on Transport network support of IMT-2020/5G*, ITU-T GSTR-TN5G , ITU-T, 2018.

[58] Y. Zhou, M. Wei , C. Hu, . X. Xu and W. Xie, "Research on Coverage and Networking Capability of 5G 40M FDD Bandwidth Enhancement Compared with 100M TDD", in *Proc. 2021 9th International Conference on Intelligent Computing and Wireless Optical Communications (ICWOC)*, Chongqing, China, June 2021, https://ieeexplore.ieee.org/abstract/document/9529964, Oct 2023.

[59] A. Esswie and K. Pedersen, "On the Ultra-Reliable and Low-Latency Communications in Flexible TDD/FDD 5G Networks", in *Proc. 2020 IEEE 17th Annual Consumer Communications & Networking Conference (CCNC)*, Las Vegas, USA, Jan 2020, https://ieeexplore.ieee.org/abstract/document/9045657, Oct 2023.

[60] P. Larsen, L. Maria, A. Checko and H. L. Christiansen, "A Survey of the Functional Splits Proposed for 5G Mobile Crosshaul Networks,", *IEEE Communications Surveys & Tutorials*, Vol. 21, No. 1, Oct 2018, pp. 146-172, https://ieeexplore.ieee.org/abstract/document/8479363, Oct 2023.

[61] T. Costa, *Analysis of Aircraft Accuracy Location in Aeronautical Multilateration Systems*, M.Sc. Thesis, Instituto Superior Técnico, Lisbon, Portugal, 2017, https://grow.tecnico.ulisboa.pt/wp-content/uploads/2017/07/mscthesis-tiago-costa.final_.pdf, Oct 2023.

[62] Y. Zeng, Q. WU and R. Zhang, "Accessing From the Sky: A Tutorial on UAV Communications for 5G and Beyond", *Proceedings of the IEEE*, Vol. 107, No. 12, Dec 2019, pp. 2327 – 2375, https://ieeexplore.ieee.org/abstract/document/8918497, Oct 2023.

[63] J. Cappele, L. Monteyne, J. Mulders, S. Goossens, M. Vergauwen and L. Perre, "Low-Complexity Design and Validation of Wireless Motion Sensor Node to Support Physiotherapy", Sensors *2020,* No.21, Nov 2021, pp. 6362, https://www.mdpi.com/1424-8220/20/21/6362, Oct 2023.

[64] S. Mangiante, G. Klas, A. Navon, Z. GuanHua, J. Ran and M. Silva, "VR is on the Edge: How to Deliver 360° Videos in Mobile Networks", in *Proc. the Workshop on Virtual Reality and Augmented Reality*

Network, Aug 2017, https://www.researchgate.net/publication/319049968_VR_is_on_the_Edge_How_to_Deliver_360_Videos_in_Mobile_Networks, Oct 2023.

[65] G. Damigos, T. Lindgren, S. Sandberg, and G. Nikolakopoulos, “Performance of Sensor Data Process Offloading on 5G-Enabled UAVs”, *Sensors,* No. 2, Jan 2023, pp. 864, https://www.mdpi.com/1424-8220/23/2/864, Oct 2023.

[66] T. Gräupl and N. Mäurer, “An Air Traffic Management Data Traffic Pattern for Aeronautical Communication System Evaluations”, in *Proc. 2019 IEEE/AIAA 38th Digital Avionics Systems Conference (DASC)*, San Diego, USA, Sep 2019, https://ieeexplore.ieee.org/document/9081745, Oct 2023.